

Copyright is owned by the Author of the thesis. Permission is given for a copy to be downloaded by an individual for the purpose of research and private study only. The thesis may not be reproduced elsewhere without the permission of the Author.

A record of natural and human- induced environmental change from Lake Horowhenua

A thesis presented in partial fulfilment of the requirements for the degree of

Master of Science

in

Earth Science

School of Agriculture and Natural Environment, Massey University,
Palmerston North, New Zealand



Celeste Bevins

2019



Lake Horowhenua at sunset.

Abstract

Lake Horowhenua is a hypertrophic turbid lake located in the western coastal plain of the lower North Island of New Zealand. In order to effectively restore or manage modified systems such as Lake Horowhenua, an understanding of past environmental change and natural variability is essential to provide a benchmark for ‘natural’ conditions. Cores from the bed of Lake Horowhenua have been analysed to reconstruct a detailed environmental record for the last c. 4,200 cal yr BP.

Prior to lake formation, the area now occupied by the lake was subject to fluvial deposition from the Ohau River sometime prior to 7,500 cal yr BP. Dune transgression began in the region c. 7,700 cal yr BP at the very earliest, and drainage of the small streams and springs was impeded, allowing for the formation of a proto lake. A tidal surge up the Hokio Stream may have occurred c. 7,100 cal yr BP. Clastic delivery into the lake from the inflowing streams was high from 4,200 cal yr BP until sometime around 3,200 cal yr BP. The lake then transitioned into a phase of increased autochthonous sedimentation. During this phase, stable bottom water oxygenation, high water quality, and little catchment disturbance dominated. The pollen record indicates that the pre-human vegetation was a lowland podocarp-hardwood forest, dominated by *Dacrydium cupressinum*. There is some evidence of vegetation response to long-term climate change associated with increasing intensification of the westerly circulation regime through the mid to late Holocene.

Proxy evidence implies human arrival to the Lake Horowhenua area occurred c. 519-486 cal yr BP, and land clearance was initiated on the plains inducing erosion within the catchment. However, sedimentation rates did not change from pre-human levels and water quality remained high. European arrival c. 1840 AD saw a further acceleration of land clearance on the plains and in the uplands, the introduction of exotic plant species for forestry, increased pastoral land for agriculture, and a reduction in water quality. Aquatic weed growth began at 1898 AD and was prolific from 1985 AD. High nutrient levels are evident from c. 1985 AD. Sedimentation rates and erosion increased significantly to 0.34 cm a^{-1} compared to pre-human (0.08 cm a^{-1}) and Māori settlement (0.07 cm a^{-1}).

Acknowledgements

First and foremost, I would like to thank the Muaūpoko Tribal Authority and the Lake Horowhenua Trust for access to Lake Horowhenua and their permission to study this taonga. I would also like to thank Noel Procter for access via his land.

I would sincerely like to thank my supervisors, Dr Kat Holt and Dr Jon Procter (Massey University) for giving me the opportunity to study Lake Horowhenua. A huge thanks to Kat for her guidance on this thesis, and introducing me to the art of pollen counting and paleoenvironmental change.

I would like to thank Massey University staff for their support in the lab, field, and during discussions. Thanks to David Feek for his help and strength during coring operations. A further thanks to Dr Anja Moebis, Ian Furkert, Dr Paramsothy Jeyakumar, Dr Qinhua Shen, and Julie Palmer for their help with answering all my questions. Thanks to Marcela Gonzalez for helping with the MP-AES. Thanks to Dr Alastair Clement for the discussions on the sand deposit.

Thanks to Piet Verburg and Max Gibbs (NIWA), and Marcus Vandergoes (GNS Science). I am grateful for their advice and the discussions on this project. I would like to express my gratitude to Andrew Rees (VUW) for arranging for me to come to VUW, answering my questions on grain size analysis, and helping with the age-depth model.

Thanks to Julia Peters, Marozane Spammers, and Wendy Payne for proofreading. Thanks to Amber Brine for photoshopping my cores back together, and Hannah Walters for helping in the lab.

I would like to thank the Graduate Women Manawatū (GWM) Charitable Trust, Massey University and the Geography Department for their financial support. This work was supported through a GWM Postgraduate Scholarship, Massey University Masterate Scholarship, and the Geography Student Research Fund. This research was funded by MBIE's Vision Maturanga Capability Fund.

I would like to thank my extended family and friends, particularly Mum, Dad, Amber, and Tyler, and their families. They never left it more than a month between visits and took my mind off things when it was needed most. Lastly, and most importantly, I dedicate this thesis to Liam Parkins, my husband, whose support both emotionally and financially allowed me to leave my job and find my passion. Without him, this would have been a pipe dream.

Table of Contents	Page
Abstract.....	i
Acknowledgements.....	ii
Table of Contents.....	iii
List of Figures.....	vi
List of Tables.....	ix
Chapter 1: Introduction	1
1.1 General introduction.....	1
1.2 Motivation for research.....	2
1.3 Research aims and objectives.....	2
1.4 Thesis structure.....	3
Chapter 2: Background information	4
2.1 Regional and geological setting.....	4
2.2 Climate.....	5
2.3 Lake description.....	6
2.4 Development of Levin and Horowhenua.....	7
2.5 Vegetation.....	8
2.6 Environmental degradation of Lake Horowhenua.....	12
2.7 Literature review.....	15
2.7.1 Introduction.....	15
2.7.2 Measuring baseline conditions and establishing reference conditions.....	15
2.7.3 Natural variability.....	17
2.7.4 Human arrival in New Zealand.....	20
2.7.5 Anthropogenic influences and evidence of impacts on lakes and surrounding environs in New Zealand.....	22
2.7.6 Summary.....	24
Chapter 3: Methodology	25
3.1 Coring.....	25
3.2 Sand deposit.....	28
3.3 Core stratigraphy.....	29
3.4 Chronology.....	29
3.4.1 Radiocarbon dating.....	29
3.4.2 Lead-210 and cesium-137 concentration dating.....	32
3.5 Bulk density measurements.....	33
3.6 Pollen analysis.....	33
3.7 Grain size analysis.....	36
3.8 Geochemistry.....	38

3.8.1 Carbon and nitrogen analysis	38
3.8.2 Organic matter content (via loss on ignition and Elementar).....	40
3.8.3 Elemental analyses (via atomic emission spectroscopy and X-ray fluorescence) .	41
Chapter 4: Results	46
4.1 Sand deposit	46
4.2 Core shortening	49
4.3 Core stratigraphy.....	49
4.4 Chronology	52
4.4.1 Radiocarbon dating	52
4.4.2 Lead-210 and cesium-137 concentration dating	56
4.5 Bulk density measurements	56
4.6 Pollen analysis	57
4.7 Grain size proxies (LPA and XRF).....	62
4.8 Geochemistry	64
4.8.1 Carbon and nitrogen	64
4.8.2 Organic matter content (via loss on ignition, Elementar, and XRF).....	65
4.8.3 Elemental and XRF proxies for oxygenation and water quality	66
4.8.4 Elemental and XRF proxies for erosion.....	67
Chapter 5: Discussion	70
5.1 Assessment of radiocarbon dating	70
5.2 Lake formation and evolution.....	72
5.2.1 Sand deposit	74
5.3 Environmental change	78
5.3.1 HW1 390-285 cm 4,213-2,924 cal yr BP.....	78
5.3.2 HW2 285-85 cm 2,924-502 cal yr BP.....	82
5.3.3 HW3 85-60 cm 502 cal yr BP – 1840 AD	87
5.3.4 HW4a 60-40 cm 1840-1898 AD	91
5.3.5 HW4b 40-0 cm 1898 AD – present.....	92
5.4 Summary of human impact	96
Chapter 6: Conclusion and recommendations for future research	97
6.1 Conclusion	97
6.2 Future research recommendations	99
References	101
Appendices	118
Appendix A: Legend for Figure 1.....	118
Appendix B: Raw pollen counts	119
Appendix C: Obscuration values	121

Appendix D: Conventional radiocarbon dating reports	122
Appendix E: Pollen diagram.....	132

List of Figures

Figure 1: The surface geology of the Horowhenua district (adapted from Begg et al., 2000). Inset: the location of Lake Horowhenua within the North Island (LINZ, 2014). The dotted red line indicates the approximate location of the inactive Levin Fault. Circled are the lobes of the Tokomaru Marine Terrace that would have acted as a barrier to the Manawatū estuary. The legend can be found in Appendix A.....	4
Figure 2: Land use in the Lake Horowhenua catchment (HRC, 2017).....	6
Figure 3: Lake Horowhenua in relation to the township of Levin, and locations of the inlets and outlets (adapted from Gibbs, 2011; Google Earth, 2018).....	7
Figure 4: Current vegetation and land cover (LAWA, n.d.). Map created by LAWA, (n.d.) using land cover database V 4.1 created by Landcare Research New Zealand Ltd.	11
Figure 5: Factors that can influence erosion and clastic grain size, and sediment geochemistry in lake sediment records.	18
Figure 6: Coring locations (Google Earth, 2018).	25
Figure 7: (A) 1-4 The corer at different snapshots during the sediment collection process. (B) Extruding the sediment into a PVC liner. (C) The winch system used to remove the corer from the sediment. (D) Example of the gravity corer used at Lake Horowhenua (PYLONEX, n.d.). (E) Gravity core about to be plugged.....	27
Figure 8: Image of the sand layer found in a core taken from near the outlet.	28
Figure 9: (A) Seed submitted for radiocarbon dating (GNS, 2018). (B) Cladocera ephippia.	30
Figure 10: Pollen processing procedure.....	34
Figure 11: (A) <i>Pediastrum</i> . (B) Example of a broken <i>Pediastrum</i> that was not included in the counts.	35
Figure 12: Stacked grain size classes of all sands.....	46
Figure 13: Images of all sands to show angularity in the >250 µm size fraction. (A) Core sand. (B) Dune sand. (C) Beach sand. (D) Ohau River sand. The images were taken at the same magnification.	47
Figure 14: Mineralogy of all sands. From top to bottom: >250 µm, >125 µm (125-250 µm), and >63 µm (125-63 µm) size fractions.	48

Figure 15: (A) Stratigraphic log and lithological descriptions of Horo 10. (B) Photographic images of Horo 10. 1: 0-0.9 m. 2: 0.9-1.9 m. 3: 1.9-2.9 m. 4: 2.9-3.9 m. Note the organic-rich silt appears more olive-grey than the image implies.	50
Figure 16: Stratigraphic log and lithological descriptions of Horo 8.	51
Figure 17: Multiplot of radiocarbon dates from the 80-90 cm range (cal yr BP). Plotted are: the seed from 85 cm (NZA 65135), lake margin plant material from 80-85 cm (NZA 65079), bulk sediment from 80-85 cm (NZA 65824), and Cladocera ehippia from 80-85 cm (NZA 65080) and 80-90 cm (NZA 65136).	53
Figure 18: Age-depth model at 95.4% confidence interval. Radiocarbon dates used in this model: NZA 65134, NZA 65135, NZA 65822, and NZA 65823. Present day and European arrival (based on pollen indicators) c. 1840 AD were also plotted. Correction of 448 ± 22 years was applied to NZA 65822 and NZA 65823 as the linear relationship between NZA 65136, NZA 65822, and NZA 65823 implies an error is present in the older dates as well (Fig. 19). Calibration carried out with SHCal13 (Hogg et al., 2013) and post-bomb SH1-2 (Hua et al., 2013) calibration curves. NZA 65824 and NZA 65136 are plotted as outliers in red.	54
Figure 19: Cladocera ehippia midpoint cal yr BP ages and 2 sigma error. Plotted are: NZA 65136, NZA 65822, and NZA 65823.	55
Figure 20: ^{210}Pb and ^{137}Cs concentration curves expressed in S.I units of Becquerels (Bq). This is equivalent to 1 radioactive disintegration per second (Swales et al., 2010).	56
Figure 21: Dry bulk density and coherent/incoherent scatter via XRF.	57
Figure 22: Relative pollen diagram of selected taxa only. A full diagram can be found in Appendix E.	61
Figure 23: Pollen moisture index.	62
Figure 24: Grain size data (LPA and XRF).	63
Figure 25: TOC wt. % and TN wt. % to determine inorganic nitrogen contribution to correct the C/N ratio.	64
Figure 26: From left to right: C/N atomic ratio. TOC wt. %. TN wt. %.	65
Figure 27: Organic matter proxies. From left to right: $\text{OM}\%^{\text{T}}$. $\text{OM}\%^{\text{L}}$. $\text{OM}\%^{\text{L}}$ stacked against $\text{OM}\%^{\text{T}}$ and $\text{OM}\%^{\text{L}}$ with 13% correction. XRF incoherent/coherent scatter.	66
Figure 28: Oxygen and water quality indicators. From left to right: Fe/Mn ratio and Fe counts via XRF as a proxy for oxygenation. Fe/Mn ratio via atomic emission spectroscopy as a proxy for oxygenation. P/CPS x 1000 via XRF as a proxy for productivity.	67

Figure 29: XRF and elemental proxies for erosion. From left to right: Magnetic susceptibility. Ti/CPS x 100, K/CPS x 100, Rb/CPS x 1000, Al/CPS x 100, all via XRF. Al% via atomic emission spectroscopy..... 69

Figure 30: Conceptual model of marine oxygen isotope stage 2 in the Manawatū Horowhenua region (adapted from Clement, 2011; Hughes, 2005). The black silhouette is the current extent of Lake Horowhenua. The dark green represents the Tokomaru Marine Terrace..... 73

Figure 31: Summary of the main proxies used to synthesise the environmental history of Lake Horowhenua. From left to right: Magnetic susceptibility via XRF. Ti/K via XRF. Ti/CPS x 100 via XRF. %OM^T. C/N ratio. Fe/Mn ratio via atomic emission spectroscopy. *Pediastrum*. *Pteridium*. Charcoal (all sizes). PMI. Stacked graph of dryland pollen. Pollen, charcoal, and *Pediastrum* are presented as relative proportions of the dryland sum. Pollen zones and age-depth model interpolated dates have been added to aid in the synthesis..... 79

Figure 32: Lake Horowhenua relative pollen and charcoal diagram to infer the point of human arrival. Data is presented as percentages of the dryland sum..... 88

List of Tables

Table 1: The seven main forest types in the Manawatū prior to human settlement (adapted from Esler, 1964, 1978).	9
Table 2: Sediment accumulation rates (SAR) from a coring site near the buoy (adapted from HRC, 2018).	15
Table 3: Graphical measures and descriptive statistics of all sands.....	46
Table 4: Grain shape, sample type, and sediment name of all sands.	47
Table 5: Radiocarbon dates.	52
Table 6: Sedimentation rates.	56
Table 7: Pollen zone ages.....	58

Chapter 1: Introduction

1.1 General introduction

Human arrival to an uninhabited area typically results in many forms of disturbance in the landscape. For example; deforestation via fire or logging, changes in catchment processes and increased rates of erosion as land use is shifted towards agriculture and horticulture, and the introduction of invasive species, to name a few. In New Zealand, the arrival of Polynesian settlers, and later European settlers, resulted in large-scale ecological impacts to the natural environment (McWethy et al., 2010; Wilmshurst et al., 1997). However, disturbance can also occur due to natural processes, such as climate variance, storms and floods, natural fire, and earthquakes, both before and during the human era. Lakes are ideal places to study such changes as their sediments capture a record of these events.

These records of natural conditions and disturbances captured in lake sediments are fundamental to understanding the pre-human and human environment. In New Zealand, research assessing pre-human and human environments largely focuses on historical monitoring and paleoenvironmental changes to natural vegetation, along with charcoal and sedimentological information (Bussell, 1988; Elliot et al., 1995; McGlone, 1983, 1989). It is these paleolimnological techniques and others that can be used to assess both pre-human and human-induced environmental change and the wider implications associated with human arrival. Such paleo-records provide a baseline for management, maintenance, and restoration of a water body and its watershed, as well as ensuring resources are not wasted on naturally degraded systems (Smol, 2008).

In order to effectively manage an ecosystem, three lines of enquiry must be made (Smol, 2008). Firstly; what were the natural conditions prior to human arrival? Without this knowledge, we cannot effectively gauge the extent of change and set realistic goals. Secondly; how dynamic is the natural system, and are the current changes within natural variability or due to anthropogenic disturbance? Thirdly; what is the critical level of stress before there is evidence of negative symptoms? (Smol, 2008).

This thesis will address the first two of these questions as they relate to Lake Horowhenua, along with investigating the formation of the lake. Lake Horowhenua is a hypertrophic turbid lake located in the western coastal plain of the lower North Island. A detailed environmental reconstruction using paleolimnological techniques will be used to examine the natural environment and the impact of human arrival at Lake Horowhenua and its watershed. This work represents one of the first comprehensive multi-proxy studies of the lakes of the Manawatū-

Horowhenua sand country and will complement the growing archive of Holocene change in New Zealand.

1.2 Motivation for research

Freshwater bodies hold intrinsic value to all New Zealanders and provide a means of sustenance, recreation and, in some cases, power generation (Cochrane, 2017). Additionally, New Zealand's natural environment is central to Māori identity and comes under the core value of *kaitiakitanga*, which means “environmental guardianship” (Harmsworth & Awatere, 2013). Thirty-two percent of New Zealand's 3,820 lakes larger than 1 ha are classed as eutrophic or worse (Verburg et al., 2010). Eutrophication of lakes results from a legacy of excess nutrients and sedimentation associated with land use change that has allowed an increase in biological productivity (Gibbs, 2011).

Lake Horowhenua is no exception and has been classified as having the 7th worst water quality in New Zealand (MfE, 2017a; Verburg et al., 2010). The current state of the lake is a result of clearance of the surrounding coastal forest, drainage of marginal wetlands, intensification of agriculture and horticulture in the catchment, urban expansion, livestock damage to riparian zones, and disposal of treated sewage into the lake from 1952 to 1987 AD. These factors have resulted in poor water quality, high turbidity, weed growth and cyanobacterial blooms, and damage and destruction to the surrounding native vegetation.

Lake Horowhenua holds a unique position in New Zealand and has a rich history. The lake is taonga (highly prized) and owned by the Muaūpoko Iwi who are spiritually connected to the lake and are the mana whenua (have historical and territorial rights) of the lake. The lake has been described as the iwi's “life blood” and has served as their ancient food bowl. The lake was a site of many battles, and the manmade islands on the western and southern shores served as places of protection. Restoration efforts are currently underway as a part of the Lake Horowhenua Accord (HRC, 2014) and Te Mana O Te Wai project (MfE, 2017b). These projects aim to enhance the mauri (life force) and the wairua (spirit) of the lake. The baseline environmental data obtained in this study will guide these and future restoration efforts, while the data from the human era will measure the extent of change and will complement modern monitoring schemes.

1.3 Research aims and objectives

This thesis aims to reconstruct a record of environmental change from the sediments within Lake Horowhenua. The following research questions are designed to achieve this:

1. When and how did Lake Horowhenua form?

2. How has the lake and catchment responded to natural and anthropogenic events over its lifetime? What are the baseline conditions, and which prior conditions form the ideal benchmark?

3. When did people arrive to the Horowhenua district, and what was the scale of change between Polynesian and European arrival?

These research questions will be answered by analysing sediment cores collected from Lake Horowhenua. Sedimentological analysis and any other indicators will be assessed to determine the formation of the lake. Ecological change will be reconstructed using pollen, charcoal, and algal indicators. Catchment disturbance will be reconstructed using grain size analysis, organic matter content, total organic carbon and total nitrogen content, magnetic susceptibility, X-ray fluorescence, and other elemental analyses. Time control and sedimentation rates will be constrained via radiocarbon dating, lead-210, and cesium-137 concentration dating. Anthropogenic impacts will be examined in high resolution and compared with pre-human conditions determined from a lower resolution analysis of the pre-human portion of the sediment record.

1.4 Thesis structure

This thesis contains six chapters. Chapter One provides a general introduction, the motivation for this study, and the aims and objectives of the research. Chapter Two presents key background information and is divided into two parts. The first part focuses on the regional geological setting, climate, lake description, and past research on Lake Horowhenua and surrounds. The second part of the chapter consists of a review of key literature on lake-based paleoenvironmental reconstructions. Chapter Three outlines the methodological approaches applied. Chapter Four presents the results of this environmental reconstruction. Chapter Five discusses the results and provides an interpretation of them in the context of the formation of the lake, environmental and catchment change, and the arrival of humans to the Horowhenua district and surrounds and their impacts. Chapter Six provides a summary of the main findings, and lastly, future research directions are explored.

Chapter 2: Background information

2.1 Regional geological setting

The Horowhenua district is located on the west coast of the southern North Island (Fig. 1). The region is underlain by a basement of quartzofeldspathic sandstone and mudstone (greywacke-argillite), originally deposited off the coast of Gondwana during the Permian and Late Jurassic (Lee et al., 2002). The uplift of the present-day range bounding the region to the southeast is thought to have occurred around 1-2 Ma (Orr, Korsch & Foley, 1991). The range is bisected into the Ruahine Range and Tararua Range by down cutting of the Manawatū River at the Manawatū Gorge. Marine cover beds and terraces (Cowie, 1963), fluvial deposits and terraces (Begg et al., 2000), dune fields (Cowie, 1963), and loess (Duguid, 1990) mantle the basement and are attributed to the region's dynamic history. The area is tectonically active, with a number of buried north-northeast striking reverse faults that manifest as anticlinal folds (Begg et al., 2000; Lamarche et al., 2005). The soils on the steep slopes are thin and friable, and pockets of volcanic ash can be found on some rolling land (Duguid, 1990).

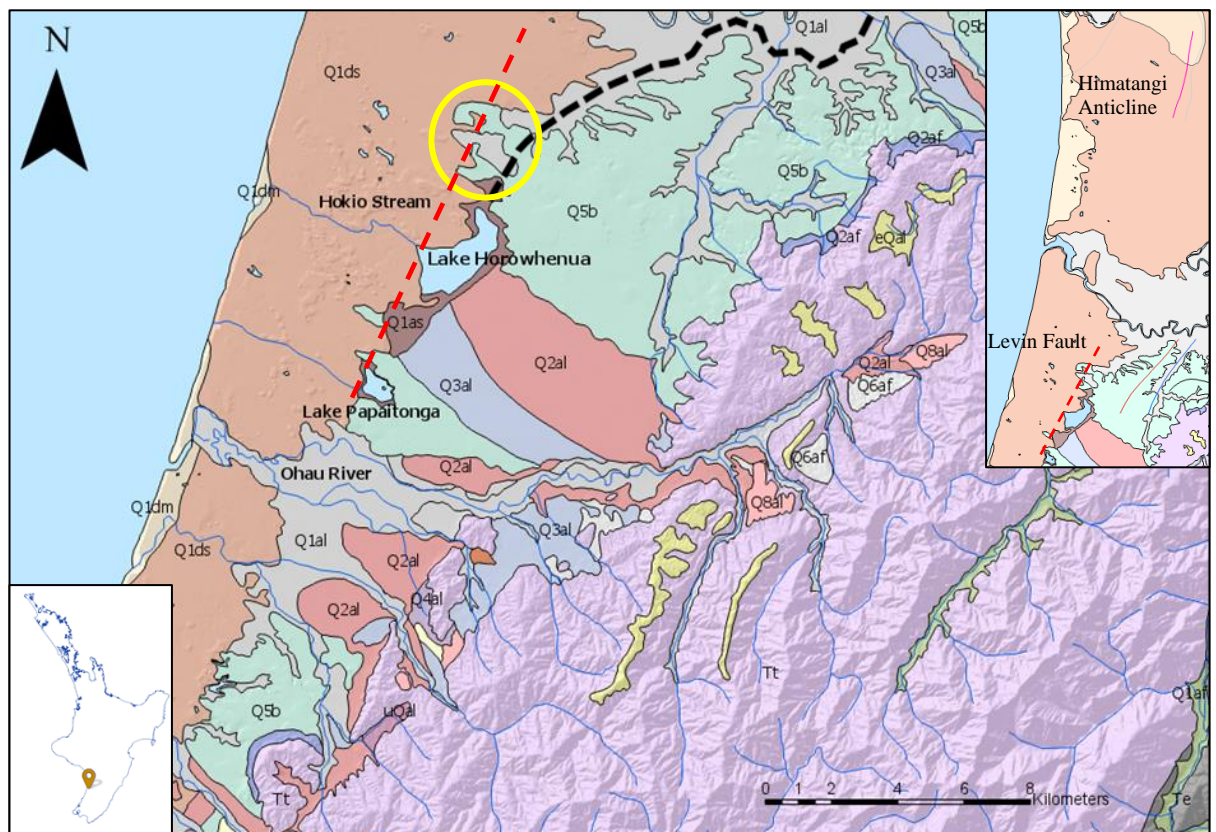


Figure 1: The surface geology of the Horowhenua district (adapted from Begg et al., 2000). Inset: the location of lake Horowhenua within the North Island (LINZ, 2014). The dotted red line indicates the approximate location of the inactive Levin Fault. Circled are the lobes of the Tokomaru Marine Terrace that would have acted as a barrier to the Manawatū estuary. The legend can be found in Appendix A.

Lake Horowhenua (40°36'39.57" S, 175°15'14.89" E) lies in the Levin Trough which extends north of Lake Horowhenua to Fielding (Rich, 1959). Lake Horowhenua is underlain by Holocene-aged gravels derived from the Ohau River sourced from headwaters in the greywacke mountain range (Gibbs, 2011; Gibbs & Quinn, 2012). A dune belt to the west of the lake stretches from the Manawatū River in the north to Paekakariki in the south (McFadgen, 1997), and is around 6 km wide and up to 11 km at its widest point (Duguid, 1990). These relic dunes of the Foxton Phase (Fig. 1) (Begg et al., 2000) accumulated between 6.6-1.6 ka (Cowie, 1963) (7,700-1,600 cal yr BP; Clement & Fuller, 2018). To the east and north of the lake, are deposits of the Tokomaru Marine Terrace of marine oxygen isotope stage 5e, alluvial gravels of the Ashhurst/Ohakea Terrace and fluvial gravels of the Milson/Rata Terrace (Fig. 1) (Begg et al., 2000).

Several authors have suggested that proto Lake Horowhenua was connected to the Manawatū estuary (e.g. Rich, 1959; Fair, 1968), which formed c. 8,300 cal yr BP (Clement et al., 2017). This significant estuary was originally thought to have extended inland to Shannon or Opiki (Fair, 1968; Rich, 1959) and Rongotea to Palmerston North (Hesp et al., 1999). Clement (2011) studied the Holocene sea-level change in the lower Manawatū valley. He found that the estuary at its maximum extent reached inland to Opiki, and across to Tokomaru and Linton. In the north, the estuary extended to Himatangi, but was abutted by the Tokomaru Marine Terrace in the south (just north of Lake Horowhenua) (circled in Fig. 1).

It is thought that, during the Holocene marine transgression, the Poroutawhao High just west of the lake (Litchfield, 2003) and the Himatangi Anticline further north, reached significant altitude to have allowed for the formation of the Manawatū estuary (Clement et al., 2010). The Poroutawhao High is around 2-2.5 km wide (Clement et al., 2017) and is fault-bounded on both sides; on the eastern side is the inactive Levin Fault (Fig. 1) (Hughes & Kennedy, 2009). This greywacke bedrock high is significant in the context of Lake Horowhenua, as it likely restricted oceanic influences in the vicinity of the lake during the Holocene sea-level high 6,800 cal yr BP (Clement, 2011).

2.2 Climate

The region has a temperate maritime climate with warm summers and mild winters (Duguid, 1990). Annual rainfall ranges from 900 mm to 2000 mm at the inland range (NIWA, n.d). In Levin, February is the driest month and July the wettest (Duguid, 1990). Summers are warm, and winters feature frequent frosts (Burgess, 1985). Temperatures differ 10 °C between summer and winter, and day and night (Clement et al., 2010; Heerdegen & Shepherd, 1992). The prevailing winds are north-westerly (Burgess, 1985).

2.3 Lake description

Lake Horowhenua is a small (2.9 km²) and shallow (<2 m deep) lake (Gibbs & White, 1994; Vant, 1985). Prior to European settlement, the lake and its streams were once a valued fishery for the Muaūpoko Iwi (HRC, 2014). The catchment is 61 km² of flat, fertile, agricultural, and horticultural land that is largely vegetated in pasture, and includes the township of Levin (Gibbs, 2011; HRC, 2014; Tempero, 2013). Land use in the catchment is dominated by dry stock (43%), dairy farming (15%), urban development (9%), and horticulture (11%) (Fig. 2) (HRC, 2017). Currently, the vegetation immediately proximal to Lake Horowhenua consists of *Phormium tenax*. Arawhata Stream and sub-catchments are the most extensive tributaries entering the lake and are primarily vegetated with crops and pasture (Roygard et al., 2015). Only 2.7% of the catchment is vegetated with native plants (Gibbs, 2011). Land use today around the Arawhata Stream is intensive dairy farming, whereas, traditionally, market gardening and horticulture dominated (Gibbs, 2011).

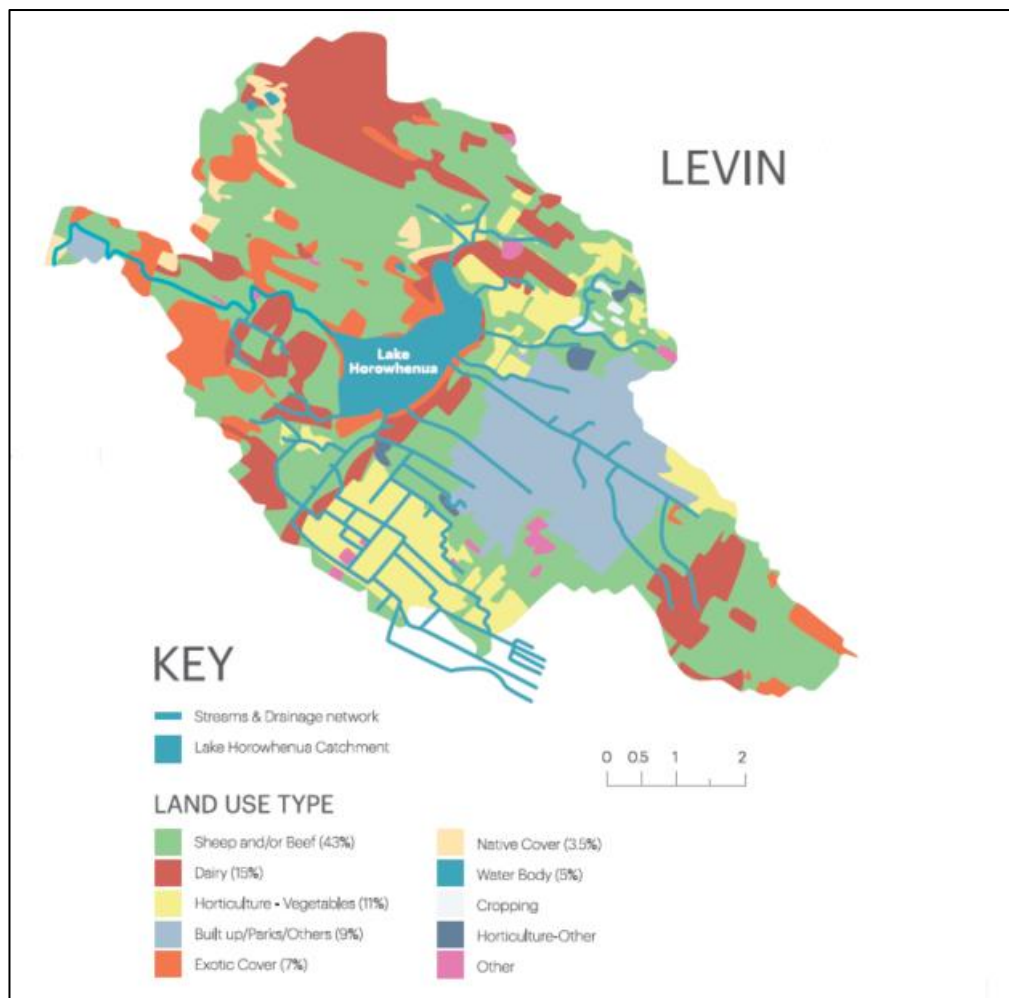


Figure 2: Land use in the Lake Horowhenua catchment (HRC, 2017).

The lake is fed by groundwater and surface runoff into eight natural and modified drains (Fig. 3). Modified natural watercourses of the Piatiki, Mangaroa, and Arawhata streams, and the Queen Street, Domain, Pa, Makomako, and Sand Road drains directly feed the lake (Chase, 2015). The spring-fed Arawhata Stream contributes 70% of the total surface input into Lake Horowhenua (Chase, 2015; MWRC, 2008). The water that feeds the stream originates from aquifers fed from the Tararua Range (Chase, 2015; MWRC, 2008). In the lake catchment, around 60% of overland flow enters highly-permeable gravels and replenishes the lake through springs along the eastern shore (Gibbs & White, 1994). The lake is also replenished by runoff water from irrigation schemes (Gibbs & White, 1994). Hokio Stream is the single outlet of the lake, and flows in a westerly direction to the coast with a discharge rate of $0.8\text{m}^3\text{ s}^{-1}$ (Gilliland, 1981). Historical data show annual rainfall of 1095 mm and annual evaporation of 722 mm, with a mean water residence time of around 50 days (Gibbs & White, 1994). The lake is artificially controlled by a weir that was installed in 1956 AD (Gibbs, 2011).

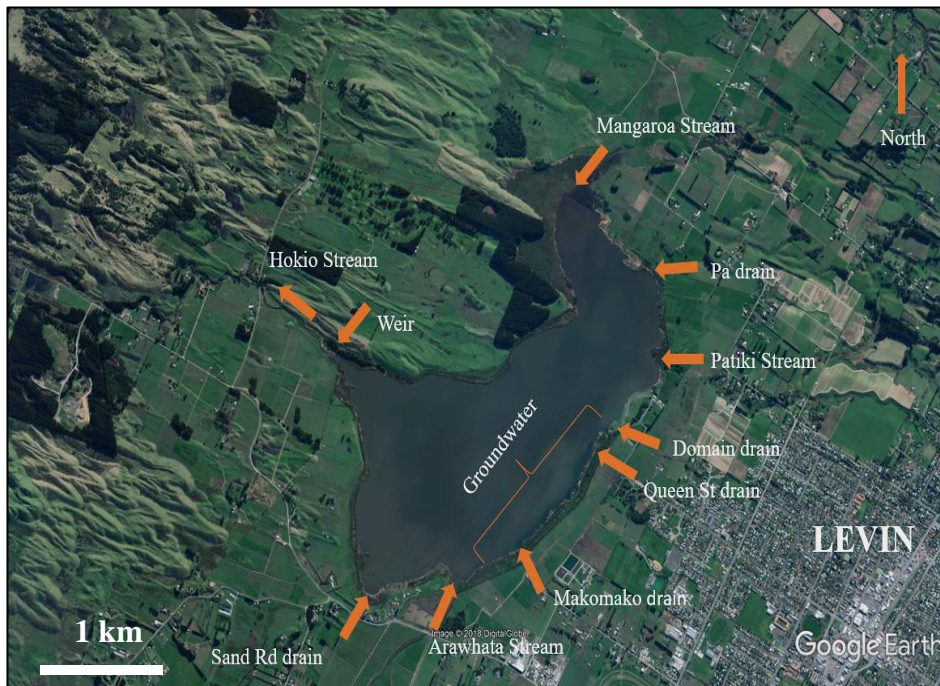


Figure 3: Lake Horowhenua in relation to the township of Levin, and locations of the inlets and outlets (adapted from Gibbs; 2011 & Google Earth, 2018).

2.4 Development of Levin and Horowhenua

In the year 1842 AD, E. J. Wakefield of the New Zealand Company, visited the area and surveyed blocks of land from the Manawatū River to Lake Horowhenua and back to the Tararua Range (Petersen, 1952). Early sheep farming began during the 1850s AD but was restricted to the already cleared sand country (Dreaver, 1984), and horticulture was mostly south of Waikanae (Dreaver, 1984). A map from 1876 AD shows that between the Manawatū and Waikanae Rivers there were

generally blank spaces with a few homes scattered throughout and the only road was the beach (Dreaver, 2006). After the opening of the Wellington to Palmerston North Railway in 1886 AD, dairy farming increased in the region (Dreaver, 1984). In 1887 AD, sections were available for lease or purchase in Levin and the first settlers of the town arrived. By 1920 AD, Levin had matured into a town due to increasingly intensive farm production (stock, dairy, wool, and flax), and by 1942 AD pasture covered 29% of the district (vs 52% in 2008) (Chase, 2015).

2.5 Vegetation

Vegetation of the past

The vegetation history of the Horowhenua district has received very little scholarly attention. The record of past vegetation in the region is generally developed through physical descriptions, and very little pollen analysis has been carried out.

It is thought that the flat plains of the Horowhenua district would have originally been one single large wetland (Ausseil et al., 2007) with extensive semi-swamp forest (Esler, 1964, 1978). Vegetation at these sites was predominantly *Phormium tenax*, *Typha orientalis*, *Austroderia*, *Dacrycarpus dacrydioides*, and *Laurelia novae-zelandiae* (Esler, 1964, 1978). In lowland areas affected by poor drainage or fire, scrub and shrubland would have been common, and succession into woody vegetation was prevented (Esler, 1964, 1978).

Esler (1964, 1978) studied the vegetation of the neighbouring Manawatū region in detail and suggested that seven main forest types persisted prior to Polynesian settlement (Table 1). McFadgen (1997) reports that in the lower North Island at the time of Polynesian settlement, the dune belt that borders the southwest coast of the North Island, including that to the immediate west of Lake Horowhenua, was forested. Only some riverbeds and active or unstable dunes would have remained unforested. Active dunes would have been vegetated with *Spinifex*, *Desmoschoenus spiralis*, and shrubs (Esler, 1964, 1978). Duguid (1990) suggests that the eastern dune belt was likely forested with *Podocarpus totara* and *Prumnopitys taxifolia*, and in partially drained areas *Dacrycarpus dacrydioides*. *P. totara* and *P. taxifolia* were also very common on the plains and foothills (Duguid, 1990). *Dacrydium cupressinum* was common on the foothills and the dune belt next to semi-swamp but was absent on the gravel plains unless clay was present.

Forest type	Location	Taxa
Semi-swamp forest	Lowland floodplain and dune country in low lying areas adjacent to rivers.	<i>Dacrycarpus dacrydioides</i> and <i>Laurelia novae-zealandiae</i> .
Totara forest	Free draining strips along the river margins and low lying areas.	<i>Podocarpus totara</i> and <i>Prumnopitys taxifolia</i> .
Mixed podocarp forest	Manawatu plains and fluvial terraces. The forest on the terraces was much older than the forest on the plains, and larger quantities of <i>Metrosideros robusta</i> occupied the terraces.	<i>Dacrydium cupressinum</i> , <i>Prumnopitys taxifolia</i> , <i>Podocarpus totara</i> , and <i>Dacrycarpus dacrydioides</i> .
Tawa forest	Low hills adjacent to the Tararua and Ruahine range. Manawatu gorge and the upper Turitea valley and in small stands on the Manawatū plains.	<i>Beilschmeidia tawa</i> .
Black beech forest	Pockets in the course of the Manawatū and Pohangina Rivers.	<i>Fuscospora solandri</i> .
Rimu and northern rata forest	Hill country (except where tawa was present). On the western flanks of the Tararua Range. <i>Dacrydium cupressinum</i> and <i>Metrosideros robusta</i> dominated above 300 m. Above 700 m was dominated by kamahi.	<i>Dacrydium cupressinum</i> and <i>Metrosideros robusta</i> .
Forests of the dune country	Dune country.	<i>Dacrycarpus dacrydioides</i> , <i>Laurelia novae-zealandiae</i> , and <i>Podocarpus totara</i> .

Table 1: The seven main forest types in the Manawatū prior to human settlement (adapted from Esler, 1964, 1978).

McFadgen (1997) cites an unpublished pollen and charcoal diagram by G.N. Park from Lake Papaitonga (6 km south of Lake Horowhenua) that is consistent with “late” clearance of forest in the area. Fox (2016) documents unpublished coarse resolution analyses of pollen and charcoal from Lake Waitawa, and pollen from Lake Horowhenua, Lake Papaitonga, and the Horowhenua Plains (Dickson, 1997). All these analyses are consistent with an initial Podocarp-hardwood forest that gives way to a reduction of tall tree taxa, and the appearance of *Pteridium esculentum* (bracken fern) and Poaceae in the upper sediments.

The iwi that settled the area (the timing of which is discussed in detail in section 2.7.4) utilised and modified the coastal sand country vegetation, as well as areas near lakes and streams for refuge and cultivation (McFadgen, 1994). Forest clearance began at the time of arrival, but its influence was not marked until later in the pre-historic record (McFadgen, 1997). The forest interior of the lowland and foothills of the Tararua Range was largely avoided during early colonisation, as the tools of the day made it difficult to occupy (Adkin, 1948; Chase, 2015). Cultivated crops consisted of kumara, taro (McFadgen, 1997), *Pteridium* (Duguid, 1990; McGlone et al., 2005), and *Cordyline australis* (cabbage tree) (Cambie & Ferguson, 2003). J. Procter *pers comm*, (2018), in addition, suggests that the cabbage tree was used around urupa (burial grounds), and that *Freycinetia banksii* (kiekie) were maintained (at least in the Horowhenua lowlands). *Corynocarpus laevigatus* (karaka) is a native northern tree (Costall et al.,

2006), and is thought to have been introduced to the area, as seeds have been found in the littoral dunes (Duguid, 1990). The dunes themselves may not have been cultivated until after European crops more suitable to the dune soils were introduced (Carkeek, 1966).

By the time of European settlement, the forest covering the dunes had been cleared (McFadgen, 1997). The patches of forest that remained on the Foxton Phase and younger dunes included: *Beilschmiedia tawa*, *Podocarpus taxifolia*, *Elaeocarpus dentatus*, *Podocarpus totara*, *Laurelia novae-zelandiae*, *Dacrycarpus dacrydioides* (Adkin, 1948), and *Alectryon excelsus* (MWRC, 1984). The plains inland of the dunes were cleared in patches, but the forest edge was largely at the inland side of the sand dunes (Adkin, 1948; McFadgen, 1997). The grassed hill-country ridges were covered in Coriariaceae and fern, and on the grassed flats *Phormium tenax* and *Austroderia toetoe* occurred (McDonald & O'Donnell, 1929). Open land was vegetated in grassland, *Leptospermum scoparium*, Coriariaceae, *Typha*, and *Austroderia toetoe*; on the wetter flats, semi-swamp forest of *Laurelia novae-zelandiae*, *Dacrycarpus dacrydioides*, and *Beilschmiedia tawa* dominated (Duiguid, 1991).

Wetlands were drained for pasture, and grazing began in the 1840s AD when European settlers arrived (Hesp, 2001; McWethy et al., 2010). By 1841 AD, the area between 'Long Reach' (actual location unknown) and Lake Horowhenua was clear of forest and forest remained in patches only (Petersen, 1952). A map from 1840 AD shows that the Manawatū dune country was vegetated with fernland, grassland, shrubland, or swamp (Anderson & McGlone, 1997; McGlone et al., 1997). Another map of the area from the 1840-1860s AD shows that the area was dominated by sand country, scrub, and fernland, with very few bush areas remaining (Esler, 1978; Flenley, 2000; Roche, 1997).

Most of the inland forest of the Horowhenua lowlands remained intact until 1886 AD, when the railway service began (Dreaver, 2006). In 1887 AD, Peter Bland Bartholemew opened a sawmill and, along with the Prouse brothers, removed most of the forest to make way for pasture (Dreaver, 2006). Timber harvesting became a race as the best timber needed to be harvested before it was burnt by farmers (Dreaver, 2006). Remnant forests remained in areas of swampland not suitable for farming, or where land had not yet been converted to farmland (Duguid, 1990).

In 1903 AD, the Sand Drift Act was passed to reduce encroachment of sand onto farmland at the coast due to deforestation (MWRC, 1984). In response to the Act, exotic plantations were established in the Horowhenua district. Holland (1983) reports that *Pinus radiata* was planted along narrow strips of active dunes in the region in 1966 AD. Duguid (1990) states that exotic plantations of *Pinus radiata* began at Waitarere in 1948 AD and may have been planted as early

as 1935 AD (Dreaver, 2006). An earlier introduction of *P. radiata* to the area is likely, as *P. radiata* was first introduced into New Zealand in the 1850s AD (Yearbook, 1990) and has been reported to have been planted in Wellington in 1865 AD (Woodward & Shulmeister, 2005).

Today, the Manawatū and Horowhenua districts have largely been converted to pasture (Fig. 4) (Roche, 2000). Forest remains on the flanks of the Ruahine and Tararua Range, as well as in isolated patches on the plains (Esler, 1962, 1964), with some preserved as reserves (Maclean & Maclean, 1988). Duguid (1990) describes the current vegetation as follows: Dune sands are vegetated with *Spinifex sericeus*, and *Ammophila arenaria*; Sand with topsoil supports pasture, *Lupinus arboreus*, and *Pteridium*; Plains near the coast are covered with rhizomatous herbs, *Leptocarpussimilis*, *Scirpus nodosus*, *Austroderia toetoe*, and *Festuca arundinace*; Where drainage was not possible, extensive peat swamps support *Phormium tenax* and some native vegetation; Inland on the rolling topography is drought-prone pasture, and shrubby weeds where the topsoil is deeper.

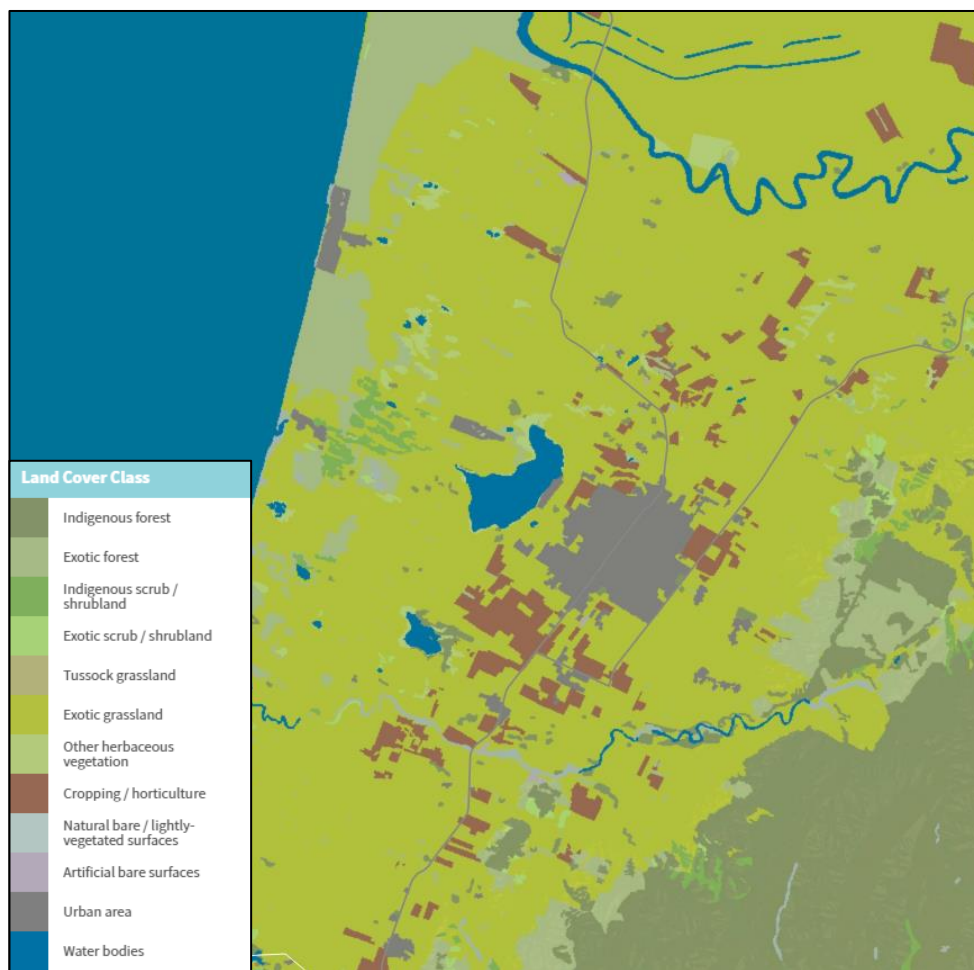


Figure 4: Current vegetation and land cover (LAWA, n.d.). Map created by LAWA, (n.d.) using land cover database V 4.1 created by Landcare Research New Zealand Ltd.

Past vegetation proximal to Lake Horowhenua

There is little reference to the past vegetation proximal to Lake Horowhenua in the literature. The Regional Management Plan: Manawatū-Wanganui (1984) states that native forest persisted at the northern end of Lake Horowhenua and ran northwards to Poroutawhao Pā until European arrival c. 1840 AD. This stand of semi-swamp forest was killed by artificial lowering of the lake water level sometime around 1931 AD (Duguid, 1990). The resultant embayment filled with *Phormium tenax*, *Austroderia toetoe*, and many other associated species. A remnant forest at Hokio Beach Road consisted of a Podocarp-hardwood forest, tree ferns, shrubs, and wetland vegetation (Duguid, 1990). The remnant forest here, and at the margins of Lake Horowhenua, was spared by a fire sometime before 1881 AD which cleared the southwest quarter where the town of Levin was settled (Duguid, 1990). Forbes (1996) drew a conclusion of what the vegetation around the lake would have been like in its natural state by comparing the vegetation of Lake Papaitonga. The vegetation around Lake Papaitonga consists of grass, scrub-covered dunes, and Podocarp-hardwood forest.

Ogle and West (1997) recorded the remnant vegetation around Lake Horowhenua in 1993 to advise restoration efforts. Their conclusion is quoted below:

The lake margins and other swampy ground would have had thickets of swamp shrubs, with flax, raupo, and other reeds on progressively wetter sites. The forest composition would have differed from site to site, according to factors such as soil moisture and fertility, and exposure to sun and wind. (p. 2)

2.6 Environmental degradation of Lake Horowhenua

Ecology

There have been a number of studies on the ecology of Lake Horowhenua. A lake weed survey was carried out by De Winton and Taumoepeau (2014). They found that the prominent pond weed in Lake Horowhenua is *Elodea canadensis*, which covers approximately 50 ha of the 300 ha lake (HRC, 2014). Historically, *Potamogeton crispus* was the dominant lake weed, but now only occurs in minor amounts (HRC, 2014). *Egeria densa* has also been found in the lake but was not found in the 2014 survey (HRC, 2014). The driver of lake weed growth is a result of the external load of nitrogen entering the lake (Gibbs & Quinn, 2012). Nitrogen levels in the lake reduce to zero during weed growth and presence (in spring and summer) (Gibbs & Quinn, 2012). Lake weed harvesting was expected to begin in 2018 to improve nitrogen concentrations, algal blooms, and sedimentation, however, this is yet to begin (HRC, 2017).

Monitoring and surveying of the aquatic native and pest species in streams that enter the lake have been carried out by Joy and Death (2002) and Curtis (1964). There have been few within-lake surveys, except for those carried out by Cunningham et al. (1953) and Tempero (2013). Six native fish species are reported to inhabit the lake: *Retropinna retropinna*, *Gobiomorphus cotidianus*, *Galaxias*, *Mugil cephalus*, *Anguilla australis*, and *Anguilla reinhardtii*, and their numbers do not appear to be affected by poor water quality (HRC, 2014). Freshwater ecologist, Dr Mike Joy, suggests that long-finned and short-finned eel (*Anguilla australis* and *Anguilla reinhardtii*) numbers and condition (e.g. smaller and fewer) are not comparable to nearby Nga Manu Lake, which is largely in a natural state (Chase, 2015).

Prior to the 1908 AD Land Drainage Act, Lake Horowhenua was thought to have an excessive stock of fish and invertebrates (Cunningham et al., 1953; Gibbs, 2011; MfE, 2001; White, 1998), which correlates well with oral tradition. Tempero (2013) studied the native and pest fish populations at Lake Horowhenua and concluded that the density of native fish populations was slightly below what would be expected for a coastal lake. The cause of this decline is thought to be a result of the weir at the Hokio Stream outlet reducing upstream migration, resulting in a reduction of diadromous species (Gibbs & Quinn, 2012; Tempero, 2013). This was confirmed when Tana and Tempero (2013) studied the abundant fish, *Retropinna retropinna*, and determined that the fish were not typical of diadromous populations. Tempero (2013) also found that eels were highly abundant, but eels larger than 1 kg were almost absent from the lake. Pest species have not been detected in large quantities.

Water quality

The earliest record of water quality data was published by Cunningham et al. (1953) and collected on 15 January 1949 AD. The study found that there was only light weed growth (*Potamogeton* sp.), no algal blooms, and good populations of fish. However, Lake Horowhenua is now hypertrophic (Burns et al., 2005). This is reflected by the lake's poor ranking as the 7th worst lake of the monitored lakes in New Zealand (HRC, 2014; Verburg et al., 2010). Clearance of coastal forest and wetland drainage, intensification of land use, urban expansion, stocking around the lake and subsequent riparian zone damage, and disposal of treated sewage at Makomako drain from 1952 to 1987 AD, has resulted in poor water quality, high turbidity, and cyanobacterial blooms and weed growth in Lake Horowhenua (Gibbs, 2011; HRC, 2014; MfE, 2001). Ecosystem disturbance by invasive fish (Gibbs, 2011), as well as the lake's shallow depth (Gibbs & Quinn, 2012) may have also contributed to the decline in water quality. However, pest species surveyed in 2013 AD were well below that which would result in negative environmental impacts (Tempero, 2013).

As a first step in remediating Lake Horowhenua, the disposal of treated sewage that began in 1952 AD (Chase, 2015) was halted in 1987 AD (Vant & Gilliland, 1991). Water quality and phosphorus loads indicated that the lake had begun to recover between 1988 and 2000 AD. The sudden decrease of total phosphorus post-diversion of the sewage has been suggested to have occurred due to rapid sedimentation rates within the lake during recent times, locking and burying phosphorus in the sediment (Gibbs, 2011). However, post 2000 AD, the water quality declined once again due to intensification of dairying and market gardening in the catchment (Gibbs, 2011; Gibbs & Quinn, 2012).

During the 1970s and 1980s AD, the water quality of Lake Horowhenua was sporadically monitored (Gilliland, 1978, 1981) until a regular monitoring program was started in 1984 AD (Vant & Gilliland, 1991). Gilliland (1978, 1981) was the first to report that the lake has a seasonal nutrient cycle, with high phosphorus concentrations in summer and high concentrations of nitrogen in winter. This was later confirmed by White et al. (1991) and Gibbs and White (1994). They also found that, in Lake Horowhenua, phosphorus limits algal growth during winter and nitrogen limits growth in summer.

From 1998-2009 AD, Horizons Regional Council (and its predecessors) collected and analysed monthly water quality indicator samples from the lake as a duty of their 'State of the Environment' monitoring (Verburg et al., 2010). An intensive monitoring programme was carried out in 2008 AD over a 6-month period (Gibbs, 2011). The recent data confirms that seasonal cycling continues, and that the summer algal blooms are being triggered by the release of dissolved reactive phosphorous as a result of weed bed collapse in late summer (Gibbs, 2011). A buoy was deployed in Lake Horowhenua and has been operational since July 2013 (HRC, 2014). The buoy collects monthly water quality data. Regular stream monitoring was established in December 2013 (HRC, 2014) and continues today (HRC, 2017).

Sedimentation

Preliminary studies on sedimentation at Lake Horowhenua suggest that the lake has been receiving large volumes of sediment derived from overland flow over farmland and parts of Levin (HRC, 2014). A comparison of total phosphorus profiles from sediment collected in 1971 and 2011 AD suggest that the lake was being infilled at a rate 10 mm per year (Gibbs, 2011). This has reduced the maximum water depth from over 2 m to around 1.6 m at present (Gibbs & Quinn, 2012). This agrees with Brougham and Currie (1976) who estimated that the entire lake surface receives 232 kg/day of sediment. Using this dry sediment weight, Gibbs (2011) calculated that the centre of the lake could accumulate around 10 mm per year. This sedimentation rate is high; however, it is plausible to occur in the centre of the lake with high suspended sediment loads

entering the lake, in addition to a redistribution of in-lake sediments (Gibbs, 2011). Gibbs and Quinn (2012) estimated that the lake has in-filled by 40 cm since 1950 AD. This was later confirmed by a sediment legacy study (Table 2) which indicated the lake has received 33 cm of sediment since 1942-1962 AD (HRC, 2018).

cm	years AD	SAR (mm y ⁻¹)
0-1.5	2015-2018	6.2
1.5-3.5	2012-2015	5.9
3.5-10	2000-2012	5.8
10-15	1991-2000	5.2
15-30	1962-1991	5
30-40	1942-1962	4.9

Table 2: Sediment accumulation rates (SAR) from a coring site near the buoy (adapted from HRC, 2018).

Sediment is received into the lake from fine soil particles and stream bed erosion (Gibbs, 2011). Plant matter and cyanobacteria also settle on the lake bed, contributing to sediment build-up (MWRC, 2008). In the past, sewage discharge contributed to sediment build-up, but was unlikely a major source (HRC, 2018). In addition, the weir at the Hokio Stream outlet eliminates the lake's ability to effectively flush suspended sediment and nutrients (Gibbs & Quinn, 2012). The presence of pond weed exacerbates this problem by the slow-down of water movement and increased sediment deposition (HRC, 2014). A sediment trap at Arawhata Stream has recently been completed. This aims to reduce the annual load of sediment entering the lake by 50% and phosphorous by 25% to 30% (HRC, 2017).

2.7 Literature review

2.7.1 Introduction

This section serves as a scientific basis for this research and contains important background information and pertinent literature on lake-based paleoenvironmental reconstructions. The first part focuses on the principles of paleoenvironmental reconstructions relating to reference conditions and a review of anthropogenic environmental change studies in New Zealand. The second part reviews natural disturbance, human arrival in New Zealand, and lastly human influences and evidence of impacts to lakes and surrounding environs.

2.7.2 Measuring baseline conditions and establishing reference conditions

Humans have undoubtedly triggered enormous change to environmental systems. It has now become clear that there is a need for environmental management and mitigation and, in some

cases, restoration. However, in recent years it has been recognised that knowledge of the baseline (natural) conditions are needed to determine restoration targets (Bennion et al., 2011; Bennion et al., 2015; Dearing et al., 2006). These are often referred to as ‘reference conditions’. Indeed, assessing an ecosystem such as a lake will return a variety of natural conditions as these environments are not static and change in response to internal and external processes (Smol, 2008; Woodward & Shulmeister, 2005).

Reference conditions may, therefore, be considered as those which existed prior to any human presence in the catchment, prior to the Industrial Revolution, or prior to the period in which human disturbance became significant (Bennion et al., 2011). The choice of which set of conditions to use as a benchmark is guided by cost, the ability of the system to be restored, and physical parameters both current and past. For example, it may be impossible to reverse certain processes occurring in the post-human period, such as changes in climate conditions and lake depth which have resulted in some deterioration of the lake. Ideally, reference conditions would be those that existed at the point prior to which human impact became significant (Bennion et al., 2011; Bennion et al., 2015). Bennion et al. (2011) suggest that reference conditions should be a benchmark rather than a target. In addition to informing restoration efforts, this baseline data can be used to compare and assess the extent of degradation. However, not all degradation during the human era can be attributed and separated from natural variability and managing and mitigating against these factors may be difficult. This type of change is discussed further in the following sections.

Extensive records of environmental history are obtained via coring of sedimentary records of lakes, bogs, estuaries, and continental shelves (Smol, 2008). These sediment records often not only capture paleoenvironmental change, including formation of the ecosystem, but also historical and modern change that can be supplemented by anecdotal evidence and modern monitoring schemes (Woodward & Shulmeister, 2005). Paleolimnological studies are used not only in New Zealand but in other parts of the world. In the Northern Hemisphere, pollen records have long been used to investigate natural and anthropogenic change to vegetation (e.g. Shennan, 2009). Detailed multi-proxy studies are now routinely used, allowing for the reconstruction of biological, chemical, and sedimentological change, and thus the development of reference conditions (Bennion et al., 2011; Bennion et al., 2015). A wide range of different environmental proxies and paleolimnological methods are available to reconstruct past environments captured in lake sediments, some of which are chosen for this study and are described further in the methodology chapter.

In New Zealand, most studies that address environmental change associated with human arrival focus on vegetation change (e.g. Bussell, 1988; Newnham et al., 1995; Wilmshurst et al., 1997) in conjunction with charcoal flux and sedimentological information. Fox (2016) compiled a table of sites where disturbance studies have been carried out in the North Island. Of the 66 sites assessed, 40 analysed pollen and charcoal only. It appears that there are few detailed studies that assess ecological, geochemical, and sedimentological change to establish reference conditions. However, as an example; a detailed multi-proxy study with the aim of aiding restoration efforts has been carried out by Cochrane (2017).

Cochrane (2017) reconstructed environmental change at Lake Pounui in Southern Wairarapa using pollen, diatoms, bacterial DNA, grain size, XRF, and loss-on-ignition. She found that the pre-human environment in Lake Pounui had varying nutrient contents, and catchment disturbance occurred due to earthquakes and storms. Post-Polynesian arrival, water quality remained high. Following European arrival, nutrient enrichment resulted in algal blooms. Cochrane (2017) also assessed which of the reference conditions would be the best restoration target by squared chord distance dissimilarity measure (SCD). Based on these statistics, 200 cal yr BP was the more realistic restoration target, as this was the time at which the lake had low productivity and where climate and physical conditions were similar to present-day conditions.

2.7.3 Natural variability

In order to outline appropriate reference conditions, it is vital to understand pre-human natural variability and to be able to separate the pre-human environment from the anthropogenic environment (Smol, 2008). Separation is usually achieved via age control and independent evidence of human arrival. However, natural variability and human-induced change are often intertwined during the so-called ‘Anthropocene’ (Fig. 5). The Anthropocene is a proposed geological era which encompasses the time period in which humans began to severely impact the environment (Bostock & Lowe, 2018; Fuller et al., 2015). In New Zealand, this is thought to have been initiated 1800 AD (Steffen et al., 2007), or the mid-20th century (Bostock & Lowe, 2018; Fuller et al., 2015; Waters et al., 2014).

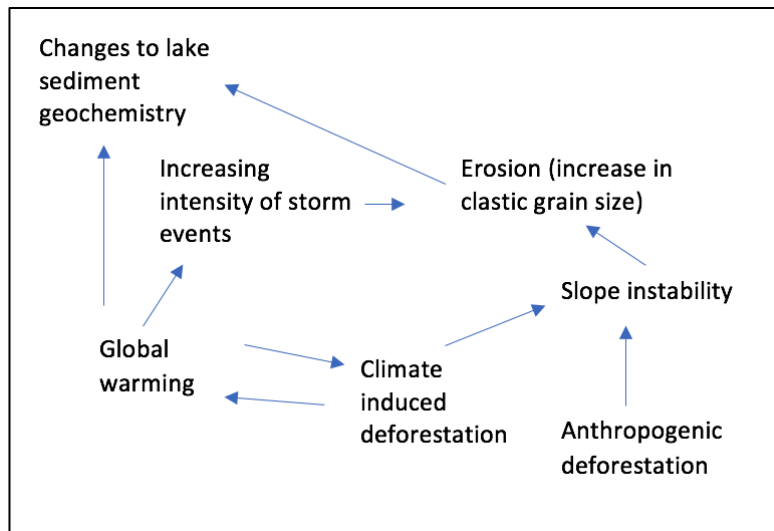


Figure 5: Factors that can influence erosion and clastic grain size, and sediment geochemistry in lake sediment records.

Natural variability comes about via a variety of mechanisms. For example, vegetation in New Zealand has been influenced by changes in climate, such as variations in temperature, drought, and fire (McGlone et al., 1992; Moar, 1967; Newnham, 1992; Newnham et al., 1998b; Newnham et al., 1989; Ogden et al., 1998; Wilmshurst et al., 2008).

Long-term climatic adjustment after the end of the last glaciation saw an increase of *Fuscospora* in the Kaimanawa, Kaweka, and Ruahine Ranges at the expense of the Podocarpaceae community (McGlone, 1989). A possible increase in the Southern Annular Mode (SAM), Walker Circulation, and El Niño-Southern Oscillation (ENSO) (Gomez et al., 2004) is purported to be responsible for driving a decrease in frost and drought sensitive species such as *Ascarina lucida* between 4,000-3,000 ya (McGlone & Moar, 1977; McGlone et al., 1993). New Zealand is particularly susceptible to climatic shifts due to its location near the westerly wind belt and its position in the Southern Ocean (Alloway et al., 2007).

One of the more ambiguous signals within Holocene records is that of fire, in that fires can be both natural and anthropogenic in origin. The fire record in sediments represented by charcoal flux, suggests that fire also occurred in pre-Holocene New Zealand, as well as throughout the Holocene (Butler, 2008; McGlone & Wilmshurst, 1999; Newnham et al., 1998b; Ogden et al., 1998; Wilmshurst et al., 1997).

During the period of 7,000-3,000 yr BP, fire events increased on the eastern part of both islands (Ogden et al., 1998; Perry et al., 2012a), although these burn events were rare, at around 1-2

events/millennia (McGlone et al., 1992; Rogers & McGlone, 1989). Post-3,000 yr BP, records of ENSO frequency (Moy et al., 2002) suggest that El Niño events became more frequent. This would have resulted in more frequent drought conditions in the eastern parts of both islands, predisposing the vegetation to ignition by lightning strike, and is recorded in the record as a further increase in charcoal during this period (Ogden et al., 1998). However, low rates of lightning strike occur in New Zealand (Christian et al., 2003), as storms are often accompanied by wet fronts (Ogden et al., 1998). It is suggested that this charcoal may be derived from fires in central Australia (Clark & Royall, 1995), as these particles are frequently small (<20 µm) (Butler, 2008). This is further evidenced by charcoal flux being coincident with an influx of *Casuarina* pollen, a common dryland Australian tree (Sutton et al., 2008).

The situation on the western coast of New Zealand is different, where natural fire is much rarer due to the considerably moister climate (McWethy et al., 2013), and ignited fires are largely self-extinguishing (Sutton et al., 2008). Thus, regular fire in dense forest in these regions is likely to be anthropogenic (Vandergoes et al., 1997; Wilmshurst et al., 1997).

Vegetation disturbance can also be caused by volcanism, which can ignite forest via hot ejected material, or cause synchronous dieback from volcanic blast wave, acid rain, or smothering from ash fall (Ogden et al., 1998). At Kaipo Bog, vegetation was reverted to a successional community on several occasions post-eruption from the Taupo Volcanic Zone, New Zealand (Newnham & Lowe, 2000). Similarly, it has been suggested that the volcanic disturbance at Otamangakau wetland, located close to the Taupo Volcanic Zone and Tongariro Volcanic Centre, may mimic climatic cooling (Alloway et al., 2007). This is not reviewed further, as volcanic eruptions during the Holocene are not thought to accompany any vegetation changes as far south as the Horowhenua district (MacDonald-Creevey, 2011).

As a further example, the short-term disturbances in tree pollen at Lake Waikaremoana may relate to both tectonic and climatic changes, such as gale force storms (Grant, 1963), heavy snowfall, landslides due to tectonic events or rainfall, lightning, and tephra fall (Newnham et al., 1998a). A different situation can be used to describe the change captured at the Waikato lowlands. Peaks and troughs of *Dacrydium cupressinum*, a canopy species, are due to ecological control. *D. cupressinum* emergents are more susceptible to damage from gale force storms, allowing other canopy competitors to emerge (Newnham et al., 1989). This, in turn, increases the susceptibility of the entire forest to fire during dry summers (Newnham et al., 1989).

In summary, a variety of natural mechanisms can be responsible for change captured in the sediments of lakes. The natural variability discussed here largely relates to mechanisms that result

in vegetation change, some of which may be short in duration or last thousands of years. However, many other mechanisms may be responsible for change captured in lake sediments. Geochemical changes, and sedimentation rate and clastic grain size increase, may result from regional or catchment-wide dynamics such as storms and floods that deliver clastic material to a lake (Augustinus et al., 2008; Augustinus et al., 2012; Lowe & Walker, 2014). These erosion events may introduce nutrient-rich sediment to the lake and result in increased productivity, which is captured as changes in elemental concentrations (Boyle, 2002) and bacterial DNA (Cochrane, 2017).

2.7.4 Human arrival in New Zealand

Polynesian arrival in New Zealand

New Zealand is thought to have been colonised by settlers from Polynesia (Penny & Murray-Mcintosh, 2002), and is one of the last landmasses to have been colonised prior to the Industrial Revolution (Hogg et al., 2002; Matisoo-Smith, 2016). The timing of colonisation by Polynesian settlers in New Zealand has been the subject of much debate, with three lines of thought: the long, the intermediate, and the short prehistory spanning: ~2000 years (Davidson, 1987; Holdaway, 1996), ~1000 years (Anderson, 1991; Spriggs & Anderson, 1993), and ~600 years (McGlone & Wilmshurst, 1999).

The long prehistory was largely based on radiocarbon dates on *Rattus exulans* bones (Holdaway & Beavan, 1999; Holdaway, 1996, 1999), which produced ages of 50-150 AD. Additionally, the discovery of *R. exulans* bones beneath the Taupo Tephra $1,717 \pm 13$ cal yr BP (Lowe et al., 2008) was used to further support this hypothesis (Yaldwyn, 2002). *R. exulans* is commensal with humans and thus its presence is also taken to indicate the presence of humans.

Published pollen diagrams, and data on charcoal and *Pteridium* from various bogs and lake sites in New Zealand, such as Lake Poukawa (McGlone, 1978), Lake Tūtira, and Lake Rotonuiaha (Wilmshurst, 1997), suggest various dates for Polynesian colonisation, ranging from 1,900 to 1,450 cal yr BP (McGlone & Wilmshurst, 1999). Sutton et al. (2008) purported that increases in *Pteridium* values between 1,933-860 cal yr BP, and increases in charcoal values between 4,400-3,100 cal yr BP, are possible evidence for anthropogenic disturbance in the landscape.

However, this evidence is weak and unconvincing, primarily due to the lack of any other supporting evidence at the sites where this early disturbance supposedly occurred. For example, there is no archaeological (Anderson, 1991; Higham et al., 1999; Higham & Hogg, 1997; McFadgen, 1994, 1997) or macrofossil evidence, such as rat-gnawed seeds dating to this time (Wilmshurst et al., 2008), suggesting that the cause of the disturbance was not human.

Additionally, radiocarbon dating of rat bones and bulk sediment (McGlone & Wilmshurst, 1999) are thought to contain significant errors (Beavan-Athfield, 2006; Beavan & Sparks, 1997; Higham et al., 2005). The most widely accepted date of colonisation by Polynesian settlers is 1250–1300 AD (Higham et al., 1999; Higham & Hogg, 1997; Hogg et al., 2002; McFadgen, 1994; Ogden et al., 1998; Wilmshurst et al., 2008), which coincides with the Kaharoa marker tephra 636 ± 12 cal yr BP (Lowe et al., 2008).

Furthermore, human mitochondrial DNA concurs with the idea of a single migration from central Polynesian, with a minimum of 70 females (Murray-McIntosh et al., 1998) and up to 190 females (Whyte et al., 2005). This is consistent with oral traditions of planned voyages using waka (canoe). Oral histories speak of the arrival of seven named waka to New Zealand from Hawaiki (a mythical land) or Polynesia. Kupe (a chieftain) is said to have arrived first, sometime around 925 AD (Simmons, 1969) on the Matahourua, then later Whatonga (another chieftain) on the Kurahaupo 1300-1505 AD (TMPR, 2017).

Human arrival in the Horowhenua district

A mixture of older and newer oral traditions can be used to describe the arrival and origin of Muaūpoko, the tangata whenua (original inhabitants) of the lake and surrounds (TMPR, 2017). A well-known Māori legend describes the fishing up of Te Ika a Maui (North Island) by Maui-tikitiki-a-Turanga and may be a figurative way of describing the discovery of the North Island (Adkin, 1948). Māori mythology also speaks of a people, referred to as Muatetangata, that originated from the land itself and have been in the lower North Island since time immemorial (TMPR, 2017). The name Muaūpoko is said to mean “the front of the head” and may describe the geographical location within Te Ika a Maui or be a reference to the Muatetangata people (Chase, 2015). Other oral histories describe the colonisation of New Zealand via waka. It is said that descendants of Whatonga, settled in the lower half of the South Island and top of the North Island (WRC, 2018). Others advocate that they are descendants of the earlier waka captained by Kupe (TMPR, 2017; J. Procter *pers comm*, 2018).

It is thought that people arrived in the adjacent Wellington region around 1319 AD (McFadgen, 1994). Forest clearance in the Horowhenua district began at the time of human arrival, but this influence was not marked until ~400 cal yr BP (McFadgen, 1994). Of interest are artefacts and hunted moa bones found on Old Waitarere Phase dunes which suggest that these are rather “late” in New Zealand’s prehistory. However, the artefacts and bones may relate stratigraphically to older dunes that were later buried by dunes of the Old Waitarere Phase (McFadgen, 1997).

Artefacts found in the dune belt, the bottom of Lake Horowhenua, and in swamps, form one of the most extensive collections in New Zealand (Adkin, 1948; McFadgen, 1997; Rolston, 1944, 1947, 1948). These items offer an important insight into Māori life, however, accurately dating them is not achievable due to a lack of knowledge of the source site and contamination potential (McFadgen, 1997). The closest sites to Lake Horowhenua dated thus far are at Paekakariki, Foxton, and Himatangi (McFadgen, 1997).

At least nine kāinga (villages) and pā (defensive settlement) were built near the shores of Lake Horowhenua, and six or seven pā were built on artificial islands in the lake as protection (Chase, 2015). Kumara storage pits were also found west of Lake Horowhenua. At least 70 middens have been located between Lake Horowhenua and the sea. Moa bones and gizzard stones found west of Lake Horowhenua and in natural deposits confirm moa hunting occurred in the area (Adkin, 1948; McFadgen, 1997), and is likely one of the reasons for forest clearance by fire.

2.7.5 Anthropogenic influences and evidence of impacts on lakes and surrounding environs in New Zealand

Human activities post-settlement can result in significant changes to the natural environment. Immediately prior to human arrival, 85-90% of New Zealand was covered with forest, and only 15% of the South Island and 1.5% of the North Island was above the timberline (McGlone, 1989; McWethy et al., 2010). The arrival of Polynesian settlers and deforestation by fire to modify the landscape in New Zealand was not unique and occurred on many islands in the Pacific (Hughes et al., 1979; Kirch, 2005; Rolett & Diamond, 2004). Human-induced ignition began at the time of arrival and peaked at 700-500 yrs BP (Ogden et al., 1998). Clearing on both Islands is thought to have occurred around the same time (Ogden et al., 1998), and the shift from forest to scrubland may have occurred within decades at drier sites (McWethy et al., 2014). Largely, the New Zealand forest was not adapted to fire; having evolved in a humid climate, very few species could survive the onslaught of fire (Anderson & McGlone, 1997).

During colonisation, fire was limited by rainfall and topography (McGlone, 1983). In the South Island, it is proposed that ignitions were targeted in areas with high flammability during years of favourable climate, which may have enhanced a positive feedback (Perry et al., 2012b). Limited clearance could be carried out where the rainfall was below 1,600 mm/a or in easily accessible areas (McGlone, 1983), and eastern areas of both islands were cleared before the wetter western areas (Ogden et al., 1998). Areas close to large lakes and rivers, and accessible portions of the coastline, were cleared first as these contained important sources of food (McGlone, 1983, 1989). The vegetation may have been cleared for timber for pā and whare (house) construction, fuel, horticulture, hunting of moa (Anderson, 1989; Sutton et al., 2008), and to encourage *Pteridium*

to grow. *Pteridium* served as an important carbohydrate source (Bussell, 1988; McGlone et al., 1994; McWethy et al., 2010) and was used as material for fishing nets (McGlone et al., 1994). The response to fire differed regionally, and in some sites grassland and *Pteridium* persisted due to slow forest regeneration (McGlone, 1983; McGlone et al., 1994). In the North Island, *Pteridium* is prominent post-fire clearance due to a more temperate climate, and regrowth after disturbance may be rapid (McGlone & Wilmshurst, 1999).

As mentioned previously, these changes in the landscape during Polynesian settlement are captured within lake sediment. Polynesian arrival in New Zealand is represented by a common pattern of vegetation change in sediment records, whereby pollen of indigenous arboreal species declines, concurrent within an increase in charcoal particles, indicating clearance of forest by fire. This is followed by an increase in spores of *Pteridium* along with pollen of other successional species such as *Weinmannia racemosa*, *Coriaria*, *Coprosma*, *Leptospermum scoparium*, Poaceae, and *Typha* (McGlone et al., 1994; McGlone & Wilmshurst, 1999; McWethy et al., 2010; Sutton et al., 2008).

Prior to European settlement in c. 1840 AD, around 40-45% (McGlone, 1983; McGlone & Wilmshurst, 1999; McWethy et al., 2010; McWethy et al., 2009) of New Zealand forest had been cleared on the plains and easily accessible areas (Glade, 2003). Today, forest covers 10% of the North Island and 60% of the South Island (Ogden et al., 1998).

European settlement coincided with a further increase of deforestation by fire and the introduction of exotic species, such as *Pinus radiata*, *Cupressus macrocarpa*, *Salix*, and many Poaceae species (Newnham et al., 1998a). The occurrence of *Pinus radiata* pollen in lake sediment records has been used in many studies to identify the arrival of Europeans (e.g. MacDonald-Creevey, 2011; McWethy et al., 2010; Wilmshurst et al., 1999; Wilmshurst et al., 1997). *Pinus* was first introduced to some places in New Zealand in the late 1850s AD (Yearbook, 1990). *Pinus* pollen can travel vast distances (Green et al., 2003) and is seen in some records around 25 years after introduction (Woodward & Shulmeister, 2005), allowing for it to be used as a reliable signal for European arrival. In some pollen records, two phases of European influence are defined (Wilmshurst, 1997). The first phase is evident by introduced pollen species, the decline in Podocarp pollen, and the stabilisation of *Pteridium*. The second phase consists of a rapid increase in Poaceae and *Pinus* pollen, and a decrease in *Pteridium* spores.

Deforestation following human arrival had a substantial impact on the rate of erosion and sedimentation into waterways due to the reduction of the soil holding capacity of roots (Pawson & Brooking, 2002). In lacustrine records, this is typically shown as a shift to larger mean and

median grain size of clastic sediments, increased sedimentation rates, a reduction of organic matter, and changes to element concentrations, e.g. aluminium and titanium (Augustinus et al., 2008; Augustinus et al., 2012; Cochrane, 2017; Lowe & Walker, 2014; McWethy et al., 2010; Trodahl, 2010). In some lakes, an increase in organic matter is evident post-human arrival as a result of more frequent eutrophic conditions (e.g. Page et al., 2010). Eutrophic conditions (McColl, 1978) can result from increased nutrients used for the fertilisation of pasture (Zabowski et al., 1996), but also due to erosion of nutrient rich soil organic matter (Issaka & Ashraf, 2017). The increase in erosion from the catchment may also alter the carbon to nitrogen ratio of the sediments. This is due to the differences of the ratios of carbon to nitrogen between soil organic matter, terrestrial plants, aquatic plants, and algae (Meyers & Teranes, 2002).

Erosion events may, in turn, be amplified by weather extremes related to natural phenomena or anthropogenic climate change (Moss et al., 2011). For example, trophic status may be altered as a result of sediment release of nutrients in response to warming temperatures (Cochrane, 2017; Søndergaard et al., 2003). These changes cannot easily be separated from other events, such as land use change and the introduction of exotic aquatic species.

2.7.6 Summary

It is clear from this literature review that there is a need for multi-proxy studies on lacustrine environments to understand the full history and impacts of humans on the environment. Paleolimnological techniques offer a way to expand upon modern monitoring and to assess pre-human variability and human impacts. Furthermore, from this literature review, it is apparent that Lake Horowhenua is in a declining state. An environmental record from Lake Horowhenua would enable expansion upon modern monitoring schemes and provide key data for current and future restoration efforts. Additionally, there has not been an in-depth study of the lakes in the Horowhenua and Manawatū districts; therefore, this study will also add to the archive of Holocene environmental change studies.

Chapter 3: Methodology

3.1 Coring

Preliminary long and short cores were collected and radiocarbon dated by Massey University and NIWA staff in October and December 2016 before the commencement of this MSc project. A total of 10 long cores (Horo 1-9) and 19 short cores (A-R) were collected during this first sampling phase (Fig. 6). The site for collection of the main core, used as the basis of this thesis, was chosen based on the results from this preliminary coring phase. While cores extracted from near the lake outlet (cores Horo 1, 2, 8, & 9a, Fig. 6) obtained the greatest total thickness of sediment, the central part of the lake (in the vicinity of Horo 3) was deemed the most appropriate for the aims of this study. Preliminary coring showed that this region had the greatest thickness of lacustrine sediment and was away from the outlet, whereas the cores near the outlet contained pre-lake sediment at the base. Also, coring away from the outlet avoided any risk of stream currents thinning the sediment sequence. However, regardless of the actual sampling site, analysing sediments from shallow lakes, such as Lake Horowhenua, can pose some difficulties due to the lack of an accumulation zone, sediment resuspension, and mixing (Anderson & Odgaard, 1994).

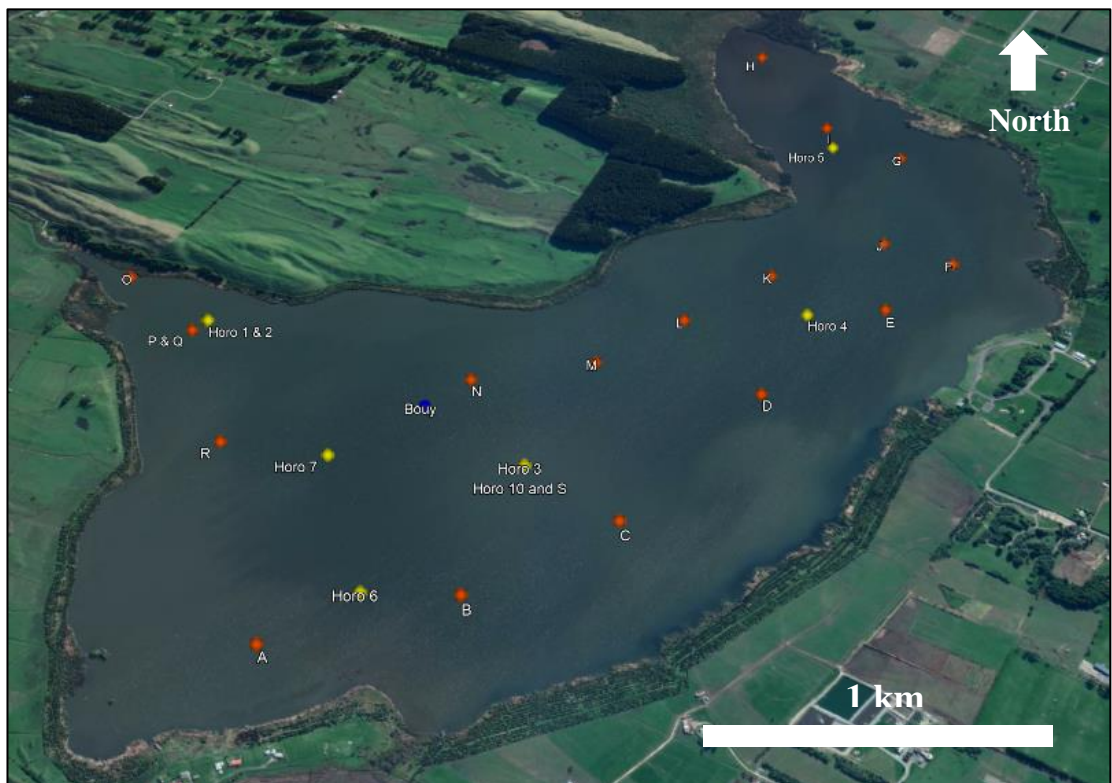


Figure 6: Coring locations (Google Earth, 2018).

Long cores, (including Horo 10) were collected using a modified Livingstone piston corer (Livingstone, 1955; Fig. 7A) operated from a raft secured by three anchors. The Livingstone piston corer contains a core barrel, a piston connected to a wire, and a core head at the penetration end (Livingstone, 1955). Extension rods were added with each successive core drive.

The master core used in this project, Horo 10, was collected on 20 July 2017 at 40°36'44.87"S 175°15'6.47"E, approximately in the middle of the lake. Accompanying short cores were collected at the same time and location (denoted short core S). The first drive of core Horo 10 began at 10 cm above the sediment-water interface to ensure that the sediment-water interface was sampled. Thus, the first drive penetrated 90 cm into the sediment. The subsequent core drives were taken at 1 m intervals. After the sediment was collected it was extruded on the raft into PVC cases (Fig. 7B). Four core drives were taken, totalling 3.9 m. A fifth drive was attempted, however, considerable difficulty in penetrating the sediment was experienced. Force was applied via a hammer, but did not produce any further penetration, and the corer was subsequently winched out (Fig. 7C), revealing blocking of the end by gravel. The core penetrated 47 cm, however, extrusion was impossible, as the gravel blocked the core head and approximately 20 cm of sediment was lost.

The Livingstone corer has difficulty in retaining the upper looser sediments, as these are typically lost or significantly disturbed during extrusion. Therefore, the upper sediments and the sediment-water interface were also sampled using an HTH gravity corer attached to a line (PYLONEX, n.d.; Fig. 7D & E). The HTH gravity corer is an open barrel corer. When lowered into the sediment and maximum penetration is reached, the line goes slack, triggering the top to snap shut. Two cores were taken at this site, with the corer penetrating 28 cm and 30 cm. All cores were transported back to Massey University where they were sealed, labelled, and refrigerated horizontally at 4 °C until sampling.

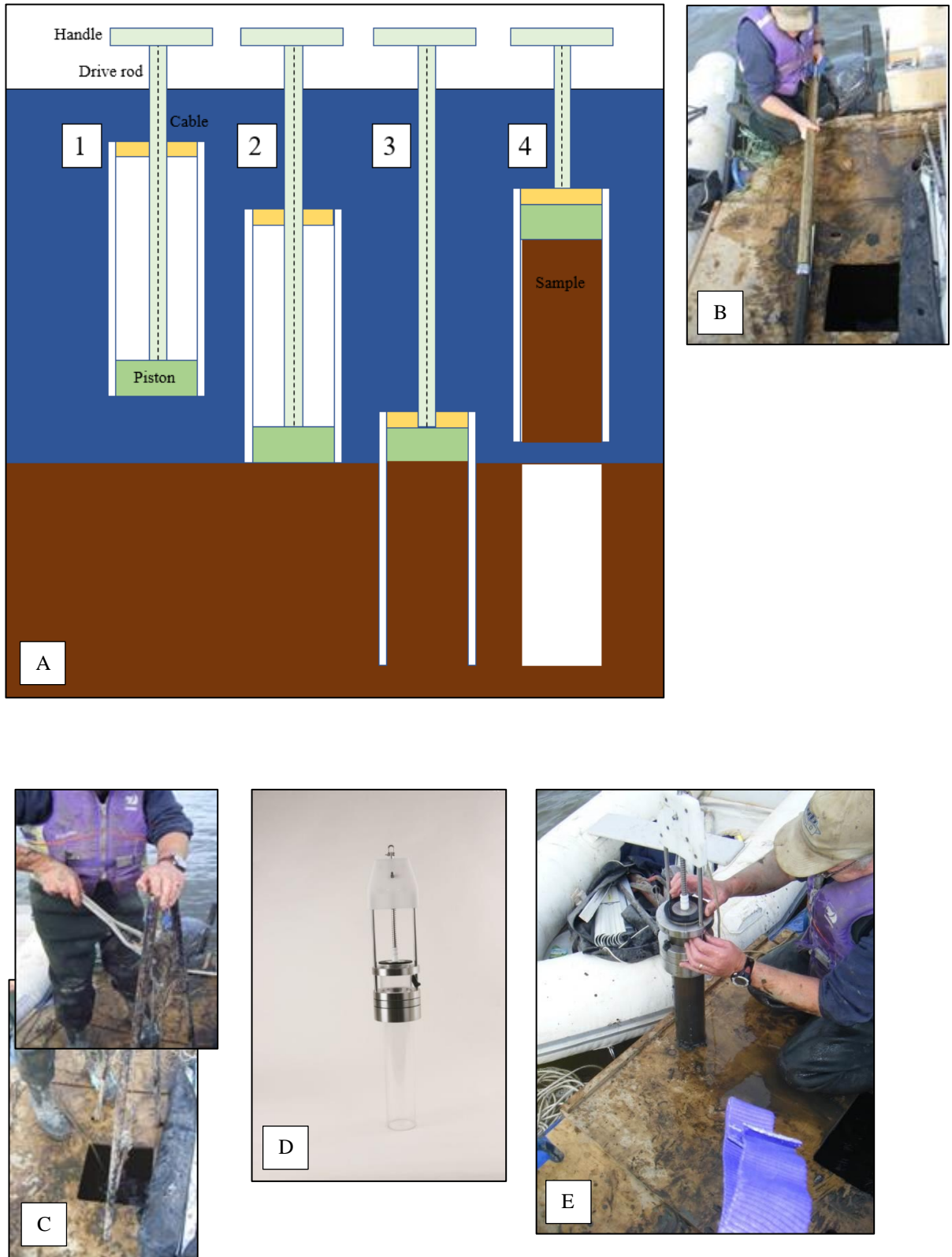


Figure 7: (A) 1-4 The corer at different snapshots during the sediment collection process. (B) Extruding the sediment into a PVC liner. (C) The winch system used to remove the corer from the sediment. (D) Example of the gravity corer used at Lake Horowhenua (PYLONEX, n.d.). (E) Gravity corer about to be plugged.

3.2 Sand deposit

While this thesis concentrates on the record captured in Horo 10, one key aspect of some of the other cores collected prior to the commencement of this project were deemed worthy of further investigation. Upon stratigraphical analysis of all long cores, a conspicuous sand layer was found in cores taken from near the outlet (Horo 1, 2, 8, and 9a; Fig. 8). Previous radiocarbon dating of bulk sediment above this layer by the supervisory staff yielded an age of 7245-7006 cal yr BP (WK-44667).

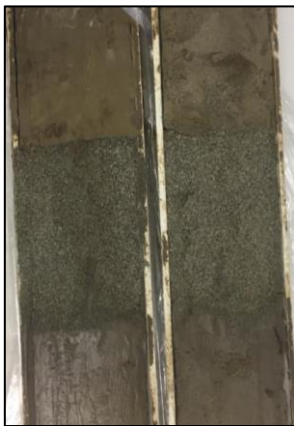


Figure 8: Image of the sand layer found in a core taken from near the outlet.

This sand layer lies near the inception of lacustrine sediment within these westerly cores, and thus it possibly relates to the early stages of the formation of the lake. Hence, it has been investigated further. Several possible scenarios may explain the deposition of the sand, namely: dune transgression or mass movement of the dunes after an earthquake, alluvial/flood deposit, tidal surge and/or tsunami, and marine transgression.

To determine the most likely origin of the sand layer, grain size analysis and componentry of mineral constituents was carried out on the core sand, as well as on beach sand collected from Hokio Beach and inactive Foxtan Phase dune sand from near Lake Horowhenua. Sand was also collected from the Ohau River, these were: overbank (OB) deposits and sand from a quiet spot in the river. Hand sieve grain size analysis was conducted using the <63-710 μm fraction in half phi intervals. Point counting to identify the proportion of mineral constituents was carried out on the >250 μm , >125 μm , and >63 μm size fractions in full phi.

Data processing

To determine any similarities between the samples, descriptive statistical analyses and graphical measures were carried out using GRADISTAT 8.0 (Blott, 2010). Sorting, skewness, and kurtosis were examined using Folk and Ward (1957) calculations. Sorting is related to the standard deviation, skewness describes the distribution of the sample, while kurtosis measures the ratio of sorting in the tails and sorting in the centre of the distribution (Last, 2002). Stacked bar graphs were plotted to examine changes in the different grain size categories and the mineral constituents.

3.3 Core stratigraphy

Once back at the laboratory, Horo 10 (hereinafter where appropriate referred to as ‘the core’) was split in half lengthways and photographed. One half was selected as the working half and the other half for archive. Prior to any analysis, the 3.9 m core was described using the modified Troels-Smith system (Kershaw, 1997) and the description was used to develop stratigraphic logs. The core was X-rayed at the Massey University School of Veterinary Sciences Radiography facility. The radiographs did not reveal any obvious stratigraphy within the cores and indicated the remarkable homogeneity of the sediments. The option to apply computed tomography (CT) scanning had been considered, however, based on the X-rays revealing a lack of any structure, the CT scanning did not proceed.

3.4 Chronology

3.4.1 Radiocarbon dating

Radiocarbon dating was applied to provide temporal control over the core sediments. The core was inspected for terrestrial plant macrofossils, as these represent ideal material for radiocarbon dating (Philippsen, 2013). For example, seasonal organs such as seeds and leaves represent a very short period of growth and should, therefore, represent a precise age. Unfortunately, due to the homogenous nature of the sediments, very little macrofossil material was found except for a single seed (of unknown species) found at 85 cm (Fig. 9A), which was dated. A periostracum (outer skin) of an *Echyridella sp.* (freshwater mussel) was found at ~380 cm, and scattered remains of aquatic plant were also found in the upper sediments. These were not dated, as they do not obtain carbon directly from the atmosphere.

As a result, bulk sediment samples were sieved through 120 µm cloth with distilled water and inspected under a binocular microscope to identify any smaller sized fractions that might be useful for dating. Numerous specimens of Cladocera ephippia were encountered. Ephippia are dry season embryos of the small crustaceans known as Cladocera (Fig. 9B) (Smirnov, 2014). Enough of these ephippia were able to be concentrated to form a sample for dating. However, given that Cladocera draw their carbon from within the lake environment, it is possible that they may

produce a reservoir effect. In order to test the likelihood of a reservoir effect in this fraction, a separate sample of Cladocera ehippia and bulk sediment were submitted for dating from a similar depth as the seed (80-90 cm range), with the assumption that the seed would return an accurate age. Lake margin plant material extracted from the bulk sediment sample was tentatively identified as *Phormium* (NZ Flax) and was also dated. In addition, a modern sample of Cladocera ehippia was dated.

The method of determining a lake water reservoir age by comparing the ages of Cladocera to a terrestrial sample has been used at other sites (e.g. Avşar et al., 2014; Vandergoes et al., 2018). The method of determining bulk sediment contamination and comparison of lake margin plants to terrestrial samples is also a common approach (e.g. Philippsen, 2013). Samples were submitted to the Rafter Radiocarbon Laboratory at GNS Science, New Zealand.

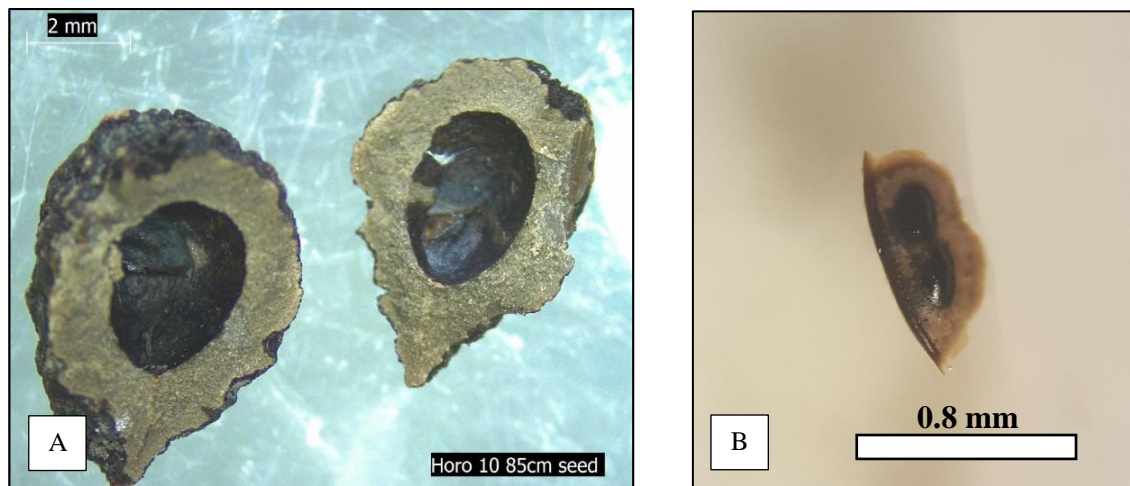


Figure 9: (A) Seed submitted for radiocarbon dating (GNS, 2018). (B) Cladocera ehippia.

Procedure

To obtain Cladocera ehippia for dating, samples of bulk sediment were sieved through 120 μm cloth with distilled water. Ten cm worth of sediment was sieved to ensure adequate remains were found. Cladocera ehippia were then picked from the $>120 \mu\text{m}$ fraction. Sample depths were: 2-12 cm (NZA 65134), 80-90 cm (NZA 65136), 200-210 cm (NZA 65137), and 297-307 cm (NZA 65138).

The following process was carried out by the laboratory technicians at the Rafter Radiocarbon Laboratory: The Cladocera ehippia concentrate samples were wet sieved, any visible contaminants were picked out by hand, and the samples then sieved at 200 μm to remove cellular detritus and algae; The bulk sediment sample from 80-85 cm was sieved at 90 μm ; Cladocera

ephippia were removed, and then sieved again at 200 μm to remove cellular detritus and algae; The bulk sediment <90 μm fraction (NZA 65824) and Cladocera ephippia (NZA 65080) were dated separately; Plant material (possibly *Phormium*; NZA 65079) was also found at this depth (80-85 cm) and was pre-treated and dated; The seed (NZA 65135) was cleaned and cut and appeared free of contamination.

The initial dates returned by Rafter suggested a possible inversion of dates returned by two of the Cladocera ephippia samples (NZA 65137 and NZA 65138). Therefore, a further two samples of Cladocera ephippia (202-208 cm/NZA 65822 and 299-305 cm/NZA 65823) were dated at the Rafter Radiocarbon Laboratory. For this second set of Cladocera ephippia dates, 6 cm of sediment was chosen as the previous 80-85 cm (NZA 65080) result suggested that a minimum of 5 cm worth of sample was required for an accurate result. This gave a total of 10 radiocarbon dates obtained from Horo 10.

All samples were subjected to AAA (alkalai, acid, alkalai) pre-treatment, followed by combustion and graphitisation. For the bulk sediment, the insoluble organic and humin fraction was dated.

Data processing

Radiocarbon dates are reported as conventional radiocarbon age and calendar years before present (cal yr BP). Calibration to calendar years was performed by the Rafter technician (Jenny Dahl) using GNS Science calibration software WinsCal V. 6.0 adapted from Stuiver and Reimer (1993). Calibration to calendar years BP was done using the Southern Hemisphere offset (SHCal13) calibration data set (Hogg et al., 2013). Cladocera ephippia from 2-12 cm (NZA 65134) were calibrated using the SH Zone1-2 calibration data set (Hua et al., 2013) to account for the bomb effect. Reservoir ages were calculated in OxCal V. 4.24, using the difference between conventional radiocarbon ages (CRA) of the seed and the other material found at a similar depth, and calibrated using the SHCal13 data set.

Age-depth model

An age-depth model for the core was constructed using OxCal V4.24 (Bronk Ramsey, 2009) with the SHCal13 (Hogg et al., 2013) and SH Zone 1-2 calibration data sets (Hua et al., 2013). OxCal utilises Bayesian statistics to combine probabilistic age determinations using a prior model into a posterior probability. This allows for the determination of a likely age at any given depth (Vandergoes et al., 2018). A P_sequence (Poisson distribution) prior outlier model was chosen. The Poisson distribution model was chosen as this accounts for variation around a constant sedimentation rate. The model was constructed using four radiocarbon dates: NZA 65135 (seed), NZA 65134, NZA 65822, and NZA 65823 (Cladocera ephippia). Present day and European

arrival c. 1840 AD constrained via pollen indicators were also added to the model. Due to the resultant age differences between the seed (NZA 65135) and Cladocera (NZA 65136) from a similar depth, a correction of 448 ± 22 years was applied to NZA 65822 and NZA 65823 with the assumption that a reservoir age was apparent in these samples due to a strong linear relationship of NZA 65136 with NZA 65822 and NZA 65823 (Fig. 19 in results). Further details of the source of the reservoir age are addressed in the discussion (section 5.1). No reservoir age correction was applied to NZA 65134, as this returned a modern equivalent age. The bulk sediment (NZA 65824) and Cladocera ehippia (NZA 65136) were also plotted as outliers and not included in the model. Average sedimentation rates were calculated based on the output of the age-depth model.

3.4.2 Lead-210 and cesium-137 concentration dating

Radionuclides have a strong affinity for clay and mud, making measuring their concentration in lake sediments ideal (Sommerfield et al., 1999). Concentrations of atmospherically produced ^{210}Pb (lead) down a sediment profile can be used to calculate sedimentation rates at discrete intervals. The half-life of ^{210}Pb is close to 22 years, and background levels are attained at less than 100 years since sedimentation (Baskaran et al., 2014). Therefore, ^{210}Pb concentrations down a profile can be used to determine the age of young sediments as well as sedimentation rates.

Cesium-137 concentration can also be used to infer age. A sharp peak of ^{137}Cs (cesium) coincides with the nuclear fallout peak associated with nuclear testing in 1963 AD, while initial detection of ^{137}C coincides with 1952 AD (Baskaran et al., 2014). The ^{137}Cs peak can also be used to determine an average sedimentation rate based on the maximum depth of the peak in the sediment column.

Procedure

Sediment was subsampled from the gravity core, as these sediments were less likely to be disturbed during extrusion compared to the sediment obtained via the Livingstone corer. The gravity core was cut open and samples were obtained from 0-1, 1-2, 2-3, 3-4, 4-5, 5-8, 8-10, 10-12, 15-17, and 28-30 cm. The samples were dried in an oven overnight at 45 °C and finely crushed. The powder was sent to the National Centre for Radiation Science in Christchurch.

Data processing

Cesium-137 and lead-210 concentrations were plotted against depth.

3.5 Bulk density measurements

Sampling for bulk density was done at continuous 2 cm intervals for the first ~1.5 m, then at 10 cm thereafter. Between 2 and 5 cubic cm of sample was dried for at least 48 hours at 45 °C before weighing. Dry bulk density was calculated using the equation:

$$P=Ms/Vt$$

Where P is the dry bulk density (g/cm³), Ms is the dry weight in grams, and Vt is the volume of the wet sample.

3.6 Pollen analysis

Pollen analysis in this study was conducted to: assess the natural vegetation and the variability of the vegetation prior to human arrival; the vegetation just prior to human arrival; and the point at which humans arrived at Lake Horowhenua and the changes to vegetation post-human arrival.

Procedure - pollen extraction

The core was sampled for pollen analysis at varying intervals. Samples were taken at 5 cm intervals within the first 115 cm, as this was the zone in which signs of human activity were likely to be present. Below this depth, samples were taken at 10 cm intervals between 120-290 cm, and at 20 cm intervals between 290 to 390 cm. The samples are referred herein as sample 1-45, with sample 1 being the youngest sample and 45 the oldest.

With the exception of samples from 5-8 cm and 15-17 cm, each sample comprised 1 cubic cm of wet sediment, obtained using a sterile 5 ml medical syringe with the tip cut off. Samples from 5-8 cm and 15-17 cm were obtained from 1 g of the dried and crushed sediment that was used for ¹³⁷Cs and ²¹⁰Pb concentration dating. Samples were processed following the treatments outlined by Faegri and Iversen (1989) and Moore et al. (1991) (Fig. 10). In addition, prior to processing, two *Lycopodium* tablets from batch number 3862 (total of 19,332 spores, approximately) were added as a control over processing, and to provide the ability to calculate pollen concentrations (Faegri & Iversen, 1989). Residues were suspended in silicone oil and mounted under coverslips on glass slides. Initially, two slides were prepared per sample. However, additional slides were subsequently prepared for some samples in which pollen was sparse, in order to produce statistically robust counts.

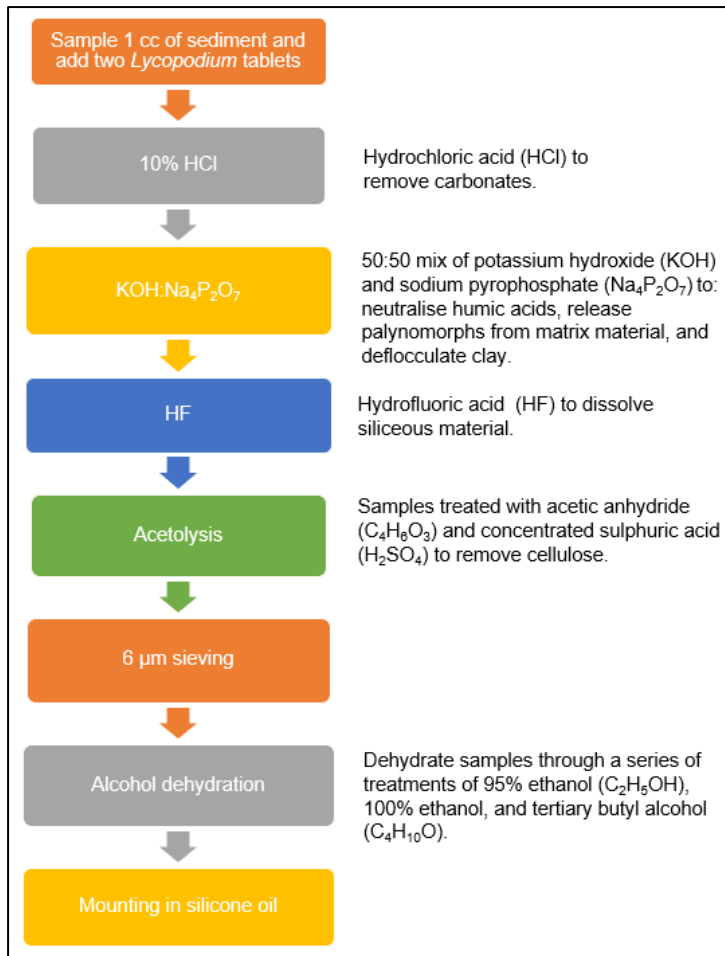


Figure 10: Pollen processing procedure.

Procedure - pollen counting

Palynomorphs were counted under a Zeiss transmitted light microscope at 400 x magnification and identified with the aid of publications by MacPhail (n.d.), Moar (1993), and Large and Braggins (1991), and reference slides in the Palynology Lab at Massey University. Slides were successively traversed and palynomorphs tabulated until a total of >125 grains of dryland pollen (i.e. excluding pollen of wetland, aquatic, fern and tree fern taxa, and *Lycopodium* marker spores) was reached. As there were two slides for each sample, this produced a minimum of 250 grains of dryland pollen per sample. Preparing two slides per sample helps to ensure that the sample counted is a homogenous representation of the pollen concentrate prepared, i.e. removing any accidental bias that may result from just counting one subsample. As mentioned above, if a slide yielded <125 grains of dryland pollen, subsequent slides were prepared and counted. Raw pollen counts can be found in Appendix B.

The bisaccate pollen of species of Podocarpaceae (specifically *Podocarpus* and *Prumnopitys*) was frequently encountered damaged. If the grain was whole but could not be distinguished for certain

as either *Podocarpus* or *Prumnopitys*, it was counted as one pollen grain and placed into a class labelled undifferentiated Podocarpaceae. In the case of broken grains, methods outlined by Woodward and Shulmeister (2005) were followed; individual saccus were counted as half and corpi were counted as half, a single corpi with one saccus was also counted as half. These grains too were classed as Podocarpaceae undifferentiated.

In addition to pollen, *Pediastrum*, (a colonial alga; Fig. 11A) were also counted when encountered during the slide traverses. As *Pediastrum* colonies can be large (50-120 μm) and are prone to breaking (Fig. 11B), they were only included in the count if at least half of the entire colony was present. *Pediastrum* numbers in some samples were particularly high, and in the case of one sample (sample 1, 0-1 cm), *Pediastrum* were counted until to a total of 750 colonies per slide was reached, in the interest of time.

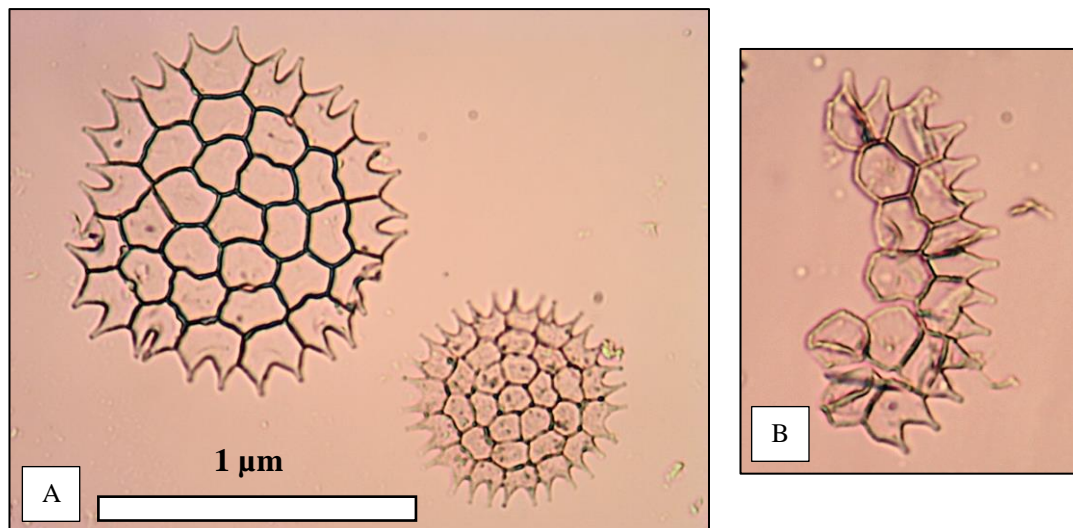


Figure 11: (A) *Pediastrum*. (B) Example of a broken *Pediastrum* that was not included in the counts.

Individual charcoal particles were also counted during the slide traverses. Each particle counted was assigned to a size class. Size was determined with the eye division piece using the longest axis of each particle, as per Clark (1982) and converted to microns. However, this approach could not be applied to samples from 5-8 cm and 15-17 cm, as these samples had been subjected to mechanical crushing (see section 3.4.2) in preparation for ^{137}Cs and ^{210}Pb concentration dating. However, as the main goal of charcoal analysis was to track human arrival or pre-human fire occurrence, the omission of these two samples from charcoal analysis has no detrimental effect, because both date to the European period, where human presence is well established.

Pollen data presentation and analysis

Pollen data were compiled into a pollen diagram prepared using the TILIA software package (Grimm, 2015). Pollen count data are presented as histograms as percentages of the dryland sum. Individual taxa were grouped into: tall trees, small trees and shrubs, herbs and grasses, ferns, and wetland and aquatics. A stacked graph of the sums of tall trees, shrubs, and herbs and grasses was created to allow for easy identification of the broad changes in vegetation cover through the core. Total pollen concentration per sample was calculated using the pollen concentration calculation presented in Faegri and Iversen (1989). A cluster analysis was also conducted using the CONISS function in TILIA (Grimm, 1987). All taxa were included in the analysis, along with charcoal and *Pediastrum*. A threshold of 5% of total dryland pollen was set for data to be included in the analysis. No data transformation was performed (i.e. the Euclidian distance was used). The results of the cluster analysis helped in delineating pollen zones. Ages interpolated from the age-depth model were added to the zones.

To assess changes to precipitation and available moisture, a pollen moisture index (PMI) was created using methods outlined in Jara et al. (2017). The PMI was calculated using the base-10 logarithm of the ratio of *Dacrydium cupressinum* to *Prumnopitys taxifolia* and Podocarpaceae undifferentiated. The results were then normalised by the record mean. The moisture index is based on the drought intolerance of *D. cupressinum* compared to *P. taxifolia* and other Podocarps (Wardle, 1991), and has been used in other studies (e.g. McGlone & Topping, 1977; Newnham et al., 1989). More positive values represent the relative dominance of the drought intolerant *D. cupressinum*, while more negative values represent a dominance of the drought tolerant *P. taxifolia* and other Podocarps.

3.7 Grain size analysis

The core sediments were also subjected to grain size analysis. Clastic grain size in lake sediments is linked to the sediment source, energy of sediment transport, turbulence and wave energy (HORIBA, 2005), and residence time on the terrestrial landscape (Trodahl, 2010). Therefore, grain size can be used to assess: lake level and proximity of the depocentre to the shoreline (Lowe & Walker, 2014), and the occurrence of events such as storms, landslides, and floods (Glade, 2003). In many studies, grain size analysis has been used to assess catchment disturbance associated with human arrival, as it can reflect increased susceptibility of the catchment to erosion following vegetation clearance (e.g. Elliot et al., 1995; Glade, 2003).

For this study, a grain size data set was produced at Victoria University of Wellington. The analysis was carried out using the Beckman Coulter LS 13 320 laser particle analyser (LPA) (BC, 2011). An LPA measures particle size via refraction and scattering of light by particles (BC, 2011;

Fox, 2016; HORIBA, 2012; Trodahl, 2010). One limitation of this approach is that an LPA assumes that all grains are spherical (BC, 2011). Thus, an irregular-shaped particle could return different sizes, dependant on which side the laser hits. Additionally, laser diffraction analysers may overestimate the size of clay-sized particles $<2 \mu\text{m}$ (Konert & Vandenberghe, 1997; McCave et al., 1986).

Due to the inherent grain size, the samples were analysed using the Mie Scattering Theory (BC, 2011). Polarization Intensity Differential Scattering (PIDS) was excluded, as particles were not expected to be less than $0.04 \mu\text{m}$. The standard operation of the Beckman Coulter allows for the detection of particles measuring $0.04 \mu\text{m}$ to $2000 \mu\text{m}$, and results are split into 113 quarter phi size fractions. These size fractions are broadly synchronous with the Blott and Pye (2001) scale.

A refractive index representative of that of quartzofeldspathic greywacke was used, as this represents the main source rock of the sediment deposited in Lake Horowhenua. A refractive index of 1.54-1.56 is usually used for quartzofeldspathic sediment (Loizeau et al., 1994; Murray, 2002; Sperazza et al., 2004). Due to the small difference in the refractive index of quartz, calcite, and feldspar, a single refractive index is usually chosen (Loizeau et al., 1994). A). In this study, the refraction index of quartz (1.55) was used.

Procedure

One cm slices of sediment were taken at 6 cm intervals from the gravity core. For the long core, sediment slices of 2 cm were taken at 6 cm intervals from 30-150 cm, then 2 cm of sediment at 12 cm intervals from the rest of the core. Sediment samples weighed between 1-1.5 g. A greater volume of sediment was taken for the upper samples as they were more water-rich.

Ideally, pre-treatment of lacustrine sediment for grain size analysis aims to eliminate all organic mass, leaving the clastic/inorganic terrigenous sediment. Thus, treatments are often aimed at removing carbonates, organic matter, and siliceous organisms such as diatoms and sponge spicules, which can skew the results (Gray et al., 2010; Mikutta et al., 2005; Vaasma, 2008; Vasskog et al., 2016). Under inspection with a microscope, the sediment samples were found to contain various diatom species and large numbers of sponge spicules. Because treatment methods can vary drastically from author to author, a thorough description of the methods used in this study is provided, as suggested by Vasskog et al. (2016).

Treatment methods were adapted from Gray et al. (2010), Mikutta et al. (2005), and Vasskog et al. (2016). Hydrochloric acid (HCl) was used to remove any carbonates and to release organic carbon. Hydrogen peroxide (H_2O_2) was used to eliminate the majority of organic material

(Vaasma, 2008). Potassium hydroxide (KOH) was used to digest biogenic silica, though it is thought to affect readily soluble clay minerals and may not remove all of the biogenic silica (Boyle, 2002). Heat was applied in the form of a heating pad at no more than 50 °C where possible to reduce any change in grain size due to heat-induced transformation of platy clay minerals (Mikutta et al., 2005). Between each pre-treatment, the sediment was washed three times with reverse osmosis (RO) water and centrifuged at 3,500 RPM for 8 minutes.

Ten ml of 10% HCl was added to a beaker containing the sample and left overnight. Following this, 20 ml of H₂O₂ was added to the beaker and left to sit for seven days. Heat was then applied. When the reaction ceased, a fresh aliquot of 20 ml was added. A total of 7 x 20 ml aliquots of H₂O₂ were used for each sample. Fifteen ml of 10% KOH was then added and the samples placed on a heat pad for 1.5 hours.

Prior to analysis, samples were sonicated and stirred in 40-80 ml of 0.5 g/L calgon solution (dependant on sample volume) for 15-20 minutes to deflocculate clay aggregates that might skew the results. Samples were added to the sample bucket until the obscuration ideally reached between 8-12%. This value ensures that enough sample has been added for measurement (J. Chewings *pers comm*, 2018). If the value was too high, the sample was drained, and more water added. Care was taken to avoid releasing too much liquid to avoid losing the fines. Most of the samples reached obscuration values of around 6%, with some as low as 3%. This was due to limited sample availability and duplicates were not able to be performed. Such low obscuration values indicate that the accuracy of the results may be limited. The obscuration values are presented in Appendix C. Samples were not sonicated during analysis.

Data processing

Mean grain size for the sediment samples was plotted against depth. The results were separated into sand, silt, and clay classes based on the grain size scale in Blott and Pye (2001). These groups were used to show percent changes in each class. The classes that were created are: clay (0.375124-2.01068 µm), fine silt (2.20725-8.14669 µm), medium silt (8.94315-15.6512 µm), coarse silt (17.1813-57.7666 µm), and sand (63.41410-2000 µm). An outlier at 109 cm returned a mean grain size of 155 µm and was excluded from data analysis.

3.8 Geochemistry

3.8.1 Carbon and nitrogen analysis

Total organic carbon (TOC) and total nitrogen (TN) can be used to infer productivity (Stephens et al., 2012), and C/N ratios can be used to distinguish between the autochthonous and allochthonous sources of organic matter (Meyers & Teranes, 2002). This is due to the inherent

differences in C/N ratios of biomass from aquatic organisms (plants and algae) to that of terrestrial organic matter (soil organic matter and terrestrial plants) (Meyers & Ishiwatari, 1993; Meyers & Teranes, 2002; Rogers & Cochran, 2017). The total nitrogen content of sediment can be affected by diagenesis, inorganic nitrogen, diatom release of nitrogen, denitrification, pH, productivity, nitrogen fixation, and (during the human era) nitrogen fertilisation, fossil fuels, and industrial processes (Talbot, 2001).

Total carbon and total nitrogen were measured at Massey University at the School of Agriculture and Environment using an Elementar vario MACRO cube (Elementar, 2016). The Elementar combusts the sample at 1800 °C and measures the gases released (N₂, CO₂, H₂O and SO₂) using chromatography (Meyers & Teranes, 2002).

Procedure

The sampling interval for carbon and nitrogen analysis was continuous 2 cm sampling for the first 1.5 m, then every 10 cm thereafter. Samples were air dried and finely crushed prior to analysis. Initially, sample weight was 50 mg, chosen based on the assumption that the sediment contained a high proportion of organic matter and therefore organic carbon. However, after the first set of results were assessed, it was found that the organic matter content may be lower. To increase reliability, the sample size was increased to 100 mg. Repeats on a selection of the initial samples using 100 mg of sediment revealed that the results from the 50 mg sample size were still reliable. Duplicates were carried out every 10 samples to ensure reproducibility.

To produce accurate measurements of organic carbon, any inorganic carbon (typically in the form of carbonate) must be removed. Given the general paucity of carbonate rocks in the Lake Horowhenua catchment, it was not expected that the samples would contain appreciable amounts of inorganic carbon. Three samples were tested via a pH probe to determine whether any carbonates were in fact present. These samples returned readings of 5.03-5.63, indicating that carbonates were largely absent (Schumacher, 2002).

Data processing

Because total nitrogen is measured, the inorganic nitrogen proportion can be quantified by plotting TOC vs TN weight percent (see Fig. 25 in results). The value of the intercept is the proportion of inorganic nitrogen and can be used to correct C/N ratio plots (Talbot, 2001). The value of the intercept was 0.06%. This correction was applied to the C/N ratio plot. C/N mass ratios were plotted using a conversion factor of 1.167 (the atomic weights of nitrogen and carbon) to yield C/N atomic ratios (Meyers & Teranes, 2002). TOC wt. % and TN wt. % were also plotted against depth.

3.8.2 Organic matter content (via loss on ignition and Elementar)

The proportion of organic matter in lacustrine sediments is influenced by a number of factors, including: in-lake productivity, organic matter content of soils in the lake catchment, catchment vegetation cover, erosion within the catchment (Lowe & Walker, 2014), and sampling location (Meyers & Teranes, 2002). Organic matter content of sediments can be estimated via induction furnace, wet oxidation, and by a conversion to values obtained from total organic carbon analysers (e.g. via the Elementar, see section 3.8.1).

For this study, organic matter (OM) was estimated via two types of analyses, loss on ignition (LOI) and through applying a conversion factor to the organic carbon content, as measured on the Elementar (section 3.8.1). These two data sets will be hereinafter referred to as OM%^L for data obtained via LOI and OM%^T for data obtained via the Elementar. Due to its low cost, LOI is one of the most common methods used to measure organic matter content (Heiri et al., 2001; Schumacher, 2002). Loss on ignition estimates the proportion of organic matter of sediment by determining the weight lost after ignition.

This approach of two data sets was chosen as the LOI method often overestimates organic matter due to the elimination of inter-crystalline water, hydroxyl groups, and volatile salts (Boyle, 2002; Goldin, 1987; Houba et al., 1997; Schumacher, 2002). Additionally, LOI temperatures of between 500 °C and 600 °C result in the combustion of inorganic carbonates, resulting in overestimations of organic matter (Hoogsteen et al., 2018). However, this should not be a problem, considering the lack of carbonates in Lake Horowhenua sediments. Meyers and Teranes (2002) suggest that TOC values are the more accurate way of determining organic matter content as the results are not inflated by volatile components.

Procedure for LOI

Methods for LOI were adapted from Hoogsteen et al. (2015), Heiri et al. (2001), and Frangipane et al. (2009). Due to recommended sample weights and heating temperatures varying between authors, again a detailed description of the methods is provided (Heiri et al., 2001; Hoogsteen et al., 2015). The minimum recommended sample weight is 2 g and an ideal sample weight is 20 g. A minimal between sample weight variance is ideal, as result variance decreases with increased sample weight (Heiri et al., 2001).

Due to sample availability, sample weight varied between 0.5 and 2 g, with the majority of samples weighing 2 g. Slices of sediment 2 cm thick were taken at 4 cm intervals from the first 150 cm, at intervals of 10 cm from 150-250 cm, and at 20 cm intervals from 250-290 cm. Samples were dried for two days in an oven at 45 °C. Samples were then crushed and re-dried at 100 °C

overnight prior to analysis to remove any remaining water. A furnace temperature of 550 °C was used to ensure complete combustion of organic matter. Samples were placed in a preheated Carbolite AAF1100 furnace to ensure equal heat distribution (Hoogsteen et al., 2015) for 4 hours. After ignition, samples were transferred into a desiccator until they had cooled to around 50°C, then the desiccator was closed. Samples were then weighed individually as quickly as possible.

Data processing for LOI OM%^L

As mentioned earlier, LOI is thought to overestimate organic matter content. This can be adjusted for via a correction factor that is dependent on temperature, ash time, and clay mineral content (Hoogsteen et al., 2015; Hoogsteen et al., 2018). The correction factor has been reported to be between 7% and up to 20% for soils and lacustrine sediments (Boyle, 2002; Heiri et al., 2001; Hoogsteen et al., 2015; Houba et al., 1997). Due to the potential for overestimation when conducting LOI analysis of organic matter (OM) content, both raw OM%^L is plotted, as well a conversion factor of 13%, as this seems closer to Elementar results.

Data processing for OM%^T

The standard conversion for TOC wt. % to organic matter % is a correction factor of 1.724 (Waksman & Stevens, 1930). This is based on the assumption that organic matter contains 58% organic carbon (Nelson & Sommers, 1996; Schumacher, 2002). Unfortunately, this correction factor is not a one-size-fits-all approach and was largely developed via studies of soil samples. A conversion factor of two is typically used for lake sediments since lacustrine sediments are thought to contain 50% organic carbon (Meyers & Teranes, 2002). This is the conversion factor chosen for this study.

3.8.3 Elemental analyses (via atomic emission spectroscopy and X-ray fluorescence)

Variations in the concentration of particular key elements in lake sediments can reflect various natural or anthropogenic processes and events operating within the lake itself and within the wider lake catchment (Davies et al., 2015). Elemental concentrations from lake sediments can be determined by destructive and non-destructive methods. Acid extractable elements can be measured quantitatively by an atomic emission spectrophotometer and qualitatively via XRF. Both acid extractable methods and X-ray fluorescence (XRF) core scanning were carried out in this study.

Atomic emission spectroscopy

An atomic emission spectrophotometer works by exciting atoms (by way of flame, plasma or arc), and measuring the wavelength of emitted light, with each element having a characteristic wavelength (Cantle, 1986). The intensity of the emitted light is proportional to the quantity of the

element (Campbell-Platt, 2017). The elements measured in this study to assess both erosion and bottom water oxygenation were manganese (Mn), iron (Fe), and Al (aluminium). This data will be supported by elemental reconstructions via XRF. Acid extractable Mn, Fe, and Al were measured on the Agilent Microwave Plasma-Atomic Emission Spectrometer (MP-AES 4200) (Elliott, 2014) at the Massey University School of Agriculture and Environment.

Iron and manganese concentrations can be used to infer bottom water oxygenation. This is because oxidised elements remain stable when oxygen remains high but can become reduced and susceptible to dissolution in reducing conditions (Boyle, 2002). In reducing conditions, Mn has a higher solubility than Fe (Boyle, 2002). An increase in the Fe/Mn ratio can be a signal for anoxic conditions brought about by stratification, or de-oxygenation via decay during enhanced biological productivity (Davies et al., 2015). This may result in a positive feedback; whereby the anoxic conditions allow for nutrient release, further enhancing eutrophication (Verburg et al., 2010). Comparison of the Fe/Mn ratio to Fe can help to ensure changes in the Fe/Mn ratio are due to redox and not catchment inputs (Kylander et al., 2011; Moreno et al., 2007). To test whether the changes in the Fe/Mn ratio are related to redox or catchment input, the Fe/Mn ratio is plotted with the Fe data (both obtained via XRF). This confirms that the Fe/Mn ratio in Lake Horowhenua sediments largely reflect redox processes, rather than detrital input. Changes in concentrations of Al will be used to infer catchment erosion. Aluminium is one of the main elemental constituents of the source rock that supplies sediment into Lake Horowhenua.

Procedure

Two cm sediment slices were taken continuously for the first 1.5 m, then every 10 cm thereafter. Samples were oven dried at 45 °C for at least 48 hours and finely crushed prior to analysis. A subsample of around 0.5 g was placed in digestion tubes before 10 ml of aqua regia ($\text{HNO}_3 + 3 \text{HCl}$) was added. The samples were left overnight before being gradually heated to a maximum of 120 °C for 4 hours. Heating was then increased to 140 °C to evaporate the acid until around 2 ml remained. Deionised water was added until the volume reached 25 ml and samples were then mixed thoroughly. The sample was then filtered and placed in the fridge at 4 °C prior to analysis. Due to high readings of Al, Fe, and Mn from the MP-AES, serial dilutions with 2% nitric acid (HNO_3) were necessary so as to not damage the MP-AES. Manganese was diluted 250 times, and aluminium and iron 12,500 times. Standards were prepared using single element reference liquids. Upon assessment of the data, outliers were detected at: 103, 251, 261, 271, 281, 301, 341, 361, and 381 cm, therefore, repeat analysis was carried out and the initial results excluded from data analysis.

Data processing

Iron, aluminium, and manganese results were converted to percentages using the equation:

$$\text{Elemental \%} = [(\text{MP-AES reading} \times \text{dilution factor}) / \text{sample weight}] \times 10000$$

Percentage data of Al and Fe/Mn were plotted against depth.

X-ray fluorescence and magnetic susceptibility via ITRAX

XRF produces rapid high-resolution qualitative elemental variations of elements from aluminium to uranium in addition to optical and radiographic imaging (Rothwell & Croudace, 2015a). XRF core scanning is non-destructive (Davies et al., 2015) and works by way of an X-ray beam irradiating the sample then measuring the emitted secondary radiation (fluorescence), which has a wavelength specific to each element (MacLachlan et al., 2015). Magnetic susceptibility sensors can be fitted to the XRF scanner and used to identify the presence of magnetic minerals within the sediment or as a means for core correlation (Rothwell & Croudace, 2015a). The presence of magnetic minerals may also indicate tephra or clastic input (Rothwell & Croudace, 2015a).

Scanning parameters

The core was submitted for ITRAX core scanning to the University of Auckland X-ray Centre. Due to the array of elements of interest and time factor constraints, detection was by way of a Molybdenum (Mo) tube with a count time of 10 seconds at 1 mm intervals. A Mo tube provides reliable counts of elements heavier than potassium but is not as efficient for the lighter elements. The elements scanned for were Al to Zr (Zircon) - with the exception of scandium, germanium, selenium, krypton, and barium. The working voltage was 60kV/50mA and 30mA/55 kV. Unfortunately, the very upper sediment of each core was unable to be scanned due to a low sediment profile.

XRF proxy for oxygen concentration

Iron and manganese ratios produced via XRF will be used to compare the reconstruction of the Fe/Mn ratio via atomic emission spectroscopy. Additionally, phosphorus concentrations are often positively correlated to higher Fe/Mn ratios due to eutrophication enhancing stratification and producing anoxic conditions (Corella et al., 2012). Phosphorus was measured by the ITRAX, thus phosphorous will also be plotted.

XRF proxy for organic matter and water content

Qualitative estimation of organic matter (and thus water content) can be assumed by assessing the scattering ratio of incoherence and coherence attained via XRF. This is due to the fact that organic

carbon has a lower atomic number than the measurable elements (Davies et al., 2015). The scatter that is produced reflects the interaction of the X-ray with water and carbon that is unable to be detected (Davies et al., 2015). Thus, higher incoherence/coherence scattering ratio indicates increased organic matter content (Davies et al., 2015; Rothwell & Croudace, 2015a), while coherence/incoherence can be used to measure fluctuations in water content (Davies et al., 2015). This data will be used to compare variations in organic matter content via $OM\%^L$ and $OM\%^T$, and water content from bulk density.

XRF proxy for erosion Ti, K, and Rb

The elements chosen for plotting are those that can potentially act as proxies for processes relating to catchment disturbance – such as deforestation resulting in increased erosion. Detrital input can be measured by the relative concentrations of lithogenic elements: Al, Si (silicon), K (potassium), Ti (titanium), Fe, Rb (rubidium), and Zr, as these elements are geochemically stable and conserved in most environments (Boës et al., 2011). As mentioned previously, the greywacke-argillite axial ranges, particularly the Rakaia sub-terrane of the Torlesse terrane, are the dominant source rock for eroded material that enters Lake Horowhenua. The main elemental constituents of the rock are Al, Si, K, Fe, Mg (magnesium), Ca (calcium), Na (sodium), and Ti (Ewart & Stipp, 1968). The trace elements in greywacke that were detected by XRF in this study, and are good measures of detrital input, are Rb and Zr (Ewart & Stipp, 1968; Ireland, 1992).

Iron is often affected by redox conditions and diagenesis (Boyle, 2002; Engstrom & Wright Jr, 1984; Mackereth, 1966). Similarly, Si levels are influenced by biogenic silica. Due to the presence of sponge spicules and diatom assemblages, Si would not be a reliable indicator for erosion in this study (Brown, 2015). Potassium is also affected by weathering, and Al counts may be insignificant due to count time and detection tube (Davies et al., 2015).

The elements chosen in this study are, therefore: Ti, Al, and K to assess catchment disturbance and deforestation related to human arrival. Rubidium was also plotted. Unfortunately, Zr counts for the 1.9-2.9 m section were not well detected, and therefore were not plotted. Although the Al counts may be unreliable, it is plotted to compare the direct measurement via atomic emission spectroscopy, and K is plotted as the results are comparable to Ti and Rb.

XRF proxy for grain size Fe/Ti and Ti/K

Fe/Ti, Ti/K, and Zr/Rb ratios can be used to infer changes in allochthonous grain size. Fe/Ti and Ti/K ratios were chosen to assess grain size, as Zr/Rb ratio is less reliable in coarse silts (Kylander et al., 2011) or in sediments with a significant proportion of Rb from K-feldspars. Although Lake Horowhenua sediments should not contain K-feldspar, the sediment does contain a relatively high

proportion of coarse silt particularly at the base of the core (see section 4.7). Increases in Fe/Ti ratio indicate sediment with a smaller grain size, while increases in Ti/K ratio indicate sediment with a larger grain size (Davies et al., 2015). These plots will be used to compare with direct grain size analysis.

Data processing

Elemental data was normalised to counts per second (CPS) or another element to account for variations in water content and organic matter or lighter elements that may affect the result (Davies et al., 2015). Data was smoothed using a 9-point moving average or 6-point moving average, dependent on the graph, to allow for trend determination.

Magnetic susceptibility

Magnetic susceptibility (κ) is the degree to which a material can be magnetised (Rothwell & Croudace, 2015b). Magnetic susceptibility via ITRAX detects both paramagnets and ferro/ferri magnets. However, Fe-Ti oxides are permanent magnets, and thus magnetic susceptibility largely reflects the occurrence of these (Rothwell & Croudace, 2015b). Magnetic susceptibility is often used to detect cryptotephra (Davies et al., 2015). In this study, magnetic susceptibility is used as an indicator of erosion. Forest clearance may result in an influx of magnetic minerals into the lake associated with catchment disturbance and erosion (Davies et al., 2015). Magnetic susceptibility $SI \times 10^{-5}$ is plotted against depth.

Chapter 4: Results

4.1 Sand deposit

Grain size analysis

In terms of grains size, the core sand sample was most similar to the dune sand and beach sand. All three are dominated by fine sand, while the river sand samples have significantly greater proportions of the coarser fractions (Fig. 12). Similarly, the mean grain size of the core sand was closest to the dune and beach sand (Table 3). All three sands are very well sorted, although the actual sorting value of the core sand is slightly higher than that of the dune sand and beach sand and is slightly coarsely skewed (Table 3). Overall, on the basis of grain size, the core sand is clearly more similar to the dune and beach sand, suggesting a coastal-marine or aeolian source as opposed to a fluvial (i.e. flood) source for this unit.

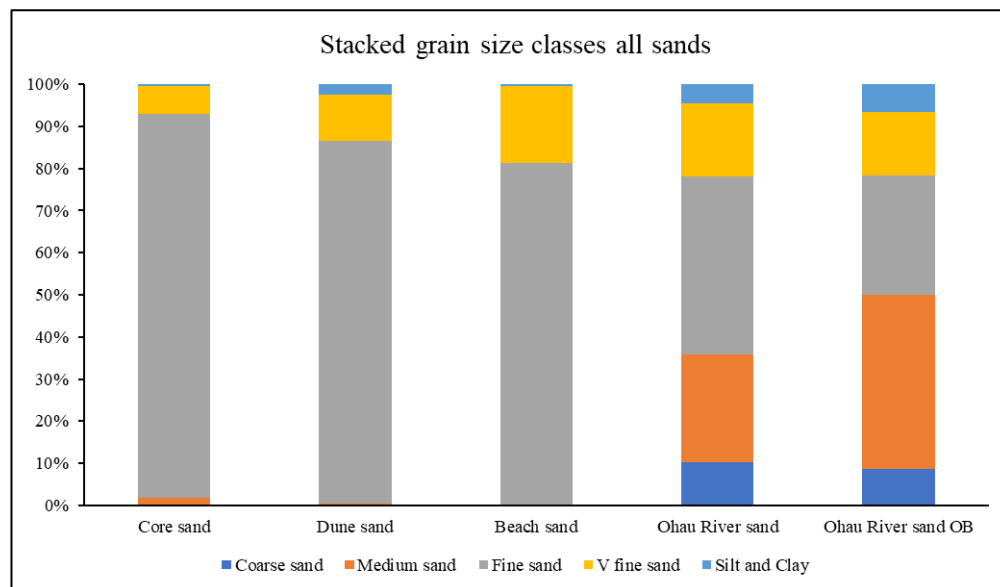


Figure 12: Stacked grain size classes of all sands.

	Core sand		Dune sand		Beach sand		Ohau River sand		Ohau River sand OB	
MEAN μm (\bar{x})	165.981	Fine Sand	153.482	Fine Sand	145.094	Fine Sand	204.877	Fine Sand	217.370	Fine Sand
SORTING (s):	1.269	Very Well Sorted	1.262	Very Well Sorted	1.245	Very Well Sorted	2.055	Poorly Sorted	2.235	Poorly Sorted
SKEWNESS (Sk):	0.100	Coarse Skewed	0.003	Symmetrical	-0.074	Symmetrical	0.097	Symmetrical	-0.341	Very Fine Skewed
KURTOSIS (K):	0.942	Mesokurtic	1.364	Leptokurtic	1.278	Leptokurtic	1.134	Leptokurtic	1.364	Leptokurtic
Sample type	Unimodal, very well sorted		Unimodal, very well sorted		Unimodal, very well sorted		Bimodal, poorly sorted		Unimodal, poorly sorted	
Sediment name	Very well sorted fine sand		Very well sorted fine sand		Very well sorted fine sand		Poorly sorted fine sand		Poorly sorted medium sand	

Table 3: Graphical measures and descriptive statistics of all sands.

Grain shape

In terms of grain shape measurements, the core sand lies in between the coastal-origin and fluvial-origin sand samples. The grain shape of the core sand in all class sizes ranges from very angular to sub-angular (Table 4, Fig. 13A). The dune sand (Fig. 13B) and beach sand (Fig. 13C) are very

angular to sub-rounded, but predominantly sub-angular to sub-rounded. Both the Ohau River sands (Fig. 13D) are very angular to sub-angular.

	Core sand	Dune sand	Beach sand	Ohau River sand	Ohau River sand OB
>500 μm	Angular to sub-angular			Angular to sub-angular	Angular to sub-angular
>250 μm	Very angular to angular	Very angular to sub-rounded	Angular to sub-angular	Very angular to angular	Very angular to angular
>125 μm	Very angular to sub-angular	Sub-angular to sub-round	Sub-angular to sub-round	Angular to very angular	Angular to very angular
>63 μm	Very angular to angular	Sub-angular to sub-round	Sub-angular to sub-round	Angular to sub-angular	Angular to sub-angular
Sediment name	Very Well Sorted Fine Sand	Very Well Sorted Fine Sand	Very Well Sorted Fine Sand	Poorly Sorted Fine Sand	Poorly Sorted Medium Sand
Sample type	Unimodal, Very Well Sorted	Unimodal, Very Well Sorted	Unimodal, Very Well Sorted	Bimodal, Poorly Sorted	Unimodal, Poorly Sorted

Table 4: Grain shape, sample type, and sediment name of all sands.

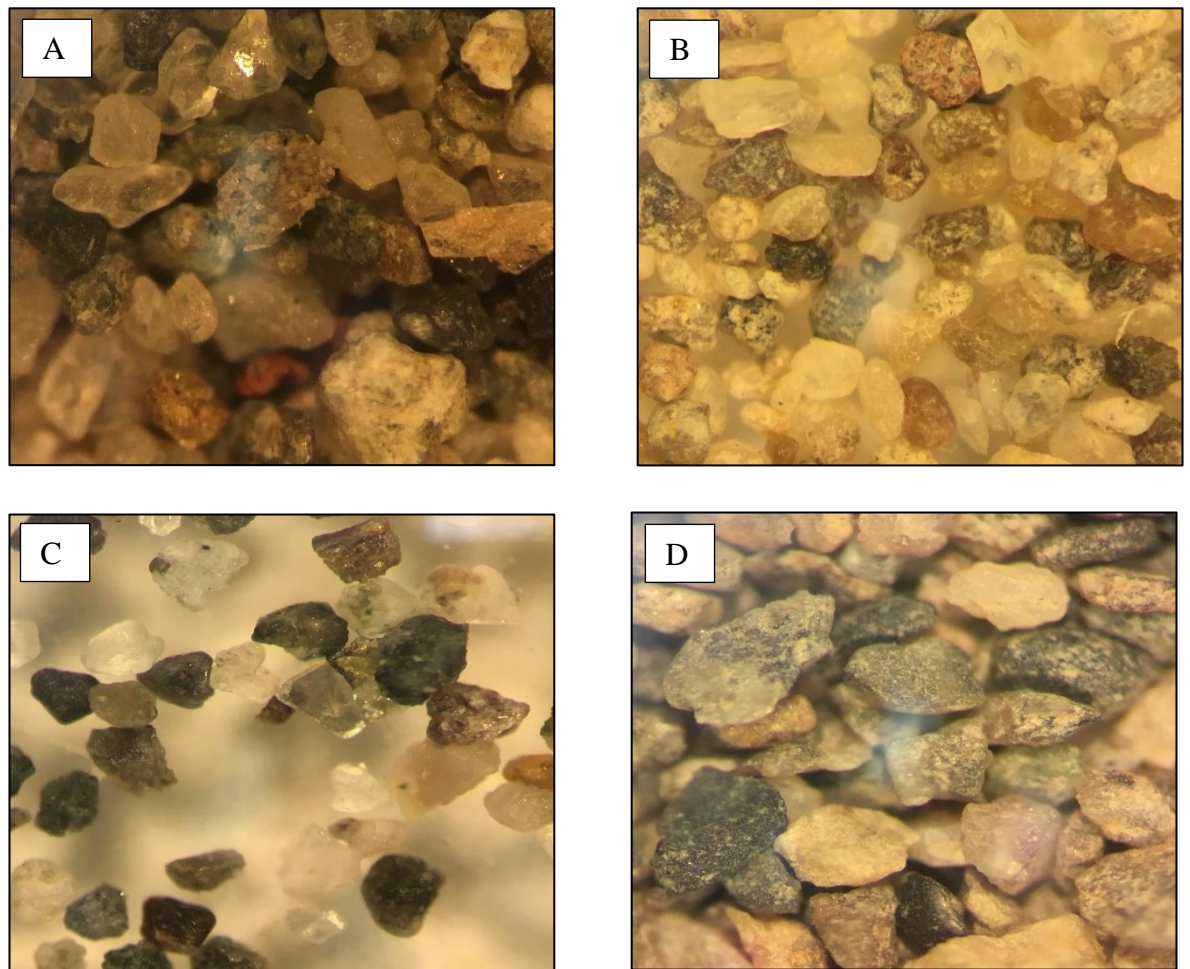


Figure 13: Images of all sands to show angularity in the $>250 \mu\text{m}$ size fraction. (A) Core sand. (B) Dune sand. (C) Beach sand. (D) Ohau River sand. The images were taken at the same magnification.

Mineralogy

Mineralogically, there was not a great deal of difference between the sand samples. The core sand is most similar to that of the dune sand and beach sand. The core sand, however, contains a greater proportion of plagioclase in the larger size fractions, and more ferromagnesian minerals (pyroxene

and magnetite) in the finer size fraction (Fig. 14). The core sand, dune sand, and beach sand also contain significant proportions of pyroxene; a silicate mineral found in volcanic rocks that would have been transported by longshore drift southwards from either Taranaki or the mouth of the Whangaehu river, which drains the Tongariro Volcanic Centre. Thus, the core sand is not fluvial in origin.

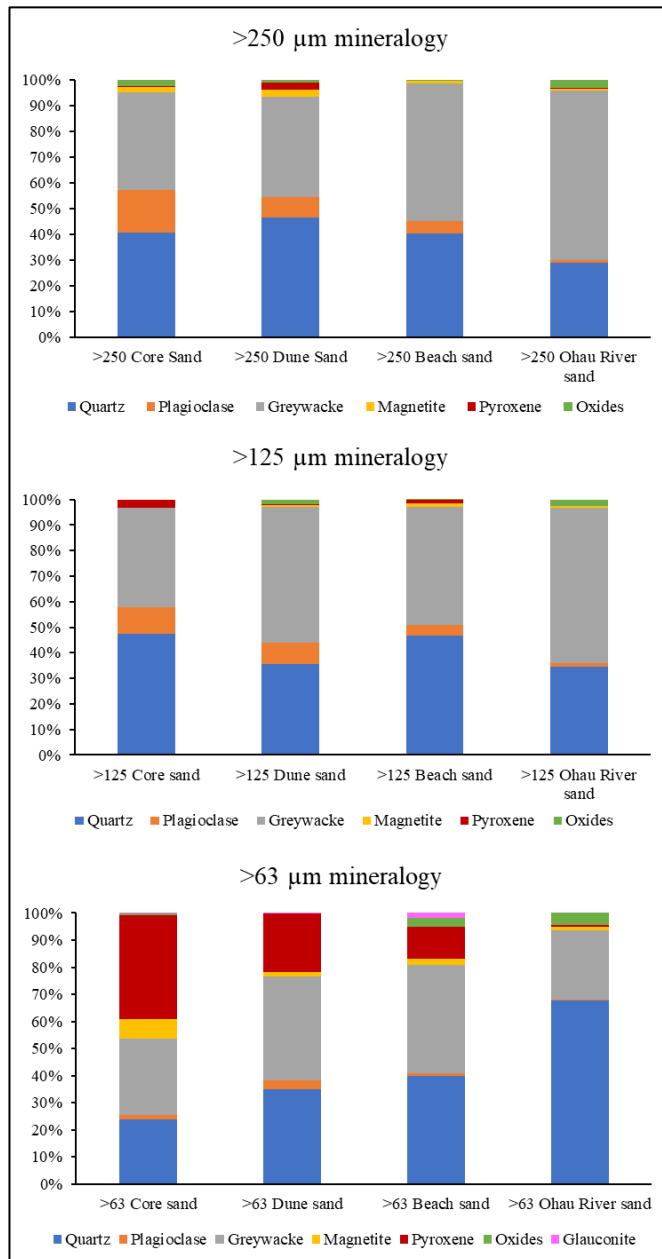


Figure 14: Mineralogy of all sands. From top to bottom: >250 µm, >125 µm (125-250 µm), and >63 µm (125-63 µm) size fractions.

4.2 Core shortening

The sediment lengths obtained for the core were 100 cm, 87 cm, 90 cm, and 93 cm, and where appropriate these cores are herein referred to as core 1 through 4, respectively. The first core penetrated to a depth of 90 cm to capture the sediment-water interface, thus it is concluded that the extra 10 cm of sediment is due to high water content; that allowed the water-rich upper rich sediment to stretch out during extrusion, transportation, and storage.

Core 2 was 13 cm short, and core 3 and 4 were short by 10 cm and 7 cm, respectively. A similar pattern of core shortening is also seen in the other long cores from the lake. Sediments obtained from open barrel corers are often shorter than the penetrated depth (Blomqvist, 1991). This results from a process called core shortening; in which the sediments are thinned progressively down core. This results from frictional and deformational forces at the leading edge of the penetrating tube plastically deforming the sediment before it enters the pipe (Glew et al., 2002; Morton & White, 1997). Other modes of sediment loss result from turbulent zones ahead of the core as it is lowered into the sediment (Blomqvist, 1991; Glew et al., 2002), bypassing, redistribution of sediments, and compaction and pore water loss (Morton & White, 1997). The core shortening in these cores is likely due to frictional and deformational forces, while the reduction of the shortening between core 1 and 4 has been attributed to the decrease in sediment pore water and sediment compaction at depth. This agrees well with the bulk density measurements and coherent/incoherent scatter (see section 4.5); in that shortening is more common in sediment with a higher water content (Glew et al., 2002).

4.3 Core stratigraphy

The sediments from Lake Horowhenua are significantly homogenous, as is confirmed via X-ray (section 3.3). The homogenous nature of the sediments is interpreted as the result of the shallow nature of the lake allowing for wind-induced mixing. The long cores taken from near the outlet grade from silt and silt-rich mud to organic-rich lake mud. While the other cores grade from silt-rich mud to organic-rich lake mud. As per section 3.4.1, very few macroscopic organic remains were found, except in the short cores and the top ~30 cm of the long cores. These consisted of scattered remains of aquatic weed, possibly *Potamogeton* sp. or *Elodea canadensis*, and other fibrous plant material. In Horo 10, a single seed was found at 85 cm and submitted for radiocarbon dating. The periostracum of a kakahi freshwater mussel (*Echyridella* sp.) specimen was also found at ~380 cm.

The 3.9 m core was divided into units using the modified Troels-Smith system (Kershaw, 1997). The stratigraphy is represented diagrammatically in Figure 15A. Figure 15B is an image of the core. From the base, the core grades from olive-brown silt-rich mud to very dark grey-brown lake

mud. The 390-335 cm section is defined as organic-rich silt and the 335-0 cm section as organic-rich lake mud. Thin fibrous material was found between 2-43 cm, and very sparse, fine aquatic plant material from 67-87 cm. A 1 cm wide, distinctive, organic-rich black band was noted at 110 cm, a 1 cm wide dark band at 319 cm, and a 1-2 mm sinuously stratified layer at 340 cm. Boundaries are all gradational, except at the dark bands, the sinuous layer, and at 87 cm and 322 cm. The dryness of the sediment greatly decreases down core from a value of 1 to a value of 3. Elasticity increases from 0-1 and darkness ranges from 2-4.

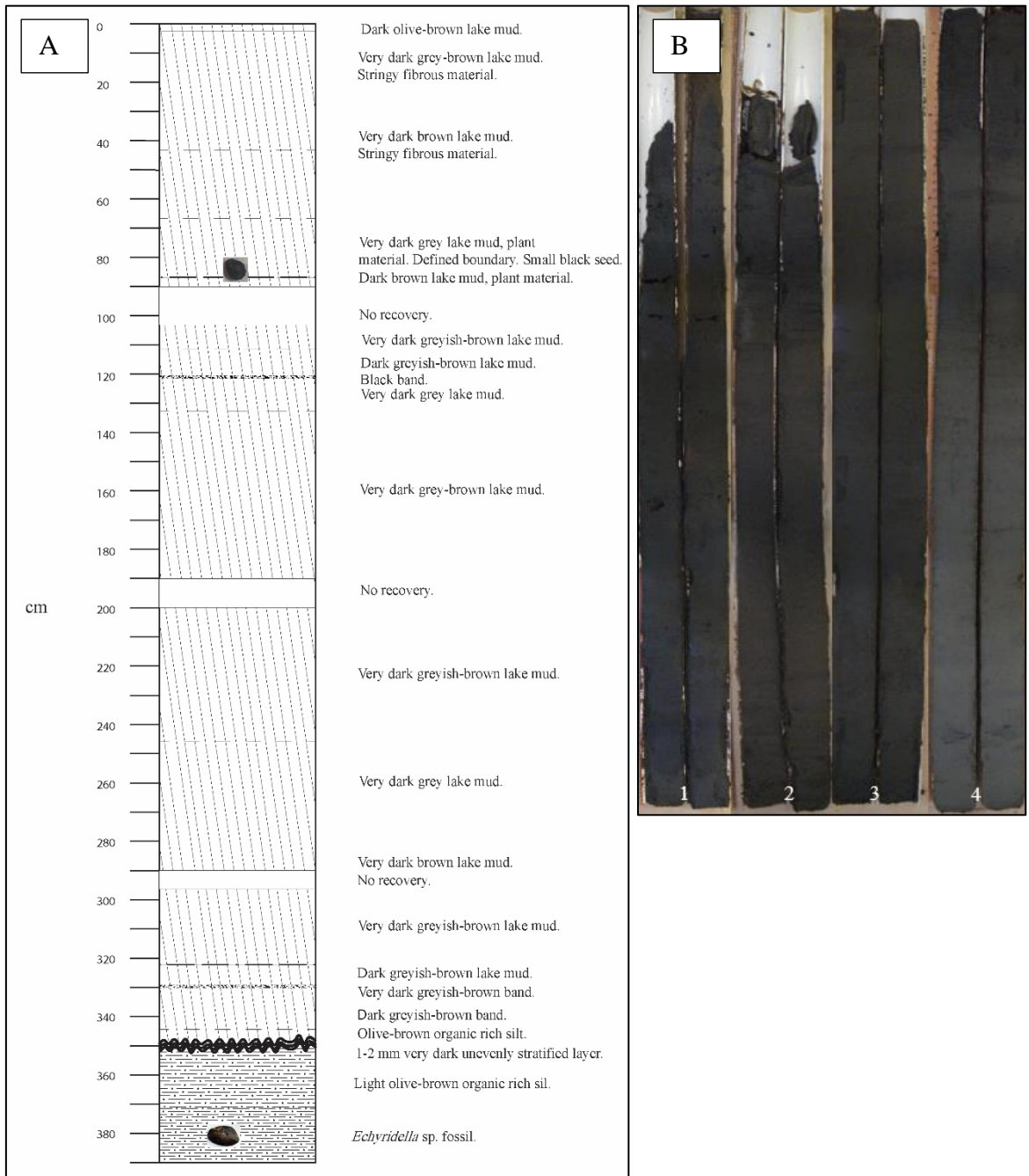


Figure 15: (A) Stratigraphic log and lithological descriptions of Horo 10. (B) Photographic images of Horo 10. 1: 0-0.9 m. 2: 0.9-1.9 m. 3: 1.9-2.9 m. 4: 2.9-3.9 m. Note the organic-rich silt appears more olive-grey than the image implies.

In all cores taken from near the outlet (i.e. Horo 1, 2, 8, & 9a), the sediments graded from fluvial grey mud, to organic-rich silt, interrupted by a paleosol and a 10 cm sand layer (Fig. 8 & Fig. 16). Following the sand layer, is a transition from organic-rich silt to organic-rich lake mud.

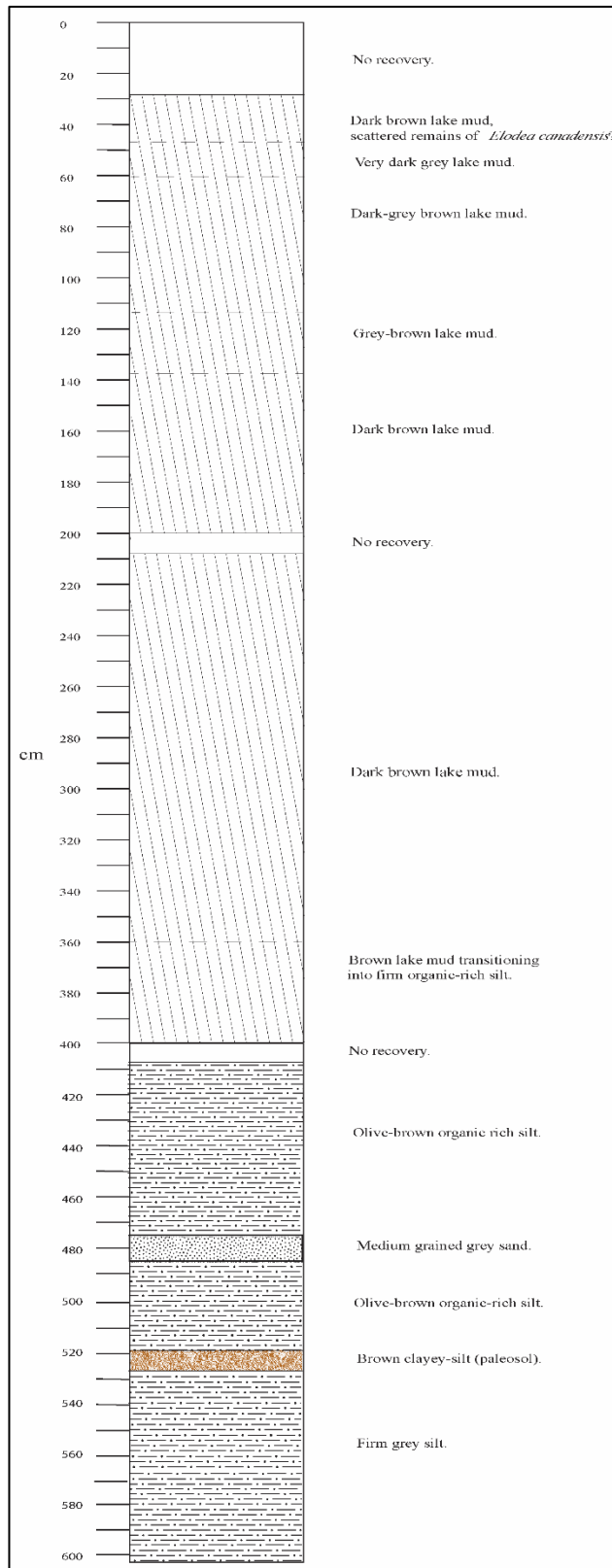


Figure 16: Stratigraphic log and lithological descriptions of Horo 8.

4.4 Chronology

4.4.1 Radiocarbon dating

Summary radiocarbon dating results are presented in Table 5, and the conventional radiocarbon age reports can be found in Appendix D. The dates from the various fractions from the 80-90 cm interval spanned a wide range ($1,094 \pm 20$, $1,077 \pm 108$, 960 ± 20 , 780 ± 50 , and 480 ± 19 yrs BP Fig. 17). The difference in years between the seed to NZA 65136, NZA 65080, NZA 65824, and NZA 65079 is: 448 ± 22 , 445 ± 19 , 344 ± 41 , and 172 ± 47 years. This is interpreted here as the result of a reservoir effect. The origin of this difference is reviewed further in the discussion. Interestingly, this reservoir age is not apparent in the Cladocera ehippia from 2-12 cm (NZA 65134), as this returned a modern age.

As mentioned previously, the Cladocera ehippia samples from 200-210 (NZA 65137) and 297-307 cm (NZA 65138) returned an inverted age. The new ages (NZA 65822 and NZA 65823) were concordant with depth (i.e. the opposite to the first batch), and thus it was determined that the earlier dates NZA 65137 and NZA 65138 were down to human error which must have resulted in swapping of the samples.

cm	Samplpe type	Lab code	14C yr BP	Cal yr BP
Horo 10				
2-12	Cladocera ehippia	NZA 65134	Modern	1959-1997 AD
80-90	Cladocera ehippia	NZA 65136	1094 ± 20	972-924
80-85	Cladocera ehippia	NZA 65080	1077 ± 108	1177-735
80-85	<90 μ m bulk sediment	NZA 65824	960 ± 20	907-770
80-85	Lake margin plant material	NZA 65079	780 ± 50	740-564
85	Seed	NZA 65135	480 ± 19	519-486
202-208	Cladocera ehippia	NZA 65822	2368 ± 21	2360-2313
299-305	Cladocera ehippia	NZA 65823	3483 ± 22	3827-3612
200-210	Cladocera ehippia	NZA 65137	3410 ± 21	3692-3510
297-307	Cladocera ehippia	NZA 65138	2259 ± 20	2315-2155

Table 5: Radiocarbon dates.

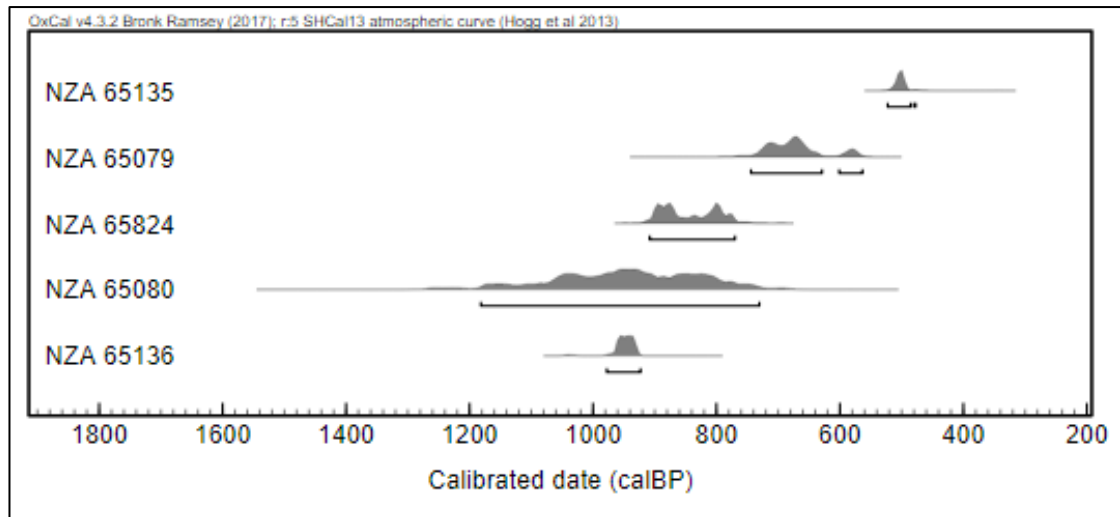


Figure 17: Multiplot of radiocarbon dates from the 80-90 cm range (cal yr BP). Plotted are: the seed from 85 cm (NZA 65135), lake margin plant material from 80-85 cm (NZA 65079), bulk sediment from 80-85 cm (NZA 65824), and *Cladocera ephippia* from 80-85 cm (NZA 65080) and 80-90 cm (NZA 65136).

Age-depth model

The age-depth model at 95.4% confidence interval is presented in Figure 18.

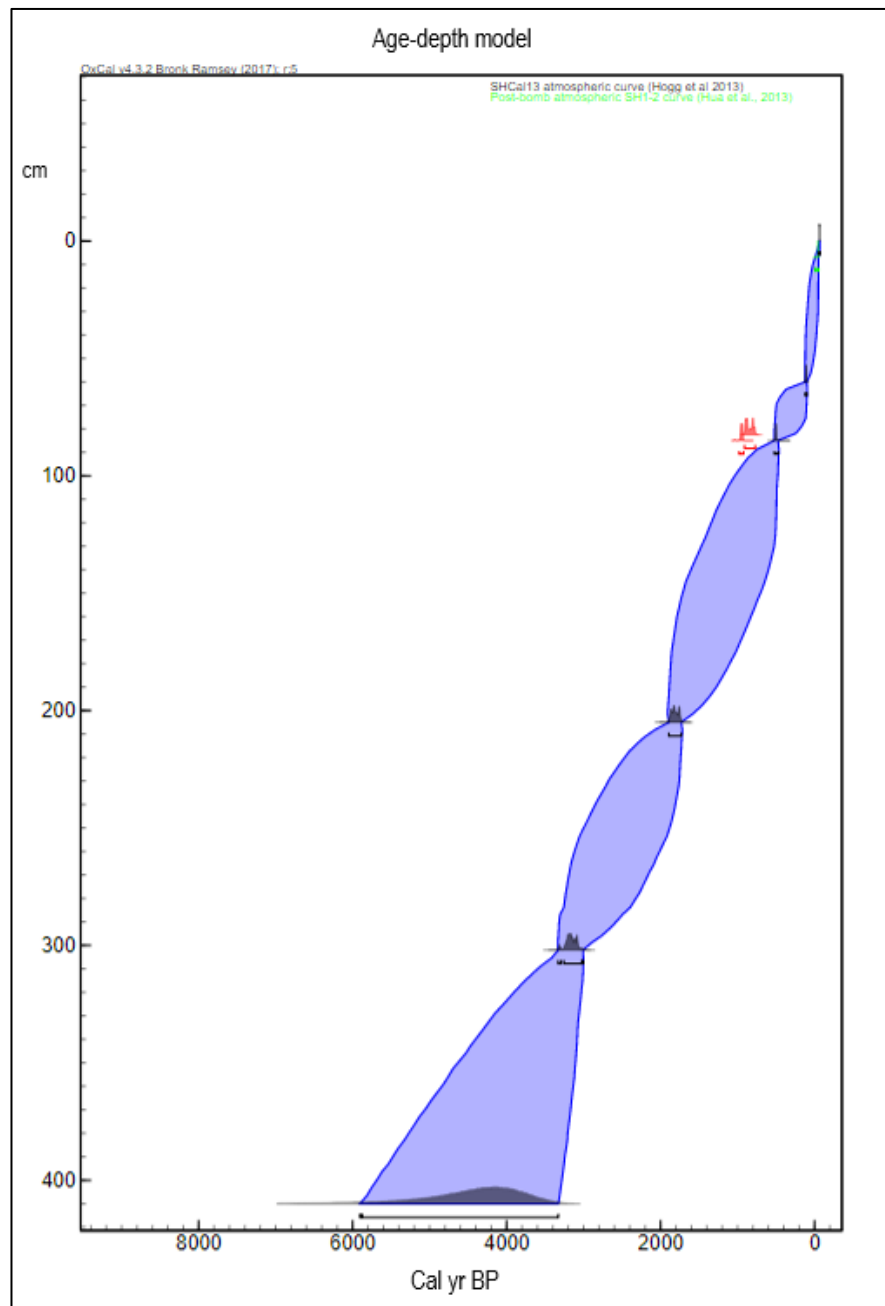


Figure 18: Age-depth model at 95.4% confidence interval. Radiocarbon dates used in this model: NZA 65134, NZA 65135, NZA 65822, and NZA 65823. Present day and European arrival (based on pollen indicators) c. 1840 AD were also plotted. Correction of 448 ± 22 years was applied to NZA 65822 and NZA 65823 as the linear relationship between NZA 65136, NZA 65822, and NZA 65823 implies an error is present in the older dates as well (Fig. 19). Calibration carried out with SHCal13 (Hogg et al., 2013) and post-bomb SH1-2 (Hua et al., 2013) calibration curves. NZA 65824 and NZA 65136 are plotted as outliers in red.

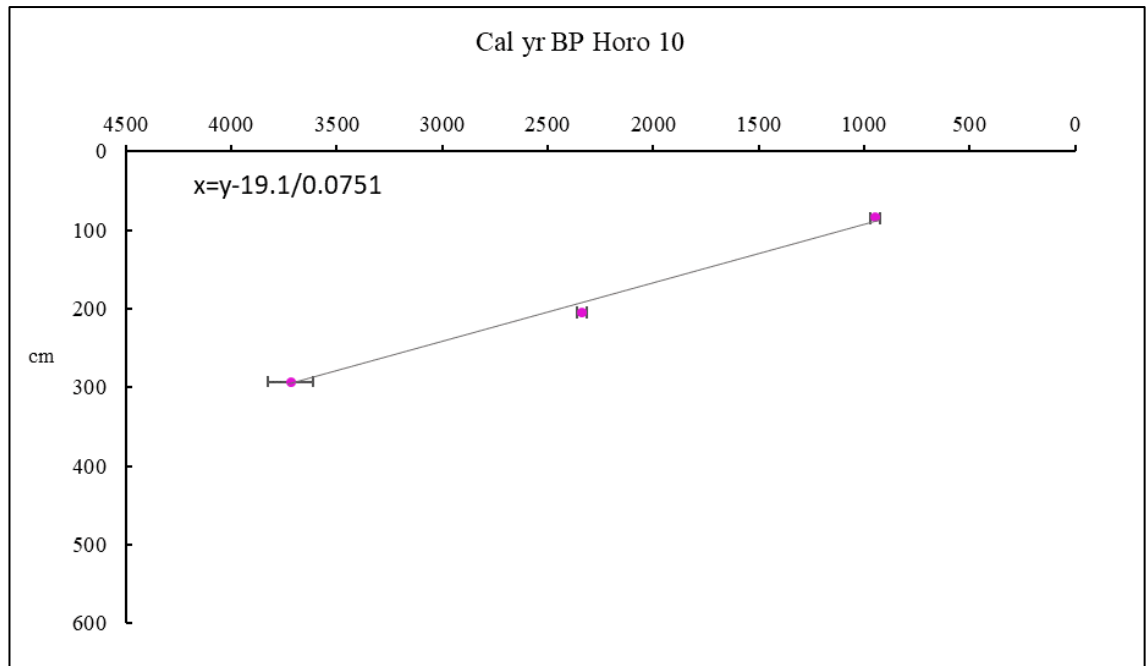


Figure 19: *Cladocera ephippia* midpoint cal yr BP ages and 2 sigma error. Plotted are: NZA 65136, NZA 65822, and NZA 65823.

Due to the low dating resolution in the core (a result of timing and budgetary constraints), age ranges at a given depth interpolated from the age-depth model are large. In this study, dates obtained via the age-depth model to infer the timing of events of interest and the pollen zones are reported as the mean cal yr BP age. Using a point estimate such as the mean or median, however, fails to account for the large uncertainties in the age-model, meaning that there is a very small likelihood that the mean represents the true age (Kennett et al., 2015). However, due to a lack of radiocarbon dates at events of interest, for interpretation purposes and simplicity, the mean age is used. It is important to keep in mind that in the discussion, there is likely to be inconsistencies in the timing of events in this study that have been correlated to events in others due to these uncertainties. When comparison is done with the timing of events in other studies, this may also be affected by difference in age models between this study and others. Further compounding this issue is the effect that core shortening will have. The material sampled for radiocarbon dating is not in its true original position, and, depending on the position in the core, originally would have been somewhere above the subsampling depth, especially in the upper sediment of each core.

Sedimentation rates

Sedimentation rates extracted from the age-depth model from depth ranges of interest are shown in Table 6. The sedimentation rate fluctuates up core between 0.08-0.07 cm a⁻¹ (pre-human and Polynesian eras) to a very high sedimentation rate of 34 cm a⁻¹ during the European era (0-60 cm).

Core	cm	cm a ⁻¹	cm a ⁻¹⁰⁰
Horo 10	0-60	0.34	34.03
	61-85	0.07	6.69
	86-285	0.08	8.35
	286-390	0.08	8.17
Average	0-390	0.12	12.15

Table 6: Sedimentation rates.

4.4.2 Lead-210 and cesium-137 concentration dating

The ²¹⁰Pb concentration profile indicates that the upper 28 cm is less than 100 years old as background levels were not reached (Fig. 20) (Baskaran et al., 2014). The ¹³⁷Cs profile lacks a distinctive peak correlating to the nuclear fallout in 1963 AD (Baskaran et al., 2014), indicating that c. 1960 AD is between the non-sampled interval of 17-28 cm.

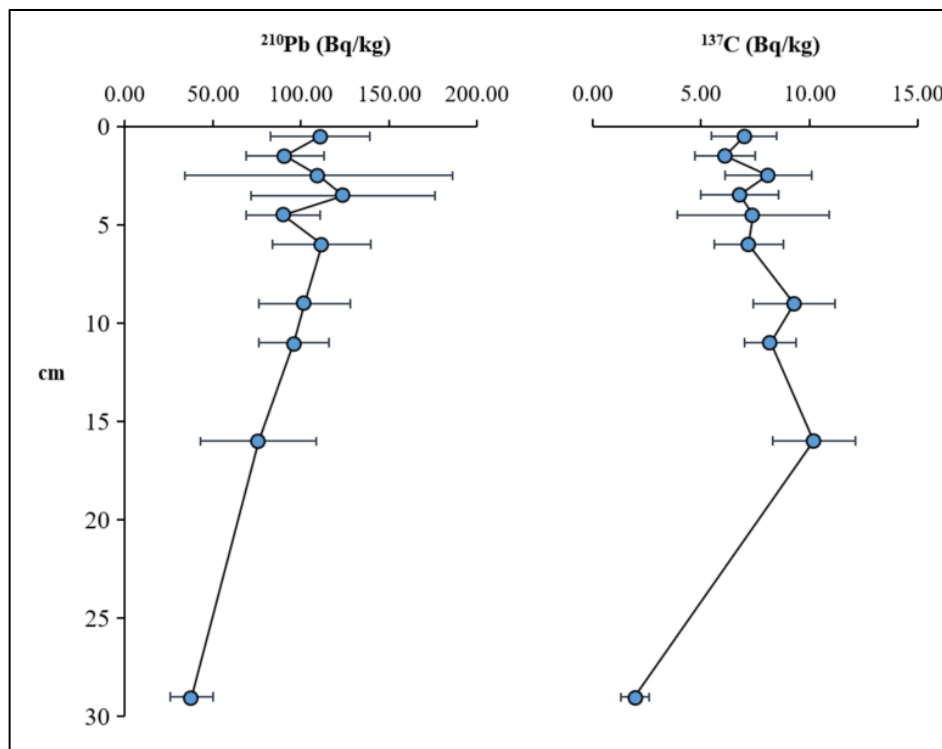


Figure 20: ²¹⁰Pb and ¹³⁷Cs concentration curves expressed in S.I units of Becquerels (Bq). This is equivalent to 1 radioactive disintegration per second (Swales et al., 2010).

4.5 Bulk density measurements

Bulk density values decrease up core and range from ~0.4 to 0.15 g/cm³ (Fig. 21). A relatively sharp decrease begins at 311 cm, which is broadly consistent with the transition from organic-rich silt to organic-rich lake mud. Following this, is a relatively smooth up core decrease in bulk

density, as would be expected as degree of compaction decreases. The coherent to incoherent scatter ratio, which measures the water content in the sediments obtained via XRF, is broadly synchronous with the bulk density trend.

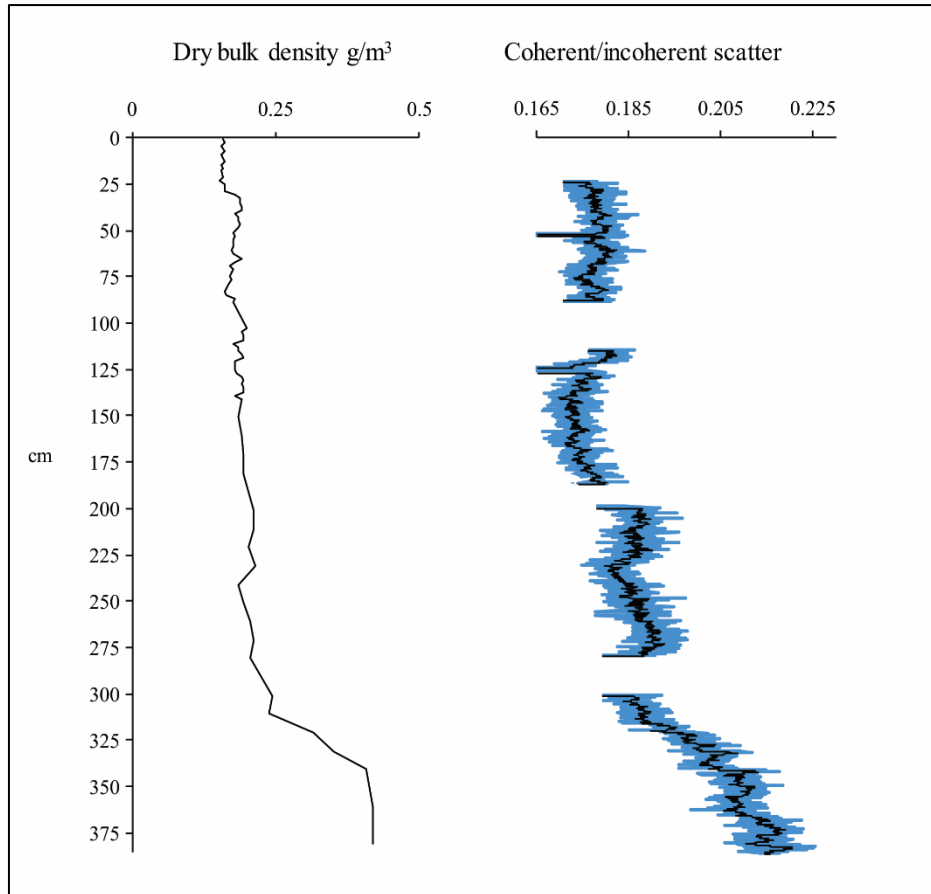


Figure 21: Dry bulk density and coherent/incoherent scatter via XRF.

4.6 Pollen analysis

Zones for the pollen diagram (Table 7 & Fig. 22) were defined using the CONISS dendrogram as a guide. Table 7 shows the age cut-offs used for the pollen zones, and the means of obtaining these cut-offs. Four zones were identified. These were: HW1 390-285 cm, HW2 285-85 cm, HW3 85-60 cm, and HW4 60-0 cm. Zones HW1 and HW2 predate human arrival in New Zealand, while zones HW3 and HW4 contain evidence of Polynesian (Māori) and then European presence. Zones are described using changes to the main taxa as well as changes to the PMI (Fig. 23).

Depth (cm)	Pollen zone	Age range	Age of pollen zone basal boundary	Supporting evidence
60	HW4		1840 AD	<i>Pinus radiata</i> pollen.
85	HW3	519-486 cal yr BP	502 cal yr BP	Mid age of radiocarbon date of seed found at 85 cm.
285	HW2	3,276-2,433 cal yr BP	2,924 cal yr BP	Mean age from age-depth model.
390	HW1	5,477-3,244 cal yr BP	4,213 cal yr BP	Mean age from age-depth model.

Table 7: Pollen zone ages.

HW1 390-285 cm 4,213-2,924 cal yr BP

This zone is dominated by pollen of tall tree taxa (~85-90%), specifically *Dacrydium cupressinum*, *Podocarpus*, and *Prumnopitys taxifolia*. These species dominate the tall tree taxa throughout the pre-human zones. *Dacrycarpus dacrydioides* and *Fuscospora* also occur in this zone and all other zones in minor amounts. Small trees and shrubs make up around 10% of the spectra in this zone, and are largely represented by *Alectryon excelsus*, *Ascarina lucida*, *Coprosma*, *Coriaria*, and Malvaceae. Additionally, *Dodonaea viscosa* and *Myrsine* also appear towards the top of the zone. Wetland and aquatics comprise mostly Cyperaceae and Haloragaceae, and *Typha orientalis* occurs in very small percentages. Ferns are represented by spores of *Cyathea* and *Phymatosorus*, which decline up zone, while monolet fern spores remain stable. Very little pollen of herbs and grasses were observed. *Pediastrum* values are relatively high at the base of this zone, equivalent to between 100 and 200% of the total dryland pollen, values then decline and remain at low concentrations throughout the rest of the pre-human zones. Small (<20 µm) and medium (20-50 µm) sized charcoal particles are also apparent in this zone (and up until HW2). Relative proportions of small trees and shrubs, and herbs and grasses decline towards the top of the zone, while tall trees increase. Pollen concentration is stable throughout this zone and until the middle of HW2 and is around 80,000 grains per cubic cm of sediment. PMI values are largely negative in this zone.

HW2 285-85 cm 2,924-502 cal yr BP

This zone is represented again by the same taxa in the previous zones. Tall tree types again dominate this zone (~90%). *Dacrycarpus dacrydioides* and *Dacrydium cupressinum* peak when *Prumnopitys taxifolia* troughs. *Fuscospora* increases from the middle to the upper part of the zone. Towards the top of the zone, *Fuscospora* and *P. taxifolia* decrease, while *D. cupressinum* increases. This zone contains a larger diversity of small trees and shrubs, but again in very low abundance (2-10%). Both the small trees and shrubs, and herbs and grasses groups almost disappear completely in the middle of this zone, while herbs and grasses disappear several more times throughout the zone. Small trees and shrubs are represented by *Coprosma*, *Coriaria*

arborea, *Dodonaea viscosa*, Malvaceae, *Myrsine*, *Phyllocladus*, *Ascarina lucida*, and *Pseudowintera*. *Cyathea*, *Dicksonia*, *Phymatosorus*, and monolete fern spores fluctuate up zone. Towards the top of this zone is a slight increase in *Pteridium*. Wetland and aquatic taxa are represented by Cyperaceae, which shows a general decline up zone, and small occurrences of *Typha orientalis*. Small (<20 µm) and medium (20-50 µm) sized charcoal particles decline from the previous zone and through this zone. Pollen concentration fluctuates from 60,000 to 130,000 grains per cubic cm of sediment. A significant increase occurs at 230 cm and 240 cm of 177,000 and 250,000 grains per cubic cm of sediment, respectively. PMI values fluctuate markedly in this zone and reach their lowest in the core at 160 cm.

HW3 85-60 cm 2,924-502 cal yr BP

This zone is characterised by a significant rise in *Pteridium*, charcoal fragments, and *Pediastrum* colonies, signalling Polynesian arrival to Lake Horowhenua and surrounds. A seed found at 85 cm has been radiocarbon dated putting the age of arrival at 519-486 cal yr BP. Tall tree taxa decline from ~95% down to 75%. Small trees and shrubs increase from ~5% up to 20%, and herbs and grasses also increase relative to previous levels. *Dacrydium cupressinum* remains stable, however, levels of pollen of all other Podocarps decline at the onset of this zone, while *Alectryon excelsus* increases. *Fuscospora* increases from prior levels. Species indicative of disturbance (*Coprosma* and *Coriaria arborea*), open conditions around the lake (*Typha orientalis*), and Poaceae also increase in this zone. Cyperaceae remain at low levels. Monolete fern spores and *Phymatosorus* also increase up zone, while *Cyathea* significantly declines. Pollen concentration decreases from prior levels and reaches the lowest throughout the profile. Pollen concentration ranges from 40,000-50,000 grains per cubic cm of sediment. PMI values are positive but fluctuate slightly in this zone and reach the highest in the profile at 70 cm.

HW4 60-0 cm 1840-present

This zone is divided into two subzones: HW4a and HW4b. HW4a (60-40 cm) comprises a decrease in tall forest taxa from 75% down to 55%, an increase Poaceae pollen, and the appearance of exotic *Pinus radiata*, signalling European arrival to the area. Levels of *Pteridium* spores and microscopic charcoal also increase. *Coprosma* and *Coriaria arborea* dominate the shrub class prior to the onset of phase two. *Typha orientalis* and Cyperaceae pollen remain somewhat stable from previous levels. *Dicksonia*, *Phymatosorus*, *Cyathea*, and monolete fern spores increase up subzone HW4a, before remaining stable and declining through HW4b. Subzone HW4b (40-0 cm) begins with a significant increase in Poaceae, and a decline in charcoal and *Pteridium* from previous levels. *Pediastrum* abundance increases at 15 cm and then dramatically rises abruptly at 10 cm. *Pediastrum* values are equivalent to between 200 to 500% of the total dryland pollen. *Potamogeton* appears at 40 cm and increases at 15 cm. *Coprosma* and

Coriaria decrease to present day and very little other shrubs are apparent. Pollen of the *Taraxacum* and Poaceae classes, and Cyperaceae, increase from previous levels, while *Typha* decline. Pollen concentration ranges from 50,000-90,000 grains per cubic cm of sediment. PMI values are positive, but decline from the previous zone, then fluctuate between 35-0 cm.

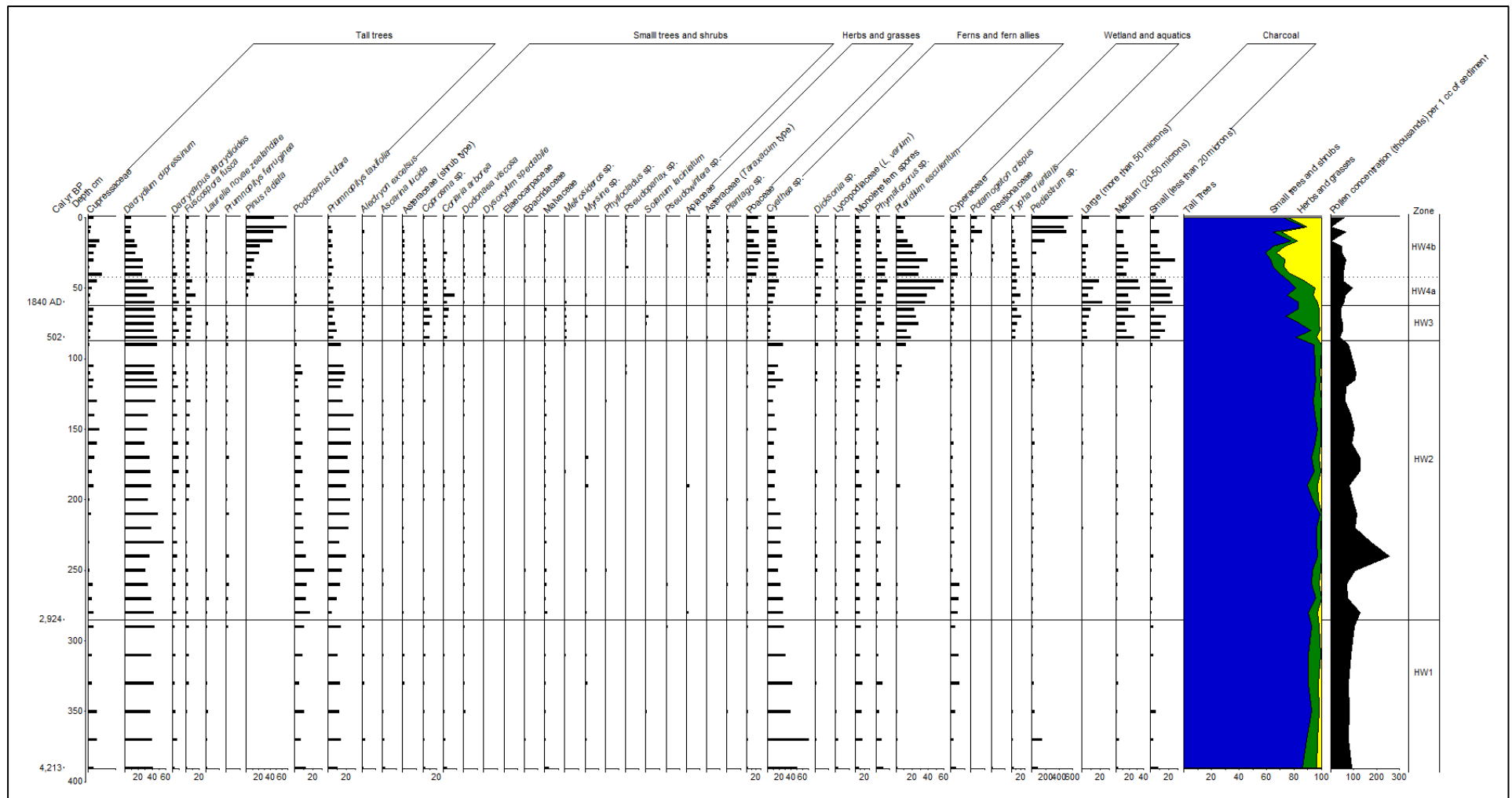


Figure 22: Relative pollen diagram of selected taxa only. A full diagram can be found in Appendix E.

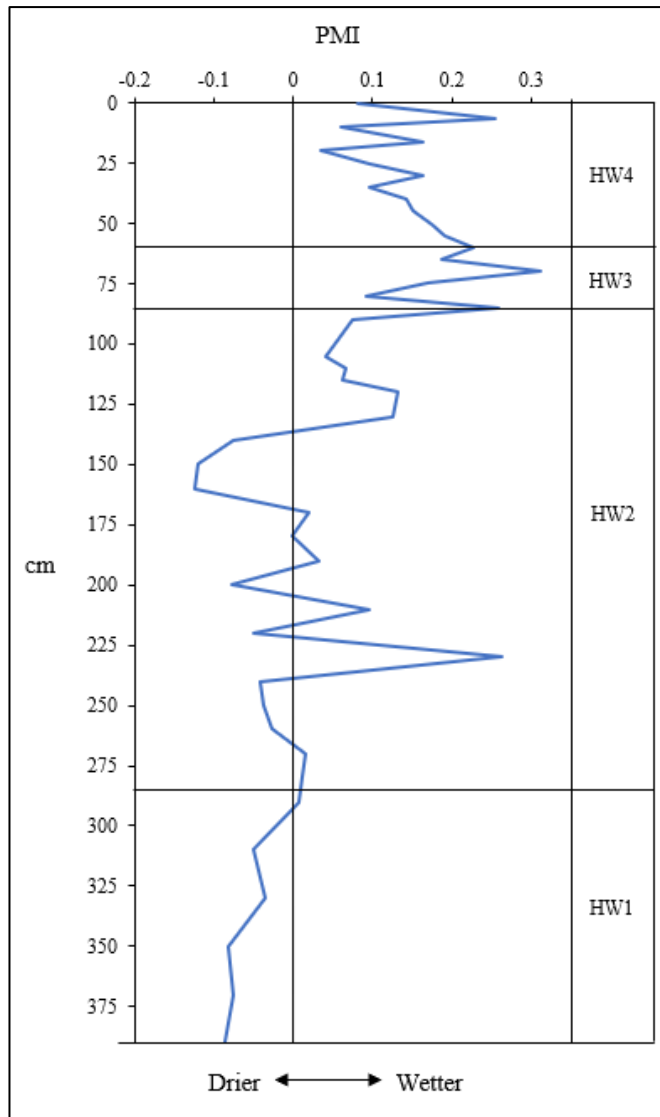


Figure 23: Pollen moisture index.

4.7 Grain size proxies (LPA and XRF)

The changes in proportions of the five grain size classes indicate that at the base of the core, the sediment is dominated by coarse silt and sand (Fig. 24). An overall trend of slight coarsening up core is evident in a reduction in the clay category, and an increase in the fine and medium silt categories. However, the sand category shows a slight reduction up core, but peaks occur at ~275, 225, 115, 85, 37, 6.5, and 0 cm. A coarsening in the fine and medium silt size classes occurs from ~150-115 cm and at 67 cm. Mean grain size varies greatly up core from 17-43 μm . A slight decreasing trend in mean grain size can be seen up core. A broad peak in mean grain size occurs at 115-103 cm. An outlier has been detected at 109 cm, as the sample returned a mean grain size of 155 μm . Unfortunately, due to sample availability, a repeat analysis was unable to be carried out, and therefore this sample has been removed from the data analysis.

The gaps in the XRF data represent where the core had a low profile and was unable to be scanned, in addition to missed recovery of sediment as a result of core shortening. The Fe/Ti ratio and the Ti/K ratio show a broadly opposite trend to one another, where a peak in the Fe/Ti ratio is matched by a trough in the Ti/K ratio, indicating that Ti is the controlling element. An increase in the Fe/Ti ratio indicates sediment with a smaller grain size, while increases in the Ti/K ratio indicates sediment with a larger grain size (Davies et al., 2015). Both the Fe/Ti and Ti/K ratio values are lowest between 390-330 cm and highest between ~80-65 cm. The overall trend indicates that at the base of the core, the lake was receiving coarser sediments, with these becoming somewhat finer up until 110 cm. At the top of the core, the plots fluctuate significantly compared to the rest of the core, with peaks in the Ti/K ratio and troughs in the Fe/Ti ratio suggesting an increase in grain size. The Fe/Ti ratio reaches very low values from 40 cm, indicative of the supply of much larger grains to the lake.

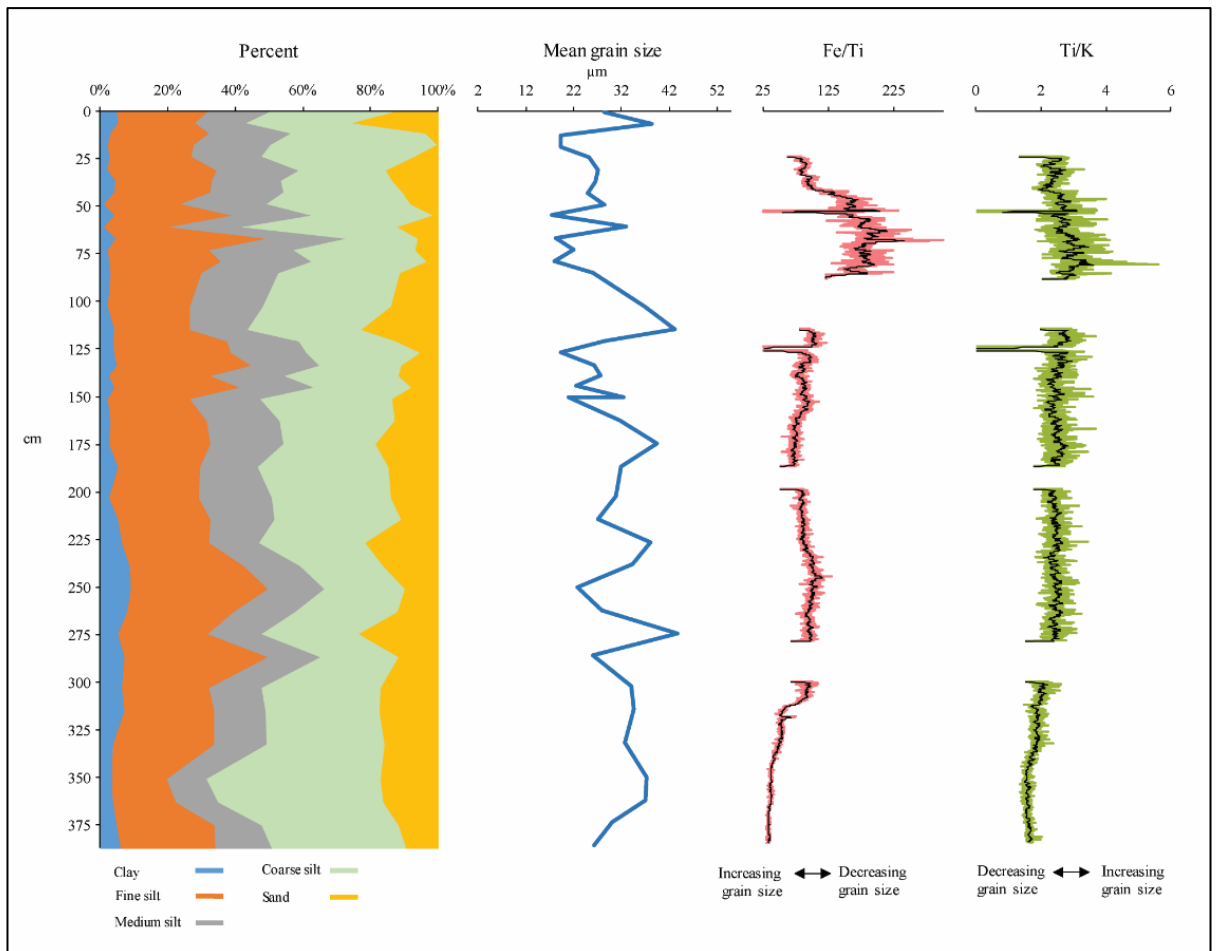


Figure 24: Grain size data (LPA and XRF).

4.8 Geochemistry

4.8.1 Carbon and nitrogen analysis

The plot below (Fig. 25) indicates that the correction to remove inorganic nitrogen is 0.06%. This value has been used to correct the C/N ratio plot.

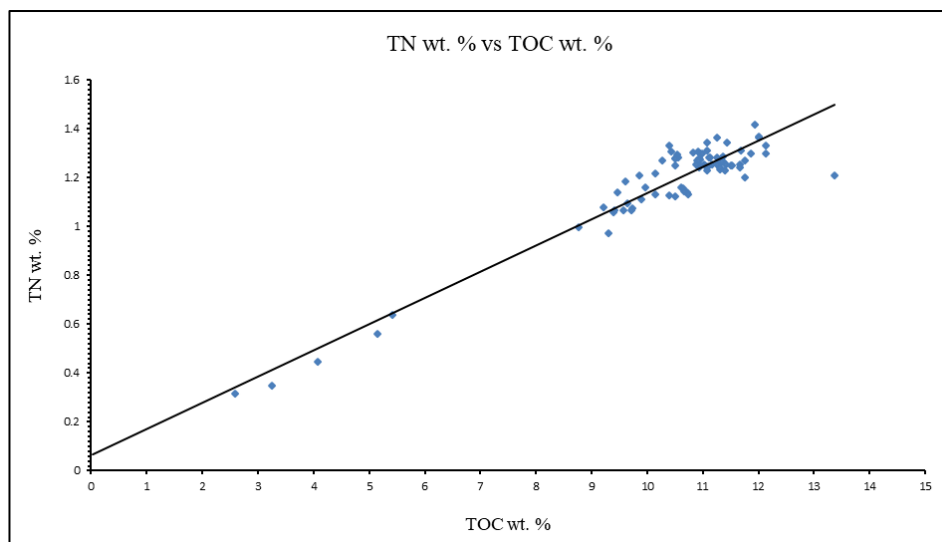


Figure 25: TOC wt. % and TN wt. % to determine inorganic nitrogen contribution to correct the C/N ratio.

The overall trend in the C/N ratio (Fig. 26) is relatively high values from 390-275 cm of 12-10.5, then a decline in values from 275-140 cm of 11-10. A peak of 12 occurs at ~120 cm and ~85 cm, before declining to the lowest value in the profile of 9.5 at ~68 cm. Values then generally increase, with an anomalously high peak of ~14 at 21 cm.

The TOC and TN plot (Fig. 26) show a broadly synchronous trend. TOC ranges from 3 to 12% with the lowest values at the base of the core. Values increase at 311 cm and remain relatively stable through the rest of the core. A sharp peak of 13% at 21 cm in the TOC plot is not apparent in the TN plot. TN values range from 0.35-1.4%, with the lowest values at the base of the core, following this, values are rather stable. In the TOC plot, the upper ~140 cm comprise of two peaks of ~12% at ~130 cm and ~80 cm. In the TN plot, there is a decrease between 130-90 cm from 1.30% to 1.10%, followed by an increase to 1.40% at ~80 cm. The TOC plot shows a slight increase from 70 cm to present, while the TN plot shows a slight decrease.

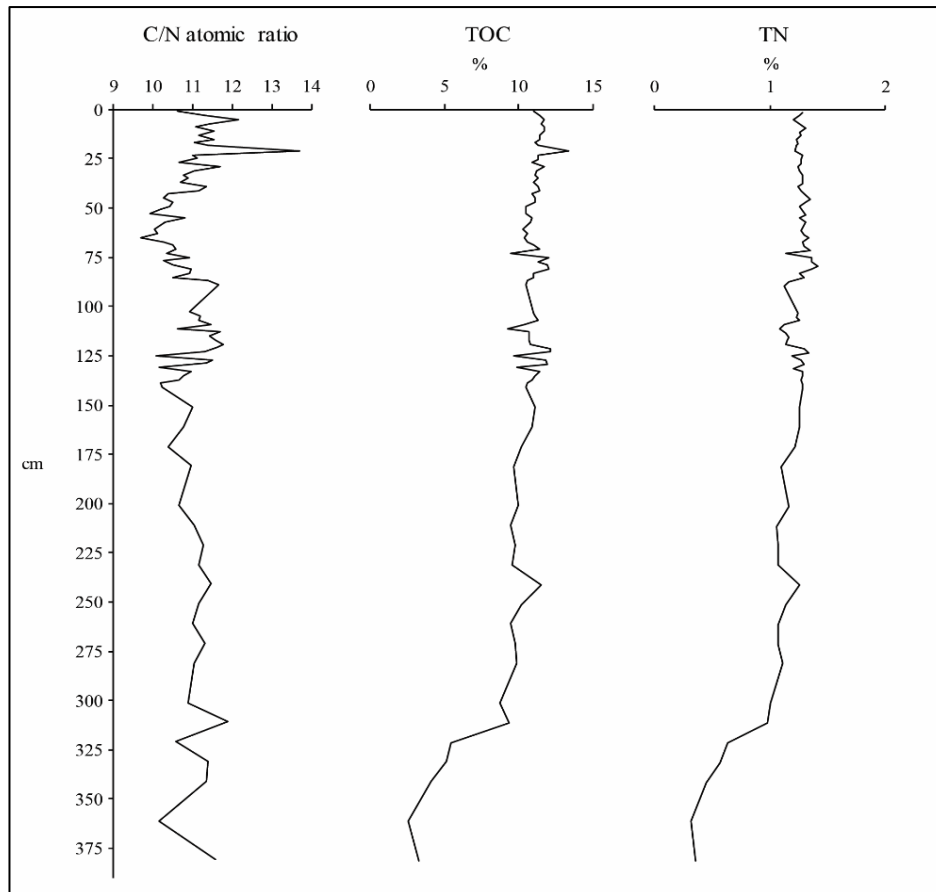


Figure 26: From left to right: C/N atomic ratio. TOC wt. %. TN wt. %.

4.8.2 Organic matter content (via loss on ignition, Elementar, and XRF)

Organic matter content (OM%) calculated via Elementar TOC values ($OM\%^T$) ranges from ~6.5-24% (Fig. 27). The low values correspond to the silt-rich organic sediments at the base of the core. From 381-311 cm, there is a sharp increase from 6.5% to 18%. From 311 cm, values generally increase up core from 18% to 23%. Between ~300 cm and 140 cm, OM% values remain relatively stable. Three small peaks occur at 245 cm, 135-115 cm, and 85-60 cm, and a sharp peak of 26% at 21 cm. There is a very slight incline from 50 cm to present.

Organic matter content via LOI $OM\%^L$ shows a similar trend to $OM\%^T$. However, there are some differences; likely due to sampling resolution. For example, a sharp peak at 21 cm and a sharp trough at 73 cm in the $OM\%^T$ plot is not apparent in the $OM\%^L$ plot. Low OM content is apparent at the base of the core, at 115-85 cm, and at 65-29 cm in both the $OM\%^L$ and $OM\%^T$ plots. High OM% is apparent in both plots at around 135-115 cm and 85-60 cm. Interestingly, the $OM\%^T$ ranges from 6.5-24% (excluding the sharp peak at 21 cm), while the $OM\%^L$ values range from 3-

28%. Using a 13% correction to the $OM\%^L$, the $OM\%^T$ and $OM\%^L$ become more agreeable. The incoherent to coherent scatter via XRF generally agrees with the $OM\%^L$ and $OM\%^T$ plots.

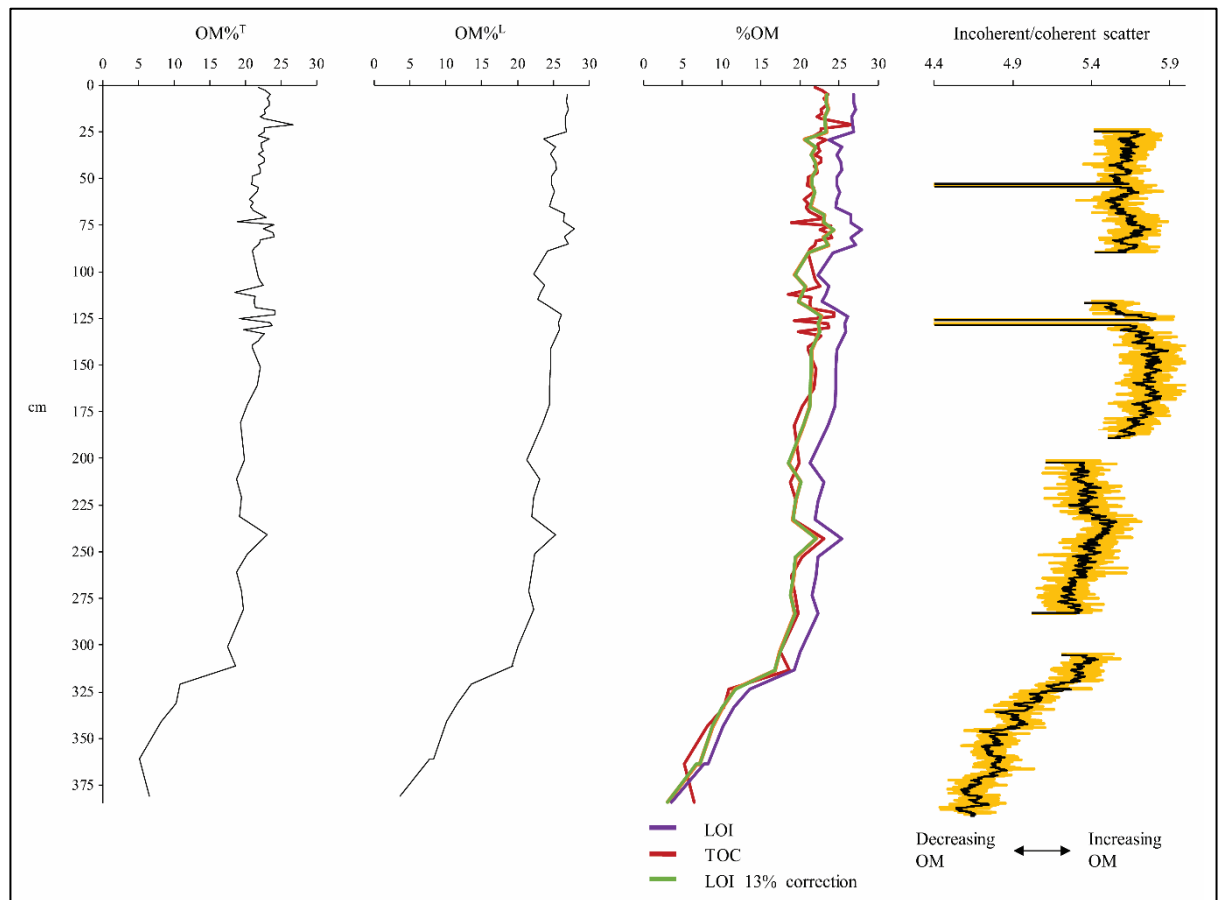


Figure 27: Organic matter proxies. From left to right: $OM\%^T$. $OM\%^L$. $OM\%^L$ stacked against $OM\%^T$ and $OM\%^L$ with 13% correction. XRF incoherent/coherent scatter.

4.8.3 Elemental and XRF proxies for oxygenation and water quality

The Fe/Mn ratio and Fe via XRF show an opposing trend through the majority of the core, except at 180-110 cm where the curves are broadly synchronous (Fig. 28). The largely opposing trend of the Fe/Mn ratio and Fe obtained via XRF confirms that the Fe/Mn ratio in Lake Horowhenua sediment largely reflects redox processes rather than catchment inputs. The Fe/Mn ratio via atomic emission spectroscopy is broadly synchronous with that of the XRF data. The Fe/Mn ratio via atomic emission spectroscopy ranges from 33-122. Distinct peaks of 90-120 occur through the profile at 281, 261, 130, and 85 cm. A distinct trough of around 60 occurs at ~310 cm. From 60 cm, values steeply decline to the present. Phosphorous values (P) via XRF are higher at the base and top of the core. The phosphorus counts do not seem to correlate well with the Fe/Mn ratio and are therefore not a reliable indicator for eutrophication.

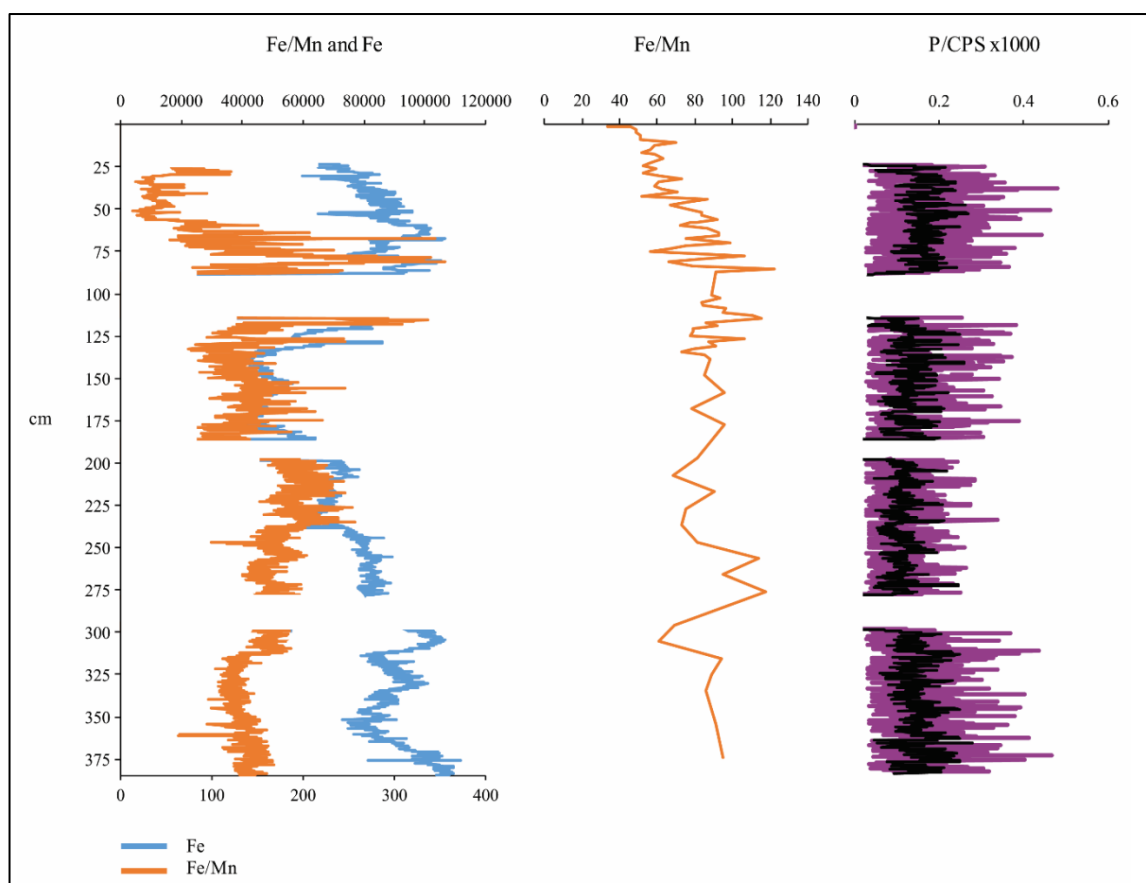


Figure 28: Oxygen and water quality indicators. From left to right: Fe/Mn ratio and Fe counts via XRF as a proxy for oxygenation. Fe/Mn ratio via atomic emission spectroscopy as a proxy for oxygenation. P/CPS x 1000 via XRF as a proxy for productivity.

4.8.4 Elemental and XRF proxies for erosion

Magnetic susceptibility varies between 178 to 2 ($\text{SI} \times 10^{-5}$), with the highest values encountered at the base of the core and lowest values between the ~170-135 cm range (Fig. 29). Values are notably high and highly variable within the basal sediments (390-310 cm), correlating with high bulk density values and low OM% (Fig. 21 & 27). From ~320 cm, values dramatically decline and then continue to gradually decline to ~230 cm before rising slightly to a small peak at ~205 cm. Following this, values decline further to the lowest values at 170-135 cm before rising again slightly into the upper 90 cm where they then remain stable. But overall, the values and degree of variation in the upper sediments is negligible compared to that seen in the basal sediments.

Values of Ti, K, Rb, and Al obtained via XRF show a similar pattern to one another and to that of the magnetic susceptibility (Fig. 29), however, there is less variability in the basal sediments compared to the magnetic susceptibility. Ti, K, Rb, and Al via XRF show a very general decrease up core from the highest counts at 390-310 cm. Between ~275-135 cm, all XRF proxies for erosion are generally low. A small increase can be seen in the Ti and K plot around 205 cm and

130 cm. Ti, K, and Rb decrease to their lowest values between ~90-50 cm, while Al shows slight increase in values from 85 to the present. Ti, K and, Rb show an increase from ~40 cm to the present day.

The Al% obtained via atomic emission spectroscopy shows a more varied pattern than that of Al via XRF. The highest values are at the base of the core, and at 80 cm and 15 cm. Al% fluctuates from 2.1-4.1% through the lower and middle portions of the core. The overall pattern for 140-115 cm is represented by relatively low values of around 1.8%, followed by increasing values between 115-75 cm of 2.5-3.25%. This is followed by a decline at ~70 cm to 1.75%, where values then steeply incline from 1.75-3.5% from 60 cm to the present day.

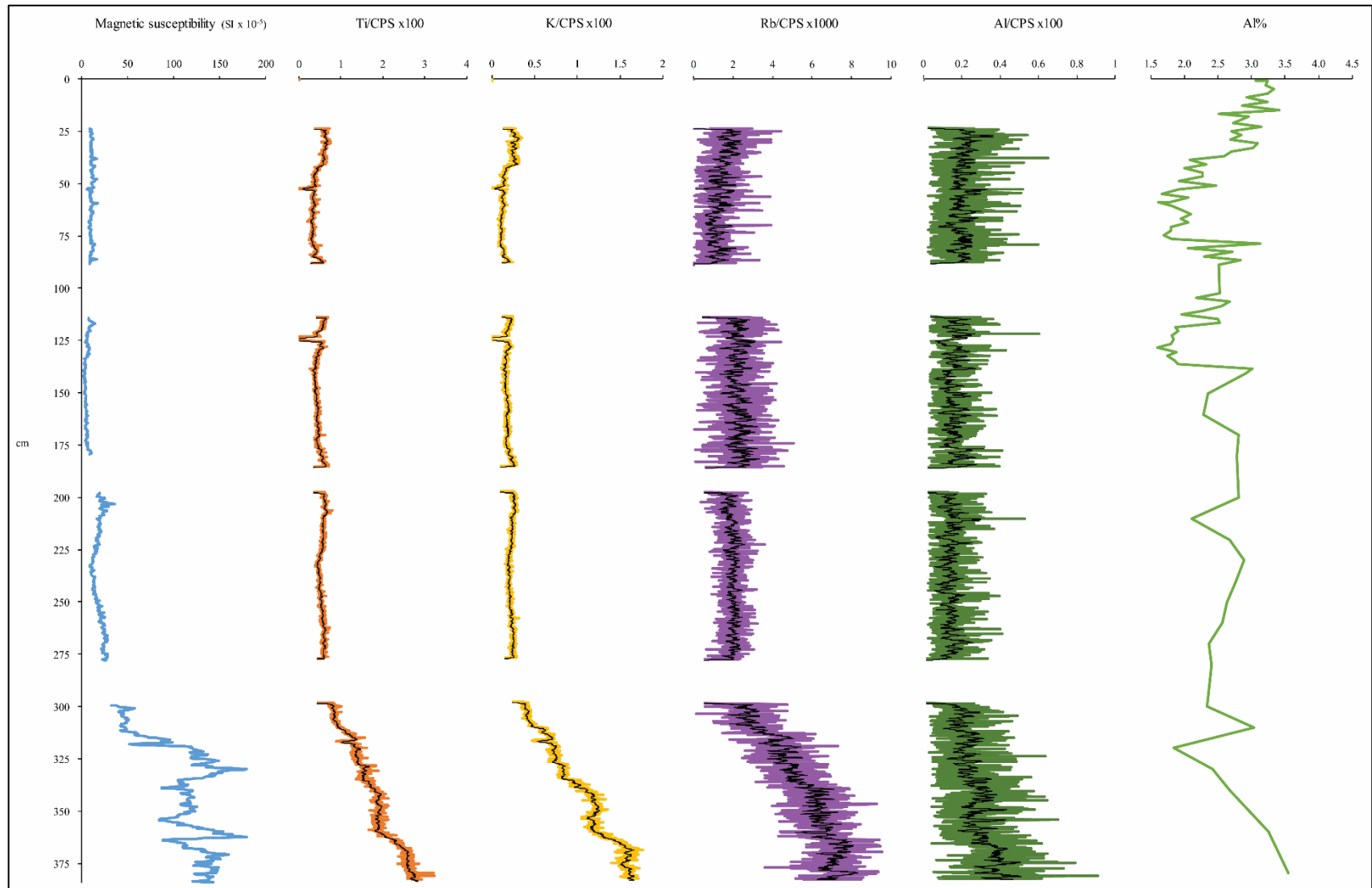


Figure 29: XRF and elemental proxies for erosion. From left to right: Magnetic susceptibility, Ti/CPS $\times 100$, K/CPS $\times 100$, Rb/CPS $\times 1000$, Al/CPS $\times 100$ via XRF. Al% via atomic emission spectroscopy.

Chapter 5: Discussion

The first part of the discussion is an interpretation and assessment of the chronology. The second part of the discussion is an interpretation of the formation and evolution of Lake Horowhenua and the source of the sand layer recognised towards the base of the cores proximal to the outlet. The third part contains a chronological interpretation using the pollen inferred zones of the environmental proxies used in this study as they relate to vegetation change, human arrival, bottom water oxygenation and water quality, and catchment disturbance.

5.1 Assessment of radiocarbon dating

As mentioned previously, a variety of different materials were submitted for radiocarbon dating. These were: bulk sediment, Cladocera ehippia, lake margin plant material, and a single seed. The results indicate discrepancies between the ages taken at the same depth. These issues are discussed in detail below.

Reservoir effect

The seed is taken to represent a true age for three reasons: the carbon in the seed was attained from the atmosphere, it is also unlikely to have been bioturbated into sediment that is much older, and the seed appeared to be free from contamination. Therefore, the difference in age between the Cladocera ehippia (NZA 65136 and NZA 65080), the lake margin plant material (NZA 65079), and the bulk sediment (NZA 65824) to the seed (NZA 65135) taken from a similar depth can be explained by a reservoir effect.

The difference between the Cladocera ehippia dates (NZA 65136 and NZA 65080) and the seed is 448 ± 22 years and 445 ± 19 years, respectively. Carbon in Cladocera can come from a variety of sources. Cladocera are known to consume algae, bacteria, detritus, and plant remains (Smirnov, 2014). The food they eat, i.e. primary producers, may uptake inorganic carbon, or in the case of detritus this may contain carbon from a variety of carbon sources, such as the remains of primary producers, terrestrial plant remains, and terrestrial particulate organic carbon. Diet also varies dependent on the Cladocera species, whether they are pelagic or littoral (Smirnov, 2014), and the availability of food source (Pulido-Villena et al., 2005).

Aquatic organisms, such as primary producers and bacteria (Branstrator & Lehman, 1991; Greenwood et al., 1999; Vandergoes et al., 2018), uptake dissolved inorganic carbon from the lake water. This inorganic carbon can come from a variety of sources (old and young), i.e. carbonate rocks in the catchment resulting in a hard water effect, old groundwater, respiration by aquatic plants and respiration of organic matter in the sediment, and atmospheric draw down (Palmer et al., 2001). Due to the lack of carbonate bearing rocks within the catchment, this is

unlikely to be the source of the reservoir age. In soft water lakes, old groundwater is a common cause of old radiocarbon dates (Philippsen, 2013).

Old groundwater can result from residence times or inputs of old carbon into the groundwater (Ascough et al., 2011) altering the $^{14}\text{C}:$ ^{12}C ratio (Vandergoes et al., 2018). Studies of the residence time of groundwater in the Manawatū and Horowhenua district using isotopic tracers has been carried out by GNS (Morgenstern et al., 2015). They found that the average residence time for groundwater on the Horowhenua plains is between 10-40 years, while the residence time of water in the lake is reported to be 50 days (Gibbs & White, 1994). These results suggest that the residence time of the groundwater and the turnover in the lake would not have a significant effect on radiocarbon ages. Other possible sources of ^{14}C depleted carbon in groundwater can result from the dissolution of old soil carbonate into the groundwater and oxidation of old organic carbon within the water (Boaretto et al., 1997).

As mentioned above, detritus consumed by Cladocera can be made up of a selection of organic remains, some of which may also be ^{14}C depleted by uptake of depleted inorganic carbon, e.g. algae, bacteria, and macrophytes (Li et al., 2018). Other organic constituents of detritus can consist of particulate organic matter from terrestrial sources (Müller-Solger et al., 2002; Smirnov, 2014) which are thought to be an important food source for littoral species (Smirnov, 2014). Terrestrial sources of organic matter may be in equilibrium with the atmosphere, e.g. recent detritus of plant remains and leaf litter. Other sources such as particulate organic matter and lignin can be many thousands of years old (McGlone & Wilmshurst, 1999), and may be used as a direct food source by Cladocera (Pulido-Villena et al., 2005) or fuel microbial respiration (Caraco et al., 2010). Consumption of highly aged particulate organic carbon by Cladocera is thought to produce old radiocarbon ages of crustacean zooplankton in the Hudson River (Caraco et al., 2010). Dissolved organic substances such as humics may also be assimilated by Cladocera (Jones, 1992; Smirnov, 2014).

The Cladocera ehippia samples (NZA 65136 and NZA 65080) and bulk sediment sample (NZA 65824) in the 80-90 cm range overlaps human arrival to Lake Horowhenua, which has been determined to occur at 85 cm. Highly aged particulate organic carbon may have entered the lake as a result of anthropogenic forest clearance post-human arrival inducing increased catchment erosion. As discussed earlier, this particular problem of in-washed soil carbon has caused much confusion with dating lake sediment post-human arrival (McGlone & Wilmshurst, 1999). This highly aged particulate carbon may have been directly used as a food source for the Cladocera; while old soil humics and other organic material would be directly incorporated into the sediment, resulting in the reservoir age of 344 ± 41 years in the bulk sediment (NZA 65824). Invertebrates

and primary producers that settle as detritus may further compound the reservoir age, as these may uptake old inorganic carbon from some of the sources mentioned previously.

The linear relationship of the Cladocera ehippia radiocarbon dates throughout the core (Fig. 19 in results) implies that a reservoir age is apparent in the deeper Cladocera ehippia radiocarbon dates. Old in-washed soil carbon contamination may not have been as significant when the catchment was forested. Therefore, the cause of the reservoir age in the older samples is likely a combination of some of the processes discussed above which may have exerted more or less influence over time.

In the case of the lake margin plant material (NZA 65079), which has tentatively been identified as *Phormium* by the GNS lab technicians, the age difference of 172 ± 47 years between the seed and plant remains is perplexing. *Phormium* is a terrestrial plant and obtains carbon for photosynthesis from the atmosphere. However, lake margin plants such as *Phormium*, may intake old dissolved inorganic carbon from the surrounding lake water when submerged, as has been found in *Typha*, *Phalaris*, and *Phragmites* (Marty & Myrbo, 2014) resulting in erroneous dates. If the plant remains were not *Phormium*, it is possible that they were of a submerged aquatic plant which are known to produce anomalously old radiocarbon ages (Marty & Myrbo, 2014; Turnbull, 2017).

Interestingly, there is no reservoir effect apparent in the Cladocera ehippia from 2-12 cm, which returned a modern equivalent age. Highly productive lakes can become atmospheric CO₂ sinks (Pacheco et al., 2014), therefore, in recent times the algae in the lake is likely to have been in isotopic equilibrium with the atmosphere (Fallu et al., 2004). The increase in primary productivity in recent decades (Gibbs & Quinn, 2012) may have resulted in Cladocera preferentially feeding on algae (Fallu et al., 2004) or algae detritus rather than old particulate organic carbon. It is thought that organic material that withstands decomposition for hundreds of years may be a poor food source (Caraco et al., 2010). Sewage effluent has been disposed of in the lake in the past and sewage detritus may also be a food source for Cladocera (Müller-Solger et al., 2002) and would be in equilibrium with the atmosphere, explaining the lack of a reservoir age in the upper sediments.

5.2 Lake formation and evolution

When considering the formation of the lake, the pre-lake sediments found in cores taken from near the outlet provide an insight into the pre-lake environment. An extrapolated age to the base of the grey silt of Horo 8, which was sampled near the outlet, gives an age of ~9,850 cal yr BP. These grey silty sediments from Horo 8 are interrupted by a paleosol deposited around 7,595-

7,480 cal yr BP. Above the paleosol, is organic-rich silt that is interrupted by the sand deposit dated at 7,245-7,006 cal yr BP. The fluvial sediments and paleosol are not seen in the master core (Horo 10). Following the sand deposit, the sediment grades from organic-rich silt to organic-rich lake mud. However, extrapolation to the base of Horo 8 may not be appropriate for three reasons. The lacustrine sediments at Lake Horowhenua have been proven to be erroneously old; the oldest radiocarbon dated sample is thought to be a paleosol, and assuming a constant sedimentation rate for and between fluvial deposits and a paleosol may be unrealistic.

These grey silts found in cores from near the outlet are interpreted to be deposits from successive flood events of the Ohau River prior to 7,538 cal yr BP. Adkin (1911) mapped the paleo Ohau River course and purported that the Ohau River meandered northwards from the range and directly through where Lake Horowhenua now sits. Furthermore, Hughes (2005) analysed borehole data between the Ohau and Manawatū Rivers and surmised that the floodplain gravels found in boreholes were deposited by the Ohau River during the Last Glacial Maximum (LGM), 28,000 to 18,000 cal yr BP (Alloway et al., 2007), and that the Ohau River did run through where Lake Horowhenua now sits (Fig. 30) (Hughes, 2005). It is these gravels that were encountered when coring Horo 10.

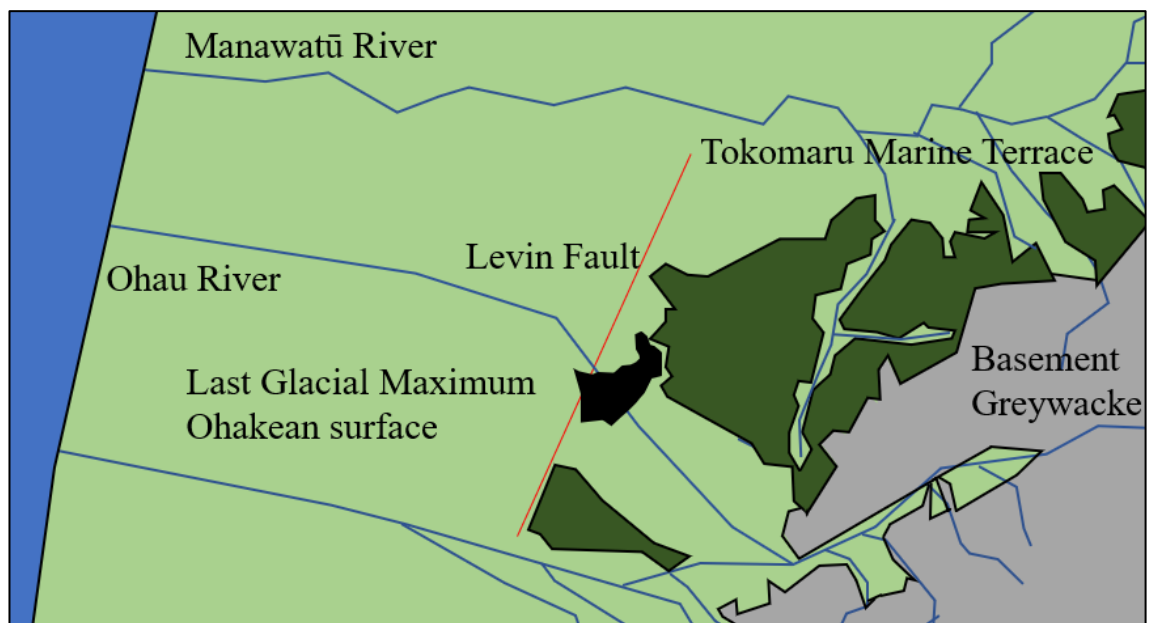


Figure 30: Conceptual model of marine oxygen isotope stage 2 in the Manawatū Horowhenua region (adapted from Clement, 2011; Hughes, 2005). The black silhouette is the current extent of Lake Horowhenua. The dark green represents the Tokomaru Marine Terrace.

The continuous nature of the deposits found in cores near the outlet may be a result of retrogressive aggradation. This mechanism is thought to be responsible for the deposition of the continuous flood plain alluvium of the Manawatū River deposited sometime around 14,000–12,500 years BP (Clement et al., 2017). The retrogressive sediments deposited by the Manawatū River were described by Clement (2011) as grey and greenish-grey silty clay or clayey silt and have been recorded by many well drillers as grey, blue or brown clays or silts, indeed very similar in nature to the deposits of the Ohau River. The silts of the Manawatū River are thought to have been deposited during the early stages of the post-glacial sea level rise as a result of the river responding with a flatter gradient which reduced stream power and the deposition of silts and clays over the top of the LGM fluvial gravels (Clement et al., 2017).

Following this, the Ohau River moved further south, as indicated by the deposition of a paleosol c. 7,595-7,480 cal yr BP. Sometime post-deposition of the paleosol, a proto lake or swamp began to form, as indicated by the olive-brown organic-rich silt overlying the paleosol. Dune transgression began around 7,700 cal yr BP (Clement & Fuller, 2018), creating around 100 dune lakes along the west coast of the lower North Island from Hawera to Otaki as a result of dune impeded drainage (Cunningham et al., 1953). At Lake Horowhenua, drainage of the small streams and the springs that enter the lake on the eastern shore would have been impeded, facilitating the formation of the lake, as indicated by the change to olive-brown organic-rich silt directly after the paleosol. While the location of the Levin Trough beneath the lake would have allowed for the persistence of a water body.

Adkin (1911) hypothesised the Ohau River became dammed by sand dunes sometime during the later Pleistocene, creating Lake Horowhenua which was around 5 to 6 square miles and 100 ft deep. He reports that the lake level was kept constant by an overflow to the sea until the enlargement of the Hokio outlet, perhaps as a result of the force from the deepening lake, which resulted in lowering of the lake level to the pre-weir level. The river moved south once the lake had reached its maximum extent, and erosion of the left bank deflected its path across the plain to its current position. The change from organic-rich silt post development of the paleosol indicates that the Ohau River was not dammed directly, as it had already moved south.

5.2.1 Sand deposit

The 10 cm thick sand deposit found in all cores near the outlet was compared to modern day beach sand, Foxton Phase dune sand, and two Ohau River sands, as these represented possible analogues of the source of the sand found in these cores. As mentioned previously, several possible scenarios may explain the deposition of the sand. These are: dune transgression or mass movement of the dunes after an earthquake, alluvial/flood deposit, tidal surge related to a tsunami, and marine

transgression. Distinguishing tsunami deposits from marine incursion deposits, or even storm surge deposits, is a known problem (Bondevik et al., 1998). Therefore, supplementing the sedimentological and mineralogical analyses will be a discussion on the geological setting that existed at the time of the sand deposition. Sediments immediately above the sand layer are dated c. 7,245-7,006 cal yr BP. These dates must be treated with caution as bulk sediment in this study have been proved to be erroneously old.

The sedimentological and mineralogical analyses indicate the sand was of a marine/coastal origin, as opposed to being derived from the ranges via fluvial transport. The core sand is also much more angular than the dune sand and more angular than the beach sand through the >125 and >63 μm size fraction, indicating that the core sand is unlikely to be dune sand. However, the beach sand (marine transgression) cannot be ruled out based on mineralogical and sedimentological analysis.

If this deposit was indicative of marine incursion, it is likely that the sand would have been found in cores taken from the southern end of the lake. The area in the vicinity of the northern end of the lake is likely to have been protected from direct incursion during the Holocene sea-level high by the Poroutawhao High (Gibb, 1986; Hesp, 1975; Te Punga, 1953), which is between 5-24 m above mean sea level (Heerdegen & Shepherd, 1982; Hesp, 1975; Hesp & Shepherd, 1978; Rich, 1959; Te Punga, 1953). Furthermore Hesp (1975) analysed bore hole data of the lower Manawatū (north of Lake Horowhenua) and found no evidence of a marine incursion in the north-eastern Levin and Lake Horowhenua area owing to the Poroutawhao High (Te Punga, 1953).

In the vicinity of Lake Horowhenua, the bedrock high is between 3 and 5 m above present sea level (PMSL) (Clement et al., 2010). Gravity anomaly and seismic studies have been conducted on the structure. Bekesi (1989) surveyed the high between Waitarere Beach Road and Hokio Beach Road. He found that at Motuere Road, some 200 m north of the Hokio Stream outlet, the high is 5 m above PMSL. Further south, Aharoni (1991) surveyed along Muhunua Road in the vicinity of Lake Papaitonga and found the southern continuation of the Poroutawhao High. This gravity data confirmed that the elevation of the high decreases southwards. The Holocene sea-level high occurred 6,800 cal yr BP at the southwest coast of the North Island and was around 1.2 m above PMSL (Clement, 2011). This indicates that a marine incursion would not have overtopped the high, nor transgressed up the proto Hokio Stream and would have come in from the southwest. Therefore, if the sand was deposited as a result of a marine incursion, it should also be found in cores 6 and 7 taken from the southern end of the lake.

Therefore, the most plausible scenario is a tidal surge up the proto Hokio Stream, probably initiated by a tsunami reaching the coast. Storm surge deposits show similar characteristics to tsunami deposits; however, storm surges do not typically transport beach sand up river valleys (Morton et al., 2007). At the time of deposition, the shoreline was located on the western side of the Poroutawhao High, which is around 2-2.5 km wide (Clement et al., 2017). It would be extremely unlikely that a storm surge travelled ~2 km up the Hokio Stream into the proto lake or swamp.

Tsunamis have been recorded at Kapiti Island to the southwest of Lake Horowhenua at $4,780 \pm 150$, $3,360 \pm 140$, $1,210 \pm 80$, and $1,100 \pm 80$ yrs BP, and at 1220 AD, 1450 AD, and 1855 AD (Goff et al., 2000). There is no evidence in the literature of a tsunami c. 7,100 cal yr BP along the west coast of the lower North Island.

Most tsunami deposits are poorly sorted and contain debris such as plants, wood or shells, and fining upwards is common (Morton et al., 2007). Mud laminae, rip-up clasts, and marine diatom and foraminifera microfossils are also a common component (Goff et al., 2001; Kortekaas, 2002; Kortekaas & Dawson, 2007; Morton et al., 2007). Homogenous and structureless deposits, such as the deposit found in Lake Horowhenua are rarely found, but indicate extremely rapid deposition (Morton et al., 2007), or are a result of the uniformity of the sediment source, or large flow velocities relative to the grain size (Peters et al., 2007). A database of tsunami deposits recorded in lakes along the Cascadia margin (from northern California USA to Vancouver Island, Canada) describes deposits as consisting of a bed of sand above and below lake mud. Some deposits contain an overlying mud cap or organic debris (Peters et al., 2001).

The depth, proximity to shoreline, lake height above mean sea level, and lake depth at the time of the tsunami, and whether the surge travelled up a stream or river prior to entering a lake may also impact the characteristics of the deposit. In Norway, the Storegga tsunami 7,860 cal yr BP surged up streams and into lakes. In a lake that was more than 5 m above the shoreline at the time of the tsunami, the deposits are described as; massive, moderately sorted to poorly sorted fine gravel to fine sand usually containing shell and foraminifera fragments that are often overlain by clasts of lake mud and peat (Bondevik et al., 1997).

It seems that the core sand has some similarities with what would be expected if a tidal surge travelled up the Hokio Stream. Without further investigation, it seems unlikely that a definitive conclusion of the source of this sand can be sought. Despite this, the sand is interpreted here to have been deposited by a tidal surge in relation to a tsunami. Assessing the sand for deep-water marine diatom and foraminifera (Dawson & Shi, 2000; Hemphill-Haley, 1996) would help to

confirm the origin of the sand. Post deposition of the sand, the lake continued to form as indicated by increasingly organic-rich sediment.

After the lake formed, it was probably restricted to the southern end of its modern-day extent as indicated by the sediment thicknesses observed during the 2016 coring expeditions. The lake deepened and widened from c. 7,000-4,200 cal yr BP until it flooded the northern end c. 5,908 cal yr BP where Horo 3 was cored. Where Horo 10 was cored, it was not flooded until sometime after c. 4,452 cal yr BP.

5.3 Environmental change

This section examines the environmental change captured in the core, which spans the last c. 4,200 cal yr BP. The discussion has been divided into sections representative of the pollen zones and primarily relates to the proxy diagrams in Figure 31.

5.3.1 HW1 390-285 cm 4,213-2,924 cal yr BP

The vegetation of zone HW1 was dominated by a Podocarp-hardwood forest. The coniferous elements were dominated by *Dacrydium cupressinum*, Podocarpus, and *Prumnopitys taxifolia*. *D. cupressinum* pollen is well-represented in pollen records and can be transported long-distance (Macphail & McQueen, 1983), suggesting that the dominance of *D. cupressinum* pollen in the record reflects the dominance of *D. cupressinum* in the catchment. *Prumnopitys taxifolia* pollen is over-represented in pollen records, which means that their presence in this zone and others can be interpreted as a much lesser presence (Wood et al., 2016). *Dacrycarpus dacrydioides* is under-represented (Macphail & McQueen, 1983) and *D. dacrydioides* pollen occurs in this zone in small numbers, and therefore would have been a common element, especially on frequently flooded or poorly drained alluvial soils (Smale, 1984; Whaley et al., 1997). *Fuscospora* occurs in this zone (and increases up the profile). *Fuscospora* pollen can be transported long-distance (McGlone, 1988; Salas, 1983) and is over-represented in pollen records (Wood et al., 2016), indicating that the occurrence of this taxa in this zone and up the profile is likely to reflect a regional source. This is expected, given that *Fuscospora* is more common in upland areas in this part of New Zealand. The predominant wind direction in the Manawatū and Horowhenua districts is north-west, while southerlies are also common (Chappell, 2015), indicating that the dominant sources of *Fuscospora* pollen are the southern Tararua Range and the South Island. *Alectryon excelsus* is an under-represented taxon and occurs in the base of this zone and throughout the profile and would have been a common component of the understory.

Ascarina lucida, *Coprosma*, *Coriaria arborea*, *Dodonaea viscosa*, and Malvaceae would have dominated the small tree and shrub elements. These taxa occur in small numbers throughout this zone and the profile and would have been common along the streams draining into Lake Horowhenua (Macphail & McQueen, 1983). Furthermore, the diversity of small tree and shrub taxa is high throughout this zone and in HW2 but in very low abundance until human arrival. Taxa are of a mixed representation and pollination mode (Macphail & McQueen, 1983; Moar et al., 2011). A little under half of these taxa are severely under-represented or under-represented. This indicates that small trees and shrubs may have made up a larger proportion of the understory of the forest than what is suggested in the pollen record. The same situation exists for herbs and grasses (Macphail & McQueen, 1983).

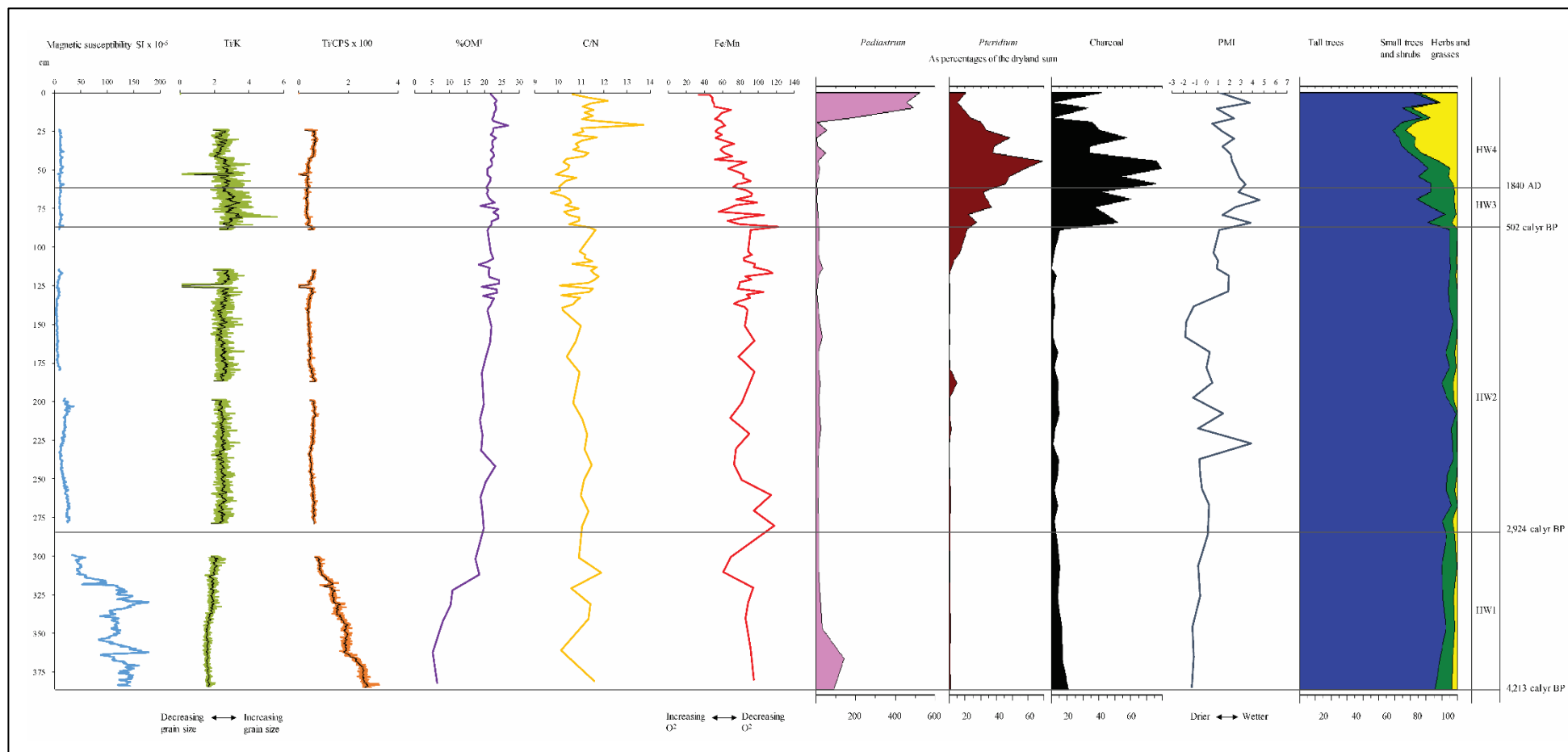


Figure 31: Summary of the main proxies used to synthesise the environmental history of Lake Horowhenua. From left to right: Magnetic susceptibility via XRF. Ti/K via XRF. Ti/CPS x 100 via XRF. %OM^T. C/N ratio. Fe/Mn ratio via atomic emission spectroscopy. Pediastrum. Pteridium. Charcoal (all sizes). PMI. Stacked graph of dryland pollen. Pollen, charcoal, and Pediastrum are presented as relative proportions of the dryland sum. Pollen zones and age-depth model interpolated dates have been added to aid in the synthesis.

High fern spore values (*Phymatosorus*, monolete fern spores, and *Cyathea*) occur in this zone and HW2 indicating their prominence around the lake and stream margins. Wetland and aquatics in this zone are dominated by Cyperaceae. Haloragaceae and *Typha* would have been present but in smaller numbers. These taxa, along with the ferns, would have been common around the lake and stream margins.

High spore values can be a result of fluvial transport (Bonny, 1978; Dunbar et al., 1997), as ferns frequently form riparian margins in New Zealand (Dawson & Lucas, 2000; Dunbar et al., 1997) leading to a bias in the record. Podocarp pollen was frequently represented by fragments such as single sacci or corpi, further indicating the contribution of fluvial transport of pollen to the sediment of Lake Horowhenua. Inflowing streams and rivers can contribute large amounts of fragmented and abraded pollen into the sediments of the lakes they flow into. This may make up to 85% of the total pollen in lake sediments (Bonny, 1978). Fern spores can also become over-represented due to open vegetation where they can be transported by wind (Wilmshurst, 1995). Furthermore, spores with thick walls are particularly resistant to damage during fluvial transport (Wilmshurst, 1995; Wilmshurst & McGlone, 2005b). Thus, it is important to interpret such high spore values with caution in this zone and throughout the profile.

The descriptions of remnant vegetation by Esler (1978) and Duguid (1990) generally agree well with that of the pre-human pollen record in this study. However, *Beilschmiedia tawa* is a severely under-represented taxa and essentially forms a blind spot in vegetation records (Macphail & McQueen, 1983). *B. Tawa* was thought to be common in the lowlands of the Horowhenua and Manawatū, and likely formed stands in areas where Podocarpus over story was limited (Esler, 1978), and as expected it was not noted in the record.

The abundance of drought tolerant *Prumnopitys taxifolia* (Leathwick & Whitehead, 2001; Vandergoes et al., 1997) in this zone is taken to indicate adequate but perhaps not excessive available moisture. As *P. taxifolia* is also over-represented, its more minor occurrence compared to HW2 supports adequate but not excessive soil water. Lower soil water is also supported by negative PMI values indicating relatively lower precipitation (Jara et al., 2017). Cyperaceae abundance has been used in other studies (e.g. Wilmshurst et al., 1999) to indicate periods of increased precipitation and/or swamp extent (Lorrey et al., 2008), and their presence is prominent in this zone. However, their affinity for water (Lorrey et al., 2008) and presence proximal to the lake margin, and the lack of correlation between the PMI in this zone (which indicates drier conditions) and through the profile indicates that the pollen record is being biased. Cyperaceae and ferns generally decline from HW1 toward the upper part of HW2, except towards the top of HW2 where there is a slight increase in ferns. While there is an increase in tall tree pollen from

HW1 and up through HW2. This suggests that there was an increasing contribution of pollen of tall trees reaching the site. This would have had a diluting effect on the representation of wetland, aquatic pollen, and fern spores. Furthermore, this may be compounded by a reduction of stream-borne pollen contribution up the profile (Newnham et al., 1998a).

The increase in *Fuscospora* towards the top of the zone and throughout HW2 is likely to relate to the late Holocene expansion of beech in upland areas as the climate deteriorated (McGlone, 1989), and as a result of the slow post-glacial adjustment (McGlone, 1989). *Ascarina lucida* also occurs in this zone in small numbers before declining up the profile. *A. lucida* is frost and drought intolerant (McGlone & Moar, 1977; McGlone et al., 1993), indicating that the climate may have been warmer than the succeeding zones (Burrows, 1996). As the lower PMI values indicate that there is adequate soil moisture, the presence of *A. lucida* cannot be attributed to wetness.

This pattern of increasing *Fuscospora* and *Ascarina* decline is recognised in many pollen records (e.g. McGlone et al., 1993; McGlone & Topping, 1977). This has been attributed to an increase in the Walker Circulation and the Southern Annular Mode (SAM), and the intensification of ENSO in the mid to late Holocene (Gomez et al., 2004; Hellstrom et al., 1998; Lorrey & Bostock, 2017; Shulmeister & Lees, 1995). This change in regime saw a shift from the previously dominant northerly flow to dominant south-westerly flow and a subsequent deterioration of the climate (Li et al., 2008). This mid-Holocene cooling is further supported by decreased sea surface temperature and glacier advance post 5 ka (Gellatly et al., 1988) as a result of the increased westerlies and south-westerlies (Li et al., 2008; Nelson et al., 2000; Porter, 2000).

Coriaria arborea and *Coprosma* are apparent in this zone and, along with *Ascarina lucida*, indicate disturbance or open sparse and regenerating forest (Burrows, 1996; McGlone, 2009). *Coriaria*, *Coprosma*, and *Ascarina* would have been common along banks of the streams entering Lake Horowhenua as a result of frequent disturbance from flooding. The decline in *Ascarina* up zone likely reflects the deterioration in climate mentioned above rather than a reduction in disturbance, as *Coprosma* and *Coriaria* remain rather constant in this zone and HW2.

Small (<20 µm) and medium (20-50 µm) sized charcoal particles are present at low levels and decrease in abundance up the profile, while large (>50 µm) sized charcoal particles appear in HW2. There has been much debate on the significance of low levels of charcoal in New Zealand lake sediment pre-human arrival (Ogden et al., 1998; Sutton et al., 2008). As mentioned previously, charcoal that is less than 20 µm can travel from Australia (Butler, 2008), while charcoal that is between 20-50 µm can travel thousands of kilometres (McGlone & Wilmshurst,

1999). The prevailing westerly circulation (Li et al., 2008) through the mid-Holocene suggests that the majority of small and perhaps some of the medium sized charcoal could have been transported from Australia. While natural ignitions of the pre-human vegetation are likely to be rare (McWethy et al., 2013), the fact that some of the charcoal particles in HW2 are relatively large ($>50\ \mu\text{m}$), suggests that they may reflect isolated local fires occurring somewhere within the broader lake catchment, as opposed to being transported long-distance (Butler, 2008).

In this zone, XRF proxies and OM% indicate that clastic sedimentation, although declining, was still high post lake formation until just prior to HW2 c. 3,255 cal yr BP and was at times dominated by SOM (soil organic matter). This can be explained by input of fluvial derived sediments and SOM from the inflowing streams during flooding and normal flow, resulting in a diluting effect. The Ohau River may have still been in the vicinity of the lake, at times delivering floodplain sediment during larger floods. Interestingly, however, is the lack of distinct peaks in mean grain size, which remain rather stable, at around 27-35 μm . The sediment in this zone also contains the largest proportion of larger size classes (coarse silt and sand) throughout the profile, except at ~115 cm.

These fluvial deposits may have at times been nutrient rich, as indicated by the presence of *Pediastrum* at the base of the core c. 4,213-3,974 cal yr BP. *Pediastrum* are indicative of nutrient-rich slow-moving environments with low salinity (Woodward & Shulmeister, 2005). An *Echyridella* specimen was found at 380 cm. Both *Pediastrum* and *Echyridella* indicate that a freshwater environment persists from the base of the core c. 4,213 cal yr BP. However, as mentioned previously, the lake was likely to have formed much earlier (post deposition of the paleosol c. 7,595-7,480 cal yr BP). Sampling for *Pediastrum* and diatom flora in Horo 8 would help in determining at which point the lake formed.

Bottom water oxygenation through this zone is stable until c. 3,255 cal yr BP, where there is a marked increase in bottom water oxygenation as inferred from the Fe/Mn ratio. This marks the beginning of a new phase representing modern Lake Horowhenua (this is discussed further in section 5.3.2), where relatively stable lake and catchment conditions dominate until just prior to human arrival in HW3.

5.3.2 HW2 285-85 cm 2,924-502 cal yr BP

The vegetation of zone HW2 again is comprised of a Podocarp-hardwood forest dominated by *Dacrydium cupressinum*, *Podocarpus*, and *Prumnopitys taxifolia*. *Dacrycarpus dacrydioides* and *Alectryon excess* again would have been common. *Fuscospora* increases in this zone and would have been common in the uplands. Small trees and shrubs are more diverse in this zone and were

dominated by *Coprosma*, *Coriaria arborea*, *Dodonaea viscosa*, Malvaceae, *Myrsine*, and *Pseudowintera*. *Coprosma*, *Coriaria*, and Malvaceae, would have been common along the stream banks along with Cyperaceae, Haloragaceae, *Typha orientalis*, *Cyathea*, and *Phymatosorus*, which would have also been common along the lake margin. Towards the top of the zone, *Pteridium* appears.

At 829-502 cal yr BP, *Pteridium* increases. *Pteridium* is a ubiquitous pioneering plant that abruptly colonises a site post disturbance (Wilmshurst, 1995). *Pteridium* is also common in open places, forest margins, in clearings, and on sand dunes (McGlone et al., 2005b). As this slight rise is not accompanied with an increase in charcoal, or a decrease in tall tree taxa, it is not attributed to humans. Potential types of disturbance that may have occurred in the catchment may be related to storms, drought, windthrow, and floods. *Pteridium* pollen is only dispersed close to source (Dodson, 1977), unless in an open landscape where wind dispersal may play an important role (Wilmshurst, 1995). *Pediastrum* also increases slightly at c. 829 cal yr BP. As mentioned above, *Pediastrum* can signal landscape disturbance or an increase in nutrients in the lake. Therefore, the increase of *Pteridium* and *Pediastrum* between 829-502 cal yr BP is determined to have been due to periodic flooding and erosion in the catchment. This is further supported by erosion proxies that also increase at 829-697 cal yr BP (discussed further in this section later). The periodic flooding would have allowed for the persistence of *Pteridium* along the stream banks, and the flooding would have resulted in nutrient delivery to the lake.

Fuscospora increases up the middle of this zone, while *Ascarina lucida* continues to decline indicating further deterioration of the climate. *Dodonaea viscosa* remains steady in this zone, indicating that, although it was cool, there was little frost in the lowlands (Macphail & McQueen, 1983). A further decline in available moisture from the previous zone is indicated by the upward increase of *Prumnopitys taxifolia* through the base and middle of the zone. While the PMI indicates periods of variable precipitation throughout the zone.

Towards the top of the zone, warmer and wetter conditions may be signalled by the sustained decrease in *Fuscospora* and *Prumnopitys taxifolia* c. 883-502 cal yr BP and an increase in the PMI c. 993-883 (increase in precipitation). A slight decrease in PMI (decrease in precipitation) is signalled around 829-502 cal yr BP. Interestingly, this period overlaps with the New Zealand correlative of the Medieval Warm Period (MWP) c. 900-600 cal yr BP (Page et al., 2010). The New Zealand correlative of the MWP is thought to have resulted from a southward expansion of the Pacific Subtropical High as the westerlies moved poleward (Newnham et al., 2018). This resulted in a climate that was dominated by warmer conditions and stable temperatures (Newnham et al., 2018). Although the period was dominated by calm, warm, and wet conditions,

the MWP included periods of increased storminess (Grant, 1985; Lusk & Ogden, 1992; Page et al., 2010) and variable precipitation (Lorrey et al., 2008). Evidence of the MWP is recorded in tree rings and speleothems in New Zealand and other sites in the Southern Hemisphere (Diaz & Pulwarty, 1994; Williams et al., 2004). In New Zealand, the MWP has been recorded in some pollen records as a decrease in *Lophozonia menziesii* (e.g. MacDonald-Creevey, 2011). However, this appears unsubstantiated. Beech trees typically live between 300-600 years, and a retreat up slope and a subsequent reduction of pollen reaching a site would take a lot longer than the short period of warming which spans some 300 years (Newnham et al., 1998a). Therefore, the decrease of *Fuscospora* at the top of this zone is likely only relative, related to an increase in Podocarp pollen production, namely *Dacrydium cupressinum*, more local to the lake site. Furthermore, the correlative increase in *Cyathea* and other ferns, perhaps as a result of increased stream-borne pollen contribution, may have led to the dilution of this long-distance pollen.

Relatively stable catchment conditions and bottom water oxygenation dominate in this zone. In this zone sediment OM is largely dominated by algae and very little SOM as inferred from the C/N ratio. XRF proxies for erosion, Al%, and OM% signal very little clastic input, except at 1,882-1,758 cal yr BP, 993-883 cal yr BP, and 829-697 cal yr BP.

Periods of increased erosion are also indicated by peaks in mean grain size and increases in larger grain size classes, as well as a slight coarsening up core by a reduction in the clay category. The decrease in mean grain size up core may be a result of the inflowing streams and the Ohau River ceasing to supply sediment to the lake later in the record. It is difficult to identify the origin of the peaks in mean grain size without further investigation, as the majority of these peaks do not correspond to changes in the other erosion proxies. Potential processes may be related to increased storminess and flood events. Distinct peaks in grain size and changes within the different size classes are apparent in the grain size analysis but not the XRF proxies for grains size. This reflects the inability of the XRF counts to adequately indicate mean grain size. Instead, it reflects changes in the overall contribution of the element to the sediment.

The small peak at 200-210 cm c. 1,882-1,758 cal yr BP in the magnetic susceptibility plot may indicate tephra, as the amplitude is within the range expected (e.g. Balascio et al., 2015). The Taupo Volcanic Zone is a prolific producer of tephra (Lowe et al., 2013). However, the majority of these are typically directed to the northeast quarter (Lowe et al., 2008) as a result of the prevailing westerly winds. Very few eruptions are known to have produced (macroscopic) layers as far south as Manawatū/Horowhenua. Ash from some of the largest eruptions in the Holocene may have made it to the lake, e.g. the ultraplinian Taupo eruption 1, 717 ± 13 cal yr BP (Lowe et al., 2008). However, the size and shallow nature of Lake Horowhenua would have resulted in

considerable reworking and mixing of what would have been a very small amount of ash in the first place, thus would be unlikely to provide a distinctive signal. This is supported by the homogenous nature of the sediments, as seen on X-ray. Therefore, the small peak in magnetic susceptibility may instead relate to increased erosion in the catchment. This is supported by the small increase in the Ti and K plots at ~205 cm.

A second period of catchment disturbance occurs prior to HW3 at c. 993-883 cal yr BP. This is shown by an increase in the C/N ratio and a very small increase in the Ti, K, and Rb plots. Coarsening in the fine and medium silt classes also occurs. However, this is not matched by Al% increase or OM% decrease, as Al% remains low and OM% remains high. This is accompanied by a slight decrease in bottom water oxygenation at 993 cal yr BP. A further episode of catchment disturbance is recognised c. 829-697 cal yr BP. At 829 cal yr BP organic matter decreases, Al% increases, and mean grain size increases (this period is not covered by XRF). The erosion in the catchment of clastic material would have had a diluting effect on OM sedimentation in the lake (as seen by the OM% decrease). The C/N ratio also increases corresponding to increased SOM sedimentation into the lake. Again, this is accompanied by a slight decrease in bottom water oxygenation at 829 cal yr BP.

Three periods of decreased bottom water oxygenation are apparent at 2,868-2,591 cal yr BP, 993 cal yr BP, and 829 cal yr BP. As Lake Horowhenua is reported to have been much deeper (Adkin, 1911), it is possible that the earlier instance of anoxia may have been compounded by stratification (Friedrich et al., 2014). Coincident with the increase in the Fe/Mn ratio, indicating the beginning of anoxic bottom water conditions c. 993 and 829 cal yr BP, is an increase in catchment disturbance. These two periods of reduced bottom water oxygenation may have resulted from eutrophication associated with nutrient delivery from erosion (Davies et al., 2015; Friedrich et al., 2014). As mentioned prior, an increase in nutrient delivery is also supported by a slight increase of *Pediastrum* at 829 cal yr BP, which is thought to have resulted from catchment disturbance. Further investigation is necessary to confirm this.

The three periods of catchment disturbance captured in the record of Lake Horowhenua at 1,882-1,758, 993-883, and 829-697 cal yr BP, may be correlated to major periods of increased storminess recorded at other sites in New Zealand. Again, the difference in ages of these events could be due to modelling uncertainties in this study, and differences between the age modelling used in the other studies.

Lake Tūtira is located in the East Coast of the North Island, and is purported to record individual storms, storm frequencies, and storm magnitude in response to changes in ENSO and the SAM.

At Lake Tūtira, corresponding storm periods occur at 2,120-1,830, 1,270-1,120, and 680-500 cal yr BP (Page et al., 2010). ENSO and the SAM along with the Interdecadal Pacific Oscillation (IPDO) are the main drivers purported to influence New Zealand's climate (Ummenhofer et al., 2009). It is well known that changes in ENSO affect the eastern and western parts of New Zealand differently, owing to the orographic effect of the axial range (Lorrey et al., 2007). However, Page et al. (2010) suggest that a comparison of the Lake Tūtira storm record with other proxy records indicate that the Lake Tūtira record is a signal for regional and wider change and is a result of the interaction between ENSO, the SAM, and IPDO and how they modulate each other.

The period of 2,120-1,830 cal yr BP is reported to be dominated by storms of particularly high magnitude and frequency at Lake Tūtira and in Antarctica (Page et al., 2010). This period may be recorded in Lake Horowhenua as a small but distant peak in magnetic susceptibility, Ti, and K. It is also noted that the record at Lake Horowhenua does not record individual storm packets like those seen in the Lake Tūtira sediments. Lake Tūtira's catchment covers steep hill country and has soft basement geology (Wilmshurst, 1997). At Lake Horowhenua, changes over longer periods of time are recorded as a result of the flat catchment and basement geology in addition to lake sediment mixing.

The latter two periods (993-883 cal yr BP and 829-697 cal yr BP) may coincide with storminess at Lake Tūtira that has been recognised to have occurred during the Medieval Warm Period c. 900-600 cal yr BP (Page et al., 2010). The latter two periods are also recorded at other sites. Increased storminess was recorded at Lake Colenso, Ruahine Range, North Island (MacDonald-Creevey, 2011) at 1,185-1,065 and 764-626 cal yr BP and is supported by storminess in other records (e.g. Grant, 1985; Lusk & Ogden, 1992; Wilmshurst et al., 1997), some of which correlate to those at Lake Tūtira (Page et al., 2010). Grant (1985) purported periods of alluvial sedimentation and erosion at several sites in the North Island at 1,192-753 and 550-530 cal yr BP.

The two erosion periods as a result of increased storminess at 993-883 and 829-697 cal yr BP, coincide with vegetation change. These were: the *Fuscospora* and *Prumnopitys taxifolia* decline c. 883-502 cal yr BP, and the *Pteridium* rise 829-502 cal yr BP. The decline in *Fuscospora* c. 883-502 cal yr BP has been attributed to an increase in local Podocarp pollen in addition to an increase in fern spore contribution to the sediment in Lake Horowhenua. However, it may also be related to stand disturbance in the uplands (the source of *Fuscospora* pollen), as this overlaps with a period of stand disturbance in Tongariro National Park c. 700-600 cal yr BP (Lusk & Ogden, 1992). The decrease in *Prumnopitys* has been attributed to increased precipitation as a result of the MWP and is not related to catchment disturbance. From 829-502 cal yr BP, the slight

Pteridium rise has been attributed to increased flooding and disturbance in the catchment as a result of this increased storminess.

Apart from the aforementioned vegetation changes, there appears to be no vegetation change that correlates to the distinct peaks in grain size or any of the other erosion proxies. Wilmshurst (1997) purported that the lack of correlation between erosion pulses and vegetation change at Lake Tūtira and Lake Rotonuiaha, both located in the Hawke's Bay, indicate that storm events resulted in increased runoff, scouring of riverbanks, in-washed sediment, and no vegetation change. Furthermore, these types of disturbance are likely to cause the most damage in the uplands, while the plains and lowlands would likely be less disturbed (Wilmshurst et al., 1997). However, an increase in pollen sampling resolution and reanalysis of the sediment for grain size may change this conclusion.

5.3.3 HW3 85-60 cm 502 cal yr BP - 1840 AD

This zone is characterised by a significant *Pteridium* rise and charcoal fragments, signalling Polynesian arrival to Lake Horowhenua and surrounds at 519-486 cal yr BP, and the initiation of anthropogenic forest clearance of the lowlands (Fig. 32). As mentioned previously, this is the common pattern used to identify Polynesian settlement (McGlone et al., 1994; McGlone & Wilmshurst, 1999; McWethy et al., 2010; Sutton et al., 2008). Charcoal in the medium (20-50 µm) and small (<20 µm) sized categories increase coincidentally with the decline in tall trees. At least two large-scale successive burn-offs are indicated by peaks in small and medium sized charcoal coinciding with a decline in tall trees. The decrease of tall tree taxa from ~95% down to 75% at 85 cm is matched by an increase in small trees and shrubs from ~5% up to 20%, and an increase in herbs and grasses from ~0% up to 5%.

The vegetation of zone HW3 was dominated by a Podocarp-hardwood forest, namely *Dacrydium cupressinum*, *Podocarpus*, *Prumnopitys taxifolia*, *Dacrycarpus dacrydioides*, and *Alectryon excelsus*. All Podocarps decline from previous levels, with the exception of *D. cupressinum* which are well-represented in pollen records and its pollen can be carried long-distance (Macphail & McQueen, 1983). *A. excelsus* also increases from prior levels as a result of a reduction of Podocarp pollen reaching the site. *Fuscospora* would have still been common in the uplands, and *Metrosideros* and *Dodonaea viscosa* would have been common in the lowlands. *Coprosma*, *Coriaria arborea*, and Malvaceae would have been common along the stream banks, and *Coprosma* and *Coriaria* increase in this zone as a result of disturbance post land clearance. *Typha orientalis* increases significantly and Cyperaceae increases, these taxa would have made up a significant portion of the lake and stream margin components, along with ferns, *Cyathea*, and *Phymatosorus*. However, *Cyathea* decreases significantly, indicating that they are no longer as

prominent in the catchment. The increase in *Typha* implies that either there was an increase in nutrients due to land clearance, or that the lake had become shallower around the margins, perhaps as a result of increased sedimentation post land clearance (McGlone, 1978). Growth of *Typha* is also thought to have been encouraged by burning lake margin vegetation by Māori, as it was used as a food source (Wilmshurst, 2007).

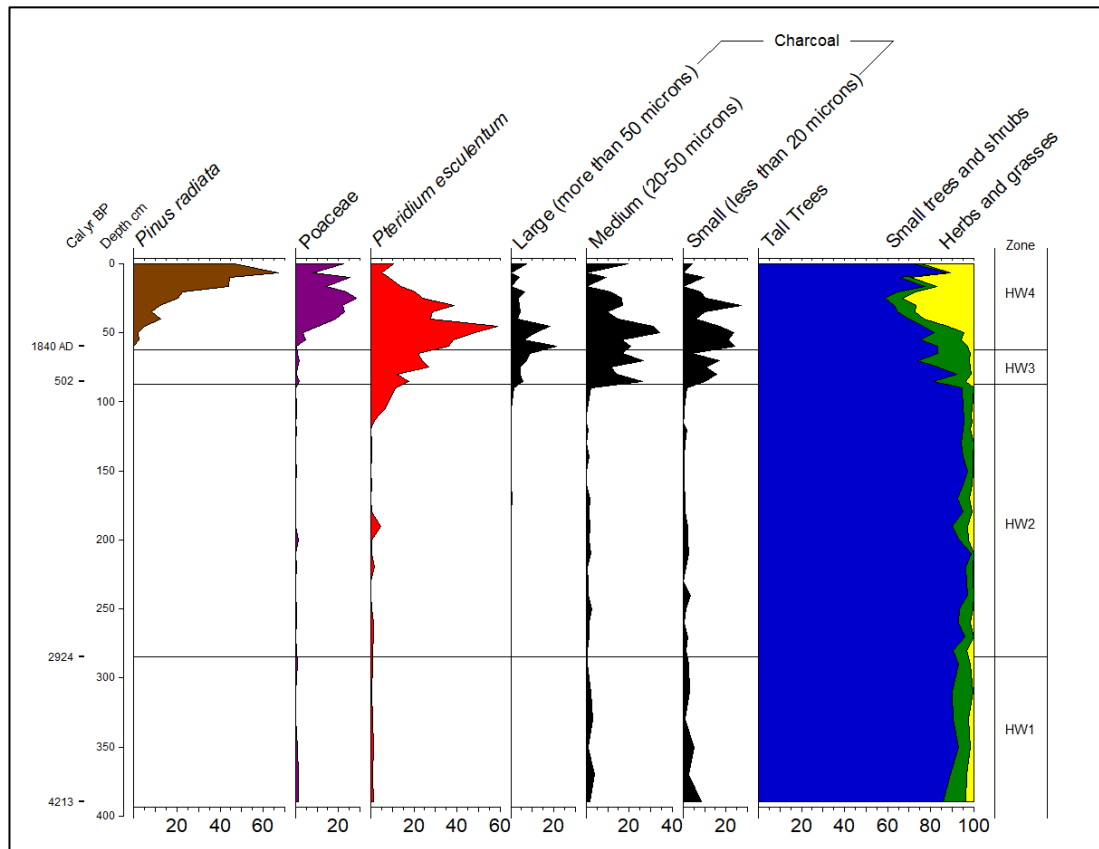


Figure 32: Lake Horowhenua relative pollen and charcoal diagram to infer the point of human arrival. Data is presented as percentages of the dryland sum.

Human arrival c. 519-486 cal yr BP (1431-1464 AD) at Lake Horowhenua is significantly later than at most sites in New Zealand by perhaps some 200 years (Higham et al., 1999; Higham & Hogg, 1997; Hogg et al., 2002; Ogden et al., 1998; Wilmshurst et al., 2008), and does not agree well with some oral traditions. The later peak in fire is contrary to most New Zealand records, which suggest that fire peaked around 700-500 yrs BP (Ogden et al., 1998), with clearance thought to have occurred over New Zealand at virtually the same time (Ogden et al., 1998). However, drier eastern areas were cleared before wetter western areas such as the Horowhenua district (Ogden et al., 1998).

Oral histories speak of people settling in the Horowhenua district 925 AD upon the arrival of waka captained by Kupe, or later when Whatonga arrived sometime between 1300-1505 AD. As mentioned previously, no artefacts from the Lake Horowhenua area have been radiocarbon dated. The closest dated sites are at Foxton and Himatangi to the north, and Paekakariki to the south (McFadgen, 1997). Shells, moa bones, and charcoal have been dated at these sites and have returned a wide range of ages. Ages range between 724-329 cal yr BP for moa bones found at Foxton. Radiocarbon ages of shells found in middens range from 662-765 cal yr BP at Himatangi, 1,070-688 cal yr BP at Foxton, and 660-555 cal yr BP at Paekakariki. Charcoal dated at Himatangi ranges from 636-465 cal yr BP.

In the Horowhenua district, it is thought that forest clearance began at the time of Polynesian arrival (c. 1319 AD) but may not have been significant until ~1515 AD as a result of population increase (McFadgen, 1994). Unfortunately, no dated, high-resolution pollen studies have been carried out on the lakes or bogs in the Horowhenua and Manawatū sand country to compare the timing of human arrival at Lake Horowhenua with. However, this late arrival at Lake Horowhenua does correlate with a second period of forest clearance at Lake Pupuke in Auckland reported by Newnham et al. (2018). The record at Lake Pupuke indicates a two-step forest clearance by fire, of which the first is absent in the Lake Horowhenua record. Localised forest clearance is indicated around 1314 AD, with a second extensive phase of clearance by fire around 1400-1450 AD (Newnham et al., 2018). Newnham et al. (2018) argue that the rapid landscape transformation as shown in records from the southern and eastern regions of New Zealand do not occur in Auckland. They propose that the western and northern areas were more humid as a result of the MWP. Therefore, sustained and persistent fire would need to occur to prevent forest regeneration (Perry et al., 2014). The MWP is thought to have persisted during the first c. 100-200 yrs of Polynesian settlement (Newnham et al., 2018). The southern and eastern forests of New Zealand were not so resistant to burning (Newnham et al., 2018) and, along with the initially warmer temperature, this resulted in the preferential colonisation of the south and east of New Zealand.

It wasn't until the culmination of the MWP and the onset of the New Zealand correlative of the Little Ice Age (LIA) c. 518 cal yr BP to 1900 AD, that a deterioration of the climate (Lorrey et al., 2008) and subsequent migration from the south allowed for the consolidation of settlements and the impact to forests in the north (Newnham et al., 2018). Late clearance is also recognised at central Taranaki (1400 AD; McGlone et al., 1988) and northern Taranaki (1600 AD; Wilmshurst et al., 2004), and has also been attributed to a superhumid mild climate limiting the ability to set and sustain fire (McGlone et al., 2005).

The LIA is thought to have been a particularly harsh period (Lorrey et al., 2008) with increased storminess (Page et al., 2010) as a result of increased westerly and southerly circulation (Lorrey & Bostock, 2017). The New Zealand correlative of the LIA is thought to have been brought about by the equatorial shift of the westerlies and subtropical front which resulted in a long-term reorganisation of the SAM and weakened ENSO teleconnection (Newnham et al., 2018). This period of cooling is recognised in many records, e.g. as a period of glacial advance in the Southern Alps (Schaefer et al., 2009) and a cooling in speleothem records (Lorrey et al., 2008).

The late clearance at Lake Pupuke and in Taranaki as a result of deteriorating conditions correlates with the late clearance at Lake Horowhenua; which also seems to coincide with a reduction of temperate conditions, as indicated by a further increase in *Fuscospora*. An increase in *Fuscospora* at this time is seen in other records (e.g. Lees, 1986; MacDonald-Creevey, 2011; Newnham et al., 1998a) and has been attributed to the downward adjustment of altitudinal limits due to the deterioration of the climate at the onset of the LIA (MacDonald-Creevey, 2011). However, as mentioned previously, the longevity of beech trees (Newnham et al., 1998a) and the relatively short duration of cooling in this record (~320 years) suggest that the *Fuscospora* rise in this record is not due to cooling. The *Fuscospora* rise in this instance, is therefore thought to result from the reduction of local Podocarp pollen (as seen by the decrease in all Podocarp pollen, except *Dacrydium cupressinum*) reaching Lake Horowhenua as a result of land clearance on the plains. Land clearance is thought to have been restricted to the lowland areas (Adkin, 1948; Chase, 2015) and agrees well with the continued input of *Fuscospora* pollen to the Lake Horowhenua record.

The land clearance by fire would have resulted in catchment instability and erosion, as signalled by the erosion proxies in this study. The slight increase in grain size in the Ti/K ratio plot (but not in mean grain size) and the rapid increase in the Fe/Ti ratio indicates that the lake was receiving quantities of both large and small sized grains. Al via XRF reaches its highest counts though 90-0 cm, however, Ti, K, and Rb reduce from previous levels. Al% reaches its peak at 80 cm then declines. C/N ratio remains high at the onset of this zone, then declines. OM% peaks at ~80 cm as a result of the deposition of SOM into the lake.

Following this, a decline in the small (<20 µm) and medium (20-50 µm) sized charcoal particles signal the culmination of large-scale land clearance in the region. Land clearance decline is also indicated by the reduction in the C/N ratio, Al%, and continued stable OM%, signalling stabilisation within the catchment and lake prior to 1840 AD. This is also supported by declining grain size, as indicated in the Ti/K ratio. Large (>50 µm) charcoal particles continue an upward rise and *Pteridium* remains high. This could indicate that around the lake site succession was prevented to allow for the cultivation and persistence of *Pteridium*. Fire is thought to have been

repeated to prevent regeneration (McGlone & Wilmshurst, 1999), and *Pteridium* is a known food source for Māori (Bussell, 1988; McGlone et al., 1994; McWethy et al., 2010).

Although clastic and SOM input into the lake increased post-Polynesian arrival, the sedimentation rate for the Polynesian era (0.07 cm a^{-1}) is similar to that of the pre-human era (0.08 cm a^{-1}), which agrees with findings by Cosgrove (2011). Cosgrove (2011) conducted a meta-analysis on sedimentation rates in aquatic ecosystems. She found that sedimentation rates post-Māori settlement do not increase significantly from pre-human sedimentation rates. Although discrete and short-lived erosion pulses do occur post deforestation, long-term sedimentation rates do not change markedly (Swales et al., 2002). However, temporary increases in sedimentation representing pulses of erosion within the soft rock hill country on the eastern coast of New Zealand are seen in Lake Tūtira post-Polynesian arrival (Wilmshurst & McGlone, 2005a). In the Lake Waikopirō and Lake Rotonuiaha catchment, rapid colonisation by *Pteridium* was thought to help to minimise erosion through its network of underground rhizomes along with the remaining intact roots of previously burnt trees (Wilmshurst & McGlone, 2005a). Lake Horowhenua catchment is small and largely flat, and would be much less susceptible to erosion under the protection of *Pteridium* and the remaining forest roots.

Bottom water oxygenation reaches its lowest throughout the profile at the onset of Polynesian arrival, then slowly increases towards the top of the zone. The reduction in bottom water oxygenation at the onset of HW3 is likely a result of preceding conditions. Nutrient levels are inferred to have remained low and water quality high, as there is no subsequent increase in *Pediastrum*. However, the contribution of eutrophication to increasing anoxic conditions cannot be ruled out on these analyses alone. Increasing bottom water oxygenation is apparent through HW3, likely as a result of recovery post land clearance.

5.3.4 HW4a (60-40 cm) 1840-1898 AD

European arrival has been determined to occur at 60 cm and has been divided into two subzones. This two-stage European impact is recognised in other records (e.g. Wilmshurst, 1997). The zone delineation was determined by: the first appearance of *Pinus radiata* pollen, a second peak in charcoal of all sizes, and a rise in Poaceae and *Pteridium*. Furthermore, this zone is characterised by an increase in Cupressaceae (most probably *Cupressus macrocarpa*), the reduction of pollen from tall tree taxa as a result of deforestation, and a decrease in small trees and shrubs namely *Coprosma* and *Coriaria arborea*. The appearance of *Pinus* and *Cupressus*, and an increase in Poaceae are typically taken to represent the arrival of Europeans in New Zealand (McWethy et al., 2010; Wilmshurst et al., 1999; Wilmshurst et al., 1997). European arrival in New Zealand is a known time marker and occurred c. 1840 AD. Although *Pinus* was not planted in the

Horowhenua district until 1935 AD, the appearance of *Pinus* pollen has been determined to occur virtually at the onset of European arrival in the Lake Horowhenua record, as signalled by the charcoal and Poaceae curve. *P. radiata* was planted in Wellington in 1865 AD (Woodward & Shulmeister, 2005), and *Pinus* pollen can travel vast distances (Green et al., 2003), suggesting that the initial *Pinus* pollen may have travelled from there.

Dicksonia and *Phymatosorus* increase during this subzone and up zone, and signal a reduction of competition from other ferns as a result of land clearance. *Cyathea* increases from prior levels and likely resulted from a reduction of the dilution of *Cyathea* spores by pollen of tall trees. Additionally, *Cyathea* spores can travel vast distances (especially in the absence of dense forest) and may also represent an increase in *Cyathea* on the plains post fire clearance (Moar et al., 2011). Cyperaceae and *Typha orientalis* would still have been prominent around the stream and lake margins during this subzone.

An increase in erosion as a result of this land clearance is signalled by an increase in AI% from 60 cm. An increase in SOM delivery to the lake also occurred as a result of increased erosion. The increase in sediment supply resulted in the dilution of autochthonous organic matter, shown by a slight decline in OM%. XRF proxies for grain size indicate that the lake began to receive quantities of sediment with a smaller grain size during this subzone. The C/N ratio begins an upward increase at the onset of this zone, while the Fe/Mn ratio declines. This is discussed in the following section to avoid repetition.

5.3.5 HW4b (40-0 cm) 1898-present

The second phase of European impact is shown by an increase in Poaceae, *Pinus radiata*, and a significant increase of *Taraxacum* and *Pediastrum* colonies towards the top of the zone. The decline in *Fuscospora* in this zone possibly signals the onset of land clearance in the uplands. A decline in charcoal, *Pteridium*, *Coprosma*, and *Coriaria arborea* indicate the culmination of land clearance towards the top of the zone. Meanwhile, the increase in Poaceae indicate the establishment of largescale agriculture and horticulture. *Cyathea*, *Dicksonia*, and *Phymatosorus* remain prominent but decline towards the top of the zone as a result of increased pastoral expansion. *Typha orientalis* decreases, indicating clearance of vegetation right to the lake edge. This clearance may have led to the increase in Cyperaceae that is seen, perhaps due to a reduction of competition with *Typha*. As mentioned previously, *Phormium tenax* has been planted around the lake margin in recent years (Gibbs & Quinn, 2012) but, as expected, was almost absent in the record.

Between c. 1883 AD and 1927 AD, tall tree taxa decline to their lowest. This agrees well with the intensification of deforestation around the Horowhenua district from 1886 AD for timber and agriculture when the railway from Wellington to Palmerston North began to run (Dreaver, 2006). A decline in charcoal and *Pteridium* signal the beginning of the decline in land clearance by fire from 1883 AD and the initiation of large-scale agriculture, as signalled by the Poaceae curve.

Sediment supply remained high, as indicated by the continued upward rise of Al% c. 1883 AD to the present day. The Ti, K and Rb plots indicate a slight increase in clastic input to the lake from 40-24 cm (where measurements stop) c.1898-1944 AD. The Fe/Ti ratio indicates that the lake began to receive sediment with an increased grain size from 40 cm c.1898 AD, however, the magnitude that is suggested by the Fe/Ti ratio is not matched by the Ti/K ratio.

The upward increase of the C/N ratio from 1840 AD may be a result of a combination of increased SOM sedimentation due to erosion post land clearance, weed growth, and sewage disposal. However, aquatic weed was not prominent until much later; sometime after 1950 AD (Cunningham et al., 1953), and sewage was disposed of in the lake from 1952 AD. This suggests that neither increased macrophyte growth nor sewage disposal are responsible for the initial rise. However, after 1950 AD they may have contributed to the upward rise. A sharp peak in the C/N ratio at 21 cm c. 1953 AD may be a result of the initiation of sewage disposal into the lake in 1952 AD. Untreated sewage has a C/N ratio value of 7-8 and treated sewage around 15 (Kabbashi, 2011). However, any change to the C/N ratio associated with sewage disposal would likely occur over a zone, rather than a specific point, suggesting that there is some other reason for the peak, or it is a result of measurement error. Unfortunately, due to sampling availability a repeat was not able to be carried out. Similarly, the upward increase in OM% during the latter European phase is likely a result of an increase in SOM supply, sewage, and even algae deposition rather than a reduction of clastic input to the lake, as this remained high. Algae productivity increased enormously sometime after 1950 AD and is a known problem at Lake Horowhenua (Gibbs, 2011). It appears that the C/N ratio has become blurred during European occupation due to high inputs of SOM, sewage disposal, and macrophyte growth, as an increase in productivity should see a declining C/N ratio.

Sewage disposal in other lakes has been recorded as the highest concentrations of total phosphorus, total organic carbon, and total nitrogen due to increased primary productivity related to the nutrient loads in sewage effluent (Atkinson & Smith, 1983). The depth at which this would be seen in the record is between 21.5-10.5 cm. Total phosphorus was not measured in this study and phosphorus counts from XRF do not cover the upper 24 cm. TN and TOC do not show the highest measurements through the profile, and TN shows a decrease from its peak at ~80 cm.

TOC slightly increases from 17-10 cm, however, this increase in TOC is a continuation of the upward trend that begins around 50 cm. The lack of sewage signal at Lake Horowhenua may be a result of in-lake sediment mixing and proximity to the sewage discharge point at Makomako drain, some 600 m from the core sampling site. Several other studies have also recorded enrichment of ^{15}N and higher $\delta^{15}\text{N}$ values post sewage disposal. Analysing the sediments for $\delta^{15}\text{N}$ would be ideal to further assess the sediments for a sewage signal.

The clastic and SOM input into the lake has had a significant impact on the sedimentation rate, which has increased from the pre-human and post-Polynesian rate of $0.08\text{-}0.07\text{ cm a}^{-1}$ to a phenomenal rate of 0.34 cm a^{-1} post-European arrival. However, as the lake began to shallow, the sediment may become more susceptible to resuspension during high winds and sediment flushing out the Hokio Stream, resulting in a reduction of sedimentation. This effect would have been mitigated post weir construction in 1956 AD. Sewage disposal and algae deposition may also have increased sedimentation into the lake in recent decades, although the contribution would have been minor (HRC, 2018). The slow downward decline of ^{210}Pb also indicates a very rapid sedimentation rate in the upper 28 cm (Swales et al., 2010), and the ^{137}Cs concentration profile indicates that the upper 17-27 cm has been deposited post 1963 AD. This agrees well with the age-depth model, which suggests 1963 AD is between 17 and 18 cm.

Using the age-depth model data, there appears to be no increase in sedimentation rate post weir construction or sewage disposal, as the rate fluctuates between 0.344 and 0.335 cm a^{-1} from c. 1940 AD to present day. This rate is much lower than that reported by HRC, (2018) using ^{210}Pb excess concentration of sediment taken from a site at the buoy. The rate varied from between $0.49\text{-}0.62\text{ cm a}^{-1}$ c. 1942-1962 to present, suggesting that there may be an increase in sedimentation rate post weir construction and sewage disposal. It has been reported previously that the weir is affecting the lakes ability to naturally flush, resulting in sediment and nutrient accumulation (Gibbs & Quinn, 2012). This indicates that further data processing to constrain incremental ^{210}Pb derived sedimentation rates for the centre of the lake would be desirable to assess whether sedimentation rates have increased in the middle of the lake post weir construction and sewage disposal. Additionally, sampling to determine the bomb peak to constrain 1963 AD rather than relying on the current age-depth model may enable more accurate age estimates for events during the latter European occupation.

Post-European arrival, increasingly intensive agriculture and horticulture, and urban development in the catchment has led to nutrient accumulation. The proliferation of *Pediastrum* (c. 1970-1985 AD) may be related to several causes. These are: intensive farming and associated nutrient leaching and runoff, intensive areal top dressing (Patterson et al., 2002), discharging treated

sewage into the lake, or accelerated deforestation. In other records, *Pediastrum* proliferation has been attributed to accelerated soil erosion following land clearance (e.g. Yasuda et al., 2000). However, deforestation was likely not intensive post 1970 AD, as intensive farming had already begun in the region (Esler, 1978; Hesp, 2001). Sewage disposal was initiated in 1952 AD and ceased in 1987 AD (Gibbs & Quinn, 2012), and areal top dressing began in New Zealand around 1950 AD (Alexander & Tullett, 1967). Therefore, it is unlikely these changes around the catchment are directly responsible.

The increase in *Potamogeton crispus* at 10 cm c. 1985 AD may be related to the increase in *Pediastrum*. *Potamogeton* appears at 40 cm c. 1898 AD, signalling the introduction of the weed into the lake. The increasingly high levels of external nitrogen entering the lake through runoff, springs (Gibbs & White, 1994), and Arawhata Stream (Gibbs, 2011) is thought to be responsible for the proliferation of aquatic weed in Lake Horowhenua (Gibbs & Quinn, 2012). *Potamogeton* and other aquatic weeds smother the lake bed during decomposition, releasing phosphorus that has accumulated in the sediment, while nitrogen is being released by weed bed decomposition (Gibbs, 2011). This process may have resulted in the proliferation of *Pediastrum* at 15-10 cm until the present, which occurs at the same time that *Potamogeton* increases.

As mentioned above, the lake is known to receive nutrients from runoff, leaching (Gibbs, 2011; Gibbs & White, 1994), and stream bed erosion (Gibbs, 2011), and the lake sediment contains a high phosphorus load as a result of sewage disposal (Gibbs, 2011). This indicates that *Pediastrum* is responding to both internal and external processes, as the weeds themselves are thought to be responding external nitrogen loads (Gibbs, 2011). Other studies (e.g. Gibbs, 2011) consider this process of weed bed collapse to be responsible for the algal blooms every summer at Lake Horowhenua. Despite the decomposition of the aquatic weed inducing anoxic conditions during late summer (Gibbs & Quinn, 2012), the Fe/Mn ratio indicates that, overall, there is increased bottom water oxygenation during the European era, likely as a result of a decreased lake level from over 2 m to 1.6 m at present (Gibbs & Quinn, 2012), that has allowed for increased wind-induced oxygen diffusion in the lake. A decrease in Fe/Mn ratio has also been reported in Laguna Potrok Aike, Argentina, as a result of a reduced lake level (Haberzettl et al., 2007). Despite increasingly high levels of nitrogen input into the lake, the TN plot shows a slight downward decrease from its highest levels during Māori settlement.

The increase in the pollen of aquatic species Cyperaceae and *Typha orientalis* during the European zone may also be related to increases in nutrient supply (Wilmshurst et al., 1999). Currently, the main pond weed is *Elodea canadensis* (De Winton & Taumoepeau, 2014). In

another study where *E. canadensis* is currently the prominent weed (Sayer et al., 1999), a lack of *E. canadensis* pollen has been noted in the palynological record.

5.4 Summary of human impact

The degree of change during European settlement is much more extensive than during Māori settlement. Land clearance for forestry and agriculture resulted in a significant decrease in native forest. During the European era, there was significant deforestation on the plains and the uplands that is not apparent during the Māori era. Catchment disturbance increased significantly post European arrival, as indicated by higher Al%, Ti, K, Rb, and C/N ratio compared to post Māori arrival. This is reflected by the significant increase in the sediment accumulation rate of 0.07 cm a⁻¹ during Māori occupation, to 0.34 cm a⁻¹ during European occupation. However, the Ti/K ratio for grain size reached a peak during Māori settlement but may also be a result of the omission of the upper 24 cm from XRF analysis. During the European era, the XRF data for grain size and grain size analysis indicates that, although clastic input was high, the grain size was relatively small until around 40 cm c. 1898 AD when it increased. Water quality is inferred to have remained high during Māori settlement, except for a decrease in bottom water oxygenation at the onset of Māori arrival. This may have been due to change that began prior to Māori arrival. The results from this study confirm oral histories, which speak of a lake with high water quality that is reported to have hosted an excessive fish stock (Cunningham et al., 1953; Gibbs, 2011; MfE, 2001; White, 1998). An increase in nutrient and sediment supply has resulted in a reduction in water quality post European arrival. In this study, this is indicated by high sedimentation rates and the proliferation of *Pediastrum* and *Potamogeton*. There does not appear to be any specific indication captured in this record of sewage disposal and weir construction. The degradation to the water quality in the lake is a result of increased sedimentation post clearance of the natural vegetation for urbanisation, agriculture and horticulture, nutrient input and subsequent weed growth and cyanobacteria blooms.

Chapter 6: Conclusion and recommendations for future research

6.1 Conclusion

Lake Horowhenua is a unique and highly prized lake and has been highly modified post-human arrival. In order to effectively restore or manage modified systems such as Lake Horowhenua, a record of past environmental change as well as natural variability is essential to determine the benchmark. A lower resolution record of pre-human change has been compared to a higher resolution record post-human arrival. This research investigated the formation of the lake and changes associated with catchment disturbance, vegetation change, and water quality. The results indicate that, prior to human arrival c. 519-486 cal yr BP, the lake had relatively high water quality, that relatively stable catchment conditions dominated in the catchment, and that a dense Podocarp-hardwood forest was present in the region.

Prior to lake formation c. 7,500 cal yr BP, fluvial deposition from the Ohau River was the source of sedimentation in the area that is now occupied by the lake. Around the same time that dune transgression began c. 7,700 cal yr BP, the river moved south, and drainage was impeded, allowing for the formation of the lake. A tidal surge may have occurred c. 7,100 cal yr BP, as indicated by a 10 cm sand deposit. Post deposition of the sand, the lake continued to widen and deepen from 7,000-4,200 cal yr BP.

The last 4,200 cal yr BP was analysed using a multi-proxy approach. The results suggest that the lake was still dominated by clastic sedimentation until sometime around 3,200 cal yr BP, when the lake then transitioned into a modern phase of increased autochthonous input, relatively stable catchment conditions and relatively stable bottom water oxygenation. The pre-human vegetation was dominated by *Dacrydium cupressinum* and vegetation largely responded to regional climatic change associated with the intensification of the westerly circulation regime.

Catchment disturbance occurred c. 2,120-1,830, 993-883, and 829-697 cal yr BP, and may relate to storminess in other records (MacDonald-Creevey, 2011; Page et al., 2010). Nutrient levels are inferred to have remained low, except for at c. 4,213-3,974 and at 829 cal yr BP where there is a small increase in *Pediastrum*, perhaps as a result of catchment disturbance. Bottom water oxygenation decreased at 2,868-2,591, 993, and 829 cal yr BP, the latter two coincide with increased catchment disturbance.

Human arrival c. 519-486 cal yr BP coincided with the onset of the LIA. This agrees well with records from Lake Pupuke in Auckland (Newnham et al., 2018) and central and northern Taranaki (McGlone et al., 1988; Wilmshurst & Higham, 2004). In which the conditions prior to the LIA were warm and humid, resulting in preferential settlement of the east and south of New Zealand,

as the forest there was not so resistant to burning (Newnham et al., 2018). At the onset of the LIA, the climate deteriorated and people migrated north. Once land clearance was initiated, this induced periods of SOM and clastic input into the lake. Bottom water oxygenation reached its lowest at the onset of Māori settlement, however, water quality is inferred to have remained high. Sedimentation rates do not differ between pre-human and Polynesian arrival. Prior to European arrival, stability within the catchment and lake then ensued as the lake and catchment reached a new equilibrium in response to the culmination of land clearance.

Two recognised phases of change are associated with European arrival. The first phase is largely related to vegetation change and catchment disturbance, while the second phase also includes a reduction in water quality, increased catchment disturbance, and the culmination of land clearance. The beginning of the first phase was marked by the introduction of exotic species and the initiation of further land clearance by fire on the plains. Deforestation was the most significant between c. 1883-1927 AD. Land clearance began in the uplands from 1883 AD and land clearance by fire began to decline at that time. A significant increase in erosion is evident around 1898 AD; around the same time that the Poaceae curve peaks, signalling the intensification of agriculture. Aquatic weed growth began in 1898 AD and was extensive by 1985 AD. *Pediastrum* increased significantly from 1970 AD and was likely responding to the release of nutrients from the sediment post weed bed collapse and to external nutrient loads. Sedimentation rates and erosion increased significantly, compared to the pre-human period and Māori settlement.

It appears that the changes associated with Polynesian arrival and European arrival are vastly different. Degradation of water quality and most of the land clearance and catchment disturbance occurred post European arrival. There does not appear to be any specific evidence of weir construction or sewage disposal in the record. But it is inferred that these processes would have contributed to the significant increase in sediment accumulation rates and water quality degradation that occurred post European arrival. Secondly, it appears that the change seen post-human occupation is not within natural variability and overall exceeds the magnitude of any change captured throughout this 4,200-year record.

It is apparent the conditions just prior to European arrival (1840 AD) may be the ideal benchmark. This is concluded for two reasons:

1. The period just prior to Polynesian arrival does not represent the most stable conditions that occurred during the natural zone. The conditions just prior and during Polynesian arrival may also be complicated by climatic change.
2. The time since c. 1840 AD was dominated by a climate that is similar to that of today.

6.2 Future research recommendations

Geology

Sedimentary logging to model the Holocene sea-level high extent on the southern end of the lake and the path of the Ohau River would be ideal.

Chronology

An increase of the resolution of radiocarbon dating to constrain the timing of particular areas of interest is desirable, including the base of fluvial sediments and the pollen zones. This will help in constructing a more accurate age-depth model and a more accurate estimation of sedimentation rates.

Further data processing to constrain incremental ^{210}Pb derived sedimentation rates for the centre of the lake, as well as sampling to determine the bomb peak to constrain 1963 AD. This would enable more accurate age estimates for events during the latter European occupation rather than relying on the current age-depth model.

Sand deposit

Diatom and foraminifera analysis can be used to determine the origin of the sand and to test for rapid deposition indicators (Hemphill-Haley, 1996). The presence of benthic and brackish marine diatoms can help in determining the source, while diatom preservation can help to identify rapid deposition associated with tsunamis.

Environmental change

A repeat of the grain size analysis samples would be desirable, due to the uncertainty of the reliability of the LPA results. Furthermore, several more investigations would be desirable, including:

1. An increase in resolution of pollen analysis to determine a more accurate record of natural variability.
2. Bacterial DNA. Bacterial DNA has been used in many studies as an indicator of water quality, as well as to assess the environment in which they lived.
3. Diatom analysis. Diatoms were found within the samples from Lake Horowhenua. Diatom analysis would aid in the interpretations of bottom water oxygenation (Lowe & Walker, 2014), as well as provide information on salinity and stratification (Rühland et al., 2015).
4. Chironomid analysis. Reconstructions of temperature, salinity, lake trophic status, and oxygenation can be interpreted from Chironomid analysis. The technique is underused in New Zealand (Vandergoes & Cochran, 2017). However, datasets for Chironomid

identification, and transfer functions of temperature and lake production are being developed (Woodward & Shulmeister, 2006).

5. Stable isotopes. $\delta^{15}\text{C}$ to further support the C/N ratio analysis of organic matter source. $\delta^{15}\text{N}$ isotopic analysis to determine the source of nitrogen entering the lake, as well as to determine if $\delta^{15}\text{N}$ increases during the period of sewage disposal. Total phosphorus concentrations would also be helpful in determining if the record contains evidence of sewage disposal.
6. Hyperspectral imaging spectroscopy. Hyperspectral imaging spectroscopy is a new promising nondestructive technique. This technique has been carried out in other studies to estimate anoxic conditions by estimating the quantity of pigments, e.g. Bacteriopheophytin *a* (BPhe *a*) in sediments (Butz et al., 2015) and would supplement the Fe/Mn ratio. While Chlorophyll *a* can be used as an estimate for productivity (Butz et al., 2017).

References

- Adkin, G. (1911). *The post-Tertiary geological history of the Ohau River and of the adjacent coastal plain, Horowhenua County, North Island*. Paper presented at the Transactions of the New Zealand Institute.
- Adkin, G. L. (1948). *Horowhenua: Its Maori place-names & their topographic & historical background*. New Zealand: Dept. of Internal Affairs.
- Aharoni, E. (1991). *Seismic reflection study across the Horowhenua coastal plain, North Island, New Zealand*. (Unpublished master's thesis), Victoria University of Wellington, Wellington, New Zealand.
- Alexander, G. I., & Tullett, J. S. (1967). *The super men: Agricultural aviation in New Zealand*: Reed.
- Alloway, B. V., Lowe, D. J., Barrell, D. J., Newnham, R. M., Almond, P. C., Augustinus, P. C., . . . McGlone, M. S. (2007). Towards a climate event stratigraphy for New Zealand over the past 30 000 years (NZ-INTIMATE project). *Journal of Quaternary Science*, 22(1), 9-35.
- Anderson, A. (1989). Mechanics of overkill in the extinction of New Zealand moas. *Journal of Archaeological Science*, 16(2), 137-151.
- Anderson, A. (1991). The chronology of colonization in New Zealand. *Antiquity*, 65(249), 767-795.
- Anderson, A., & McGlone, M. (1997). A forceful impact. The East Polynesians effect on fauna and flora, plate 12. In M. McKinnon, B. Bradley, & R. Kirkpatrick (Eds.), *New Zealand historical atlas: Ko Papatuanuku e Tatoto Nei*. New Zealand: David Bateman.
- Anderson, N., & Odgaard, B. (1994). Recent palaeolimnology of three shallow Danish lakes. *Hydrobiologia*, 275(1), 411-422.
- Ascough, P., Cook, G., Hastie, H., Dunbar, E., Church, M., Einarsson, Á., . . . Dugmore, A. (2011). An Icelandic freshwater radiocarbon reservoir effect: Implications for lacustrine ¹⁴C chronologies. *The Holocene*, 21(7), 1073-1080.
- Atkinson, M., & Smith, S. (1983). C: N: P ratios of benthic marine plants¹. *Limnology and Oceanography*, 28(3), 568-574.
- Augustinus, P., Bleakley, N., Deng, Y., Shane, P., & Cochran, U. (2008). Rapid change in early Holocene environments inferred from Lake Pupuke, Auckland city, New Zealand. *Journal of Quaternary Science: Published for the Quaternary Research Association*, 23(5), 435-447.
- Augustinus, P., Cochran, U., Kattel, G., D'Costa, D., & Shane, P. (2012). Late Quaternary paleolimnology of Onepoto maar, Auckland, New Zealand: Implications for the drivers of regional paleoclimate. *Quaternary International*, 253, 18-31.
- Ausseil, A.-G. E., Dymond, J. R., & Shepherd, J. D. (2007). Rapid mapping and prioritisation of wetland sites in the Manawatu–Wanganui Region, New Zealand. *Environmental Management*, 39(3), 316-325.
- Avşar, U., Hubert-Ferrari, A., Batist, M. D., & Fagel, N. (2014). A 3400 year lacustrine paleoseismic record from the North Anatolian Fault, Turkey: Implications for bimodal recurrence behavior. *Geophysical Research Letters*, 41(2), 377-384.
- Balascio, N., Francus, P., Bradley, R., Schupack, B., Miller, G., Kvisvik, B., . . . Thordarso, T. (2015). Investigating the use of scanning x-ray fluorescence to locate cryptotephra in minerogenic lacustrine sediment: Experimental results. In I. Croudace & R. Rothwell (Eds.), *Micro-XRF studies of sediment cores: Applications of a non-destructive tool for the environmental sciences* (pp. 305-324).
- Baskaran, M., Nix, J., Kuyper, C., & Karunakara, N. (2014). Problems with the dating of sediment core using excess ²¹⁰Pb in a freshwater system impacted by large scale watershed changes. *Journal of Environmental Radioactivity*, 138, 355-363.
- BC. (2011). Beckman Coulter LS 13 320 laser diffraction particle size analyser. Retrieved from <https://www.beckmancoulter.com/wsrportal/techdocs?docname=B05577AB.pdf>

- Beavan-Athfield, N. (2006). Comment on “*diet-derived variations in radiocarbon and stable isotopes: A case study from Shag River mouth, New Zealand*”. *Radiocarbon*, 48(1), 117-121.
- Beavan, N. R., & Sparks, R. J. (1997). Factors influencing ¹⁴C ages of the Pacific rat *Rattus exulans*. *Radiocarbon*, 40(2), 601-613.
- Begg, J., Johnston, M., & McSaveney, E. (2000). *Geology of the Wellington area*. New Zealand: GNS.
- Bennion, H., Battarbee, R. W., Sayer, C. D., Simpson, G. L., & Davidson, T. A. (2011). Defining reference conditions and restoration targets for lake ecosystems using palaeolimnology: A synthesis. *Journal of Paleolimnology*, 45(4), 533-544.
- Bennion, H., Simpson, G. L., & Goldsmith, B. J. (2015). Assessing degradation and recovery pathways in lakes impacted by eutrophication using the sediment record. *Frontiers in Ecology and Evolution*, 3, 94.
- Blomqvist, S. (1991). Quantitative sampling of soft-bottom sediments: Problems and solutions. *Marine Ecology Progress Series*, 72(3), 295-304.
- Blott, S. (2010). GRADISTAT V. 8.0. A grain size distribution and statistics package for the analysis of unconsolidated sediments by sieving or laser granulometer. *Kenneth Pye Associates Ltd*: UK.
- Blott, S. J., & Pye, K. (2001). Gradistat: A grain size distribution and statistics package for the analysis of unconsolidated sediments. *Earth Surface Processes and Landforms*, 26(11), 1237-1248.
- Boaretto, E., Thorling, L., Sveinbjörnsdóttir, A., Yechieli, Y., & Heinemeier, J. (1997). Study of the effect of fossil organic carbon on ¹⁴C in groundwater from Hvinningdal, Denmark. *Radiocarbon*, 40(2), 915-920.
- Boës, X., Rydberg, J., Martinez-Cortizas, A., Bindler, R., & Renberg, I. (2011). Evaluation of conservative lithogenic elements (Ti, Zr, Al, and Rb) to study anthropogenic element enrichments in lake sediments. *Journal of Paleolimnology*, 46(1), 75-87.
- Bondevik, S., Svendsen, J. I., & Mangerud, J. (1997). Tsunami sedimentary facies deposited by the Storegga tsunami in shallow marine basins and coastal lakes, western Norway. *Sedimentology*, 44(6), 1115-1131.
- Bondevik, S., Svendsen, J. I., & Mangerud, J. (1998). Distinction between the Storegga tsunami and the Holocene marine transgression in coastal basin deposits of western Norway. *Journal of Quaternary Science: Published for the Quaternary Research Association*, 13(6), 529-537.
- Bonny, A. P. (1978). The effect of pollen recruitment processes on pollen distribution over the sediment surface of a small lake in Cumbria. *The Journal of Ecology*, 385-416.
- Bostock, H. C., & Lowe, D. J. (2018). Update on the formalisation of the Anthropocene. *Quaternary Australasia*, 35(1), 14.
- Boyle, J. (2002). Inorganic geochemical methods in palaeolimnology. In W. Last & J. Smol (Eds.), *Tracking environmental change using lake sediments: Physical and geochemical methods* (Vol. 2, pp. 83-141). London, England: Dordrecht and London: Kluwer Academic, Developments in Paleoenvironmental Research.
- Branstrator, D. K., & Lehman, J. T. (1991). Invertebrate predation in Lake Michigan: Regulation of *Bosmina longirostris* by *Leptodora kindtii*. *Limnology and Oceanography*, 36(3), 483-495.
- Bronk Ramsey, C. (2009) Bayesian analysis of radiocarbon dates. *Radiocarbon*, (1), 337-360.
- Brougham, G. G., & Currie, K. J. (1976). *Progress report on water quality investigations: Lake Horowhenua*: Manawatu Catchment Board and Regional Water Board.
- Brown, E. T. (2015). Estimation of biogenic silica concentrations using scanning XRF: Insights from studies of Lake Malawi sediments. In I. Croudace & R. G. Rothwell (Eds.), *Micro-XRF studies of sediment cores: Applications of a non-destructive tool for the environmental sciences* (pp. 267-277): Springer.
- Burgess, S. (1985). *The climate and weather of Manawatu and Horowhenua*. NZMS Miscellaneous Publication. (No. 115/18): New Zealand Meteorological Service, Wellington.

- Burns, N., McIntosh, J., & Scholes, P. (2005). Strategies for managing the lakes of the Rotorua District, New Zealand. *Lake and Reservoir Management*, 21(1), 61-72.
- Burrows, C. (1996). Germination behaviour of seeds of the New Zealand woody species *Ascarina lucida*, *Coprosma grandifolia*, *Melicactus lanceolatus*, and *Solanum laciniatum*. *New Zealand Journal of Botany*, 34(4), 509-515.
- Bussell, M. R. (1988). Mid and late Holocene pollen diagrams and Polynesian deforestation, Wanganui district, New Zealand. *New Zealand Journal of Botany*, 26(3), 431-451.
- Butler, K. (2008). Interpreting charcoal in New Zealand's palaeoenvironment—What do those charcoal fragments really tell us? *Quaternary International*, 184(1), 122-128.
- Butz, C., Grosjean, M., Fischer, D., Wunderle, S., Tylmann, W., & Rein, B. (2015). Hyperspectral imaging spectroscopy: A promising method for the biogeochemical analysis of lake sediments. *Journal of Applied Remote Sensing*, 9(1), 096031.
- Butz, C., Grosjean, M., Goslar, T., & Tylmann, W. (2017). Hyperspectral imaging of sedimentary bacterial pigments: A 1700-year history of meromixis from varved Lake Jaczno, northeast Poland. *Journal of Paleolimnology*, 58(1), 57-72.
- Cambie, R. C., & Ferguson, L. R. (2003). Potential functional foods in the traditional Maori diet. *Mutation Research/Fundamental and Molecular Mechanisms of Mutagenesis*, 523, 109-117.
- Campbell-Platt, G. (2017). *Food science and technology*: John Wiley & Sons.
- Cantle, J. E. (1986). *Atomic absorption spectrometry* (Vol. 5). Amsterdam, Netherlands: Elsevier Scientific.
- Caraco, N., Bauer, J. E., Cole, J. J., Petsch, S., & Raymond, P. (2010). Millennial-aged organic carbon subsidies to a modern river food web. *Ecology*, 91(8), 2385-2393.
- Carkeek, W. (1966). *The Kapiti Coast*. Wellington, New Zealand: AH and AW Reed.
- Chappell, P. (2015). *The climate and weather of Manawatu-Wanganui* (No. 66). New Zealand: NIWA.
- Chase, L. (2015). *Muaūpoko evidence and traditional history report* (No. Wai 2200, #A160). Retrieved from https://forms.justice.govt.nz/search/Documents/WT/wt_DOC_94599308/Wai%202200%2C%20A160.pdf
- Christian, H. J., Blakeslee, R. J., Boccippio, D. J., Boeck, W. L., Buechler, D. E., Driscoll, K. T., . . . Mach, D. M. (2003). Global frequency and distribution of lightning as observed from space by the Optical Transient Detector. *Journal of Geophysical Research: Atmospheres*, 108(D1), ACL 4-1-ACL 4-15.
- Clark, J. S., & Royall, P. D. (1995). Particle-size evidence for source areas of charcoal accumulation in late Holocene sediments of eastern North American lakes. *Quaternary Research*, 43(1), 80-89.
- Clark, R. L. (1982). Point count estimation of charcoal in pollen preparations and thin sections of sediments. *Pollen et Spores*, 24, 523-535.
- Clement, A. J., & Fuller, I. C. (2018). Influence of system controls on the Late Quaternary geomorphic evolution of a rapidly-infilled incised-valley system: The lower Manawatu valley, North Island New Zealand. *Geomorphology*, 303, 13-29.
- Clement, A. J., Fuller, I. C., & Sloss, C. R. (2017). Facies architecture, morphostratigraphy, and sedimentary evolution of a rapidly-infilled Holocene incised-valley estuary: The lower Manawatu valley, North Island New Zealand. *Marine Geology*, 390, 214-233.
- Clement, A. J., Sloss, C. R., & Fuller, I. C. (2010). Late Quaternary geomorphology of the Manawatu coastal plain, North Island, New Zealand. *Quaternary International*, 221(1-2), 36-45.
- Clement, A. J. H. (2011). *Holocene sea-level change in the New Zealand archipelago and the geomorphic evolution of a Holocene coastal plain incised-valley system: The lower Manawatu valley, North Island, New Zealand*. (Doctoral dissertation, Massey University, Palmerston North, New Zealand). Retrieved from <https://mro.massey.ac.nz/handle/10179/2678>
- Cochrane, L. (2017). *Reconstructing ecological change, catchment disturbance, and anthropogenic impact over the last 3000 years at Lake Pounui, Wairarapa, New Zealand*.

- (Master's Thesis, Victoria University of Wellington, Wellington, New Zealand). Retrieved from <http://researcharchive.vuw.ac.nz/xmlui/handle/10063/6665>
- Corella, J. P., Brauer, A., Mangili, C., Rull, V., Vegas-Vilarrúbia, T., Morellón, M., & Valero-Garcés, B. L. (2012). The 1.5-ka varved record of Lake Montcortès (southern Pyrenees, NE Spain). *Quaternary Research*, 78(2), 323-332.
- Cosgrove, S. (2011). *Anthropogenic impacts on Waituna Lagoon: Reconstructing the environmental history*. (Master's thesis, University of Dunedin, Otago, New Zealand). Retrieved from <https://ourarchive.otago.ac.nz/handle/10523/2294>
- Costall, J., Carter, R., Shimada, Y., Anthony, D., & Rapson, G. (2006). The endemic tree *Corynocarpus laevigatus* (karaka) as a weedy invader in forest remnants of southern North Island, New Zealand. *New Zealand Journal of Botany*, 44(1), 5-22.
- Cowie, J. (1963). Dune-building phases in the Manawatu district, New Zealand. *New Zealand Journal of Geology and Geophysics*, 6(2), 268-280.
- Cunningham, B. T., Moar, N., Torrie, A., & Parr, P. (1953). A survey of the western coastal dune lakes of the North Island, New Zealand. *Marine and Freshwater Research*, 4(2), 343-386.
- Curtis, C. (1964). Notes on eel weirs and Maori fishing methods. *The Journal of the Polynesian Society*, 73(2), 167-170.
- Davidson, J. (1987). *The Prehistory of New Zealand*: Longman Paul.
- Davies, S. J., Lamb, H. F., & Roberts, S. J. (2015). Micro-XRF core scanning in palaeolimnology: recent developments. In I. Croudace & R. Rothwell (Eds.), *Micro-XRF studies of sediment cores: Applications of a non-destructive tool for the environmental sciences* (pp. 189-226): Springer.
- Dawson, A. G., & Shi, S. (2000). Tsunami deposits. *Pure and Applied Geophysics*, 157(6-8), 875-897.
- Dawson, J., & Lucas, R. (2000). *Nature guide to the New Zealand forest*: Godwit.
- de Winton, M., & Taumoepeau, A. (2014). *Delimitation of submerged weed bed areas in Lake Horowhenua*. (No. HAM2014-015). New Zealand: NIWA. Retrieved from <https://www.horizons.govt.nz/HRC/media/Media/Reserves%20and%20Projects/Delimitation-of-submerged-weed-bed-areas-in-Lake-Horowhenua.pdf?ext=.pdf>
- Dearing, J., Battarbee, R., Dikau, R., Larocque, I., & Oldfield, F. (2006). Human–environment interactions: Learning from the past. *Regional Environmental Change*, 6, 1-16.
- Diaz, H. F., & Pulwarty, R. S. (1994). An analysis of the time scales of variability in centuries-long ENSO-sensitive records in the last 1000 years. *Climatic Change*, 26(2-3), 317-342.
- Dickson, M. (1997). *A mid to late Holocene pollen diagram, Horowhenua Lowlands, New Zealand*. Massey University, New Zealand.
- Dodson, J. (1977). Pollen deposition in a small closed drainage basin lake. *Review of Palaeobotany and Palynology*, 24(4), 179-193.
- Dreaver, A. (1984). *Horowhenua County and its people: A centennial history*: Dunmore [for] Horowhenua County Council.
- Dreaver, A. (2006). *Levin: The making of a town*: Horowhenua District Council.
- Duguid, F. C. (1990). Botany of northern Horowhenua lowlands, North Island, New Zealand. *New Zealand Journal of Botany*, 28(4), 381-437.
- Dunbar, G. B., McLea, B., & Goff, J. R. (1997). Holocene pollen stratigraphy and sedimentation, Wellington Harbour, New Zealand. *New Zealand Journal of Geology and Geophysics*, 40(3), 325-333.
- Elementar. (2016). Vario MACRO cube. Retrieved from https://www.elementar.de/fileadmin/user_upload/Elementar_Website/Downloads/Flyer/Flyer-vario-MACRO-cube-EN.pdf
- Elliot, M., Striewski, B., Flenley, J., & Sutton, D. (1995). Palynological and sedimentological evidence for a radiocarbon chronology of environmental change and Polynesian deforestation from Lake Taumatawhana, Northland, New Zealand *Radiocarbon*, 37(3), 899-916.

- Elliott, S. (2014). Overview of the MP-AES. Retrieved from <https://www.agilent.com/cs/library/eseminars/public/4200%20MP-AES%20for%20Mining%20Playlist.pdf>
- Engstrom, D. R., & Wright Jr, H. (1984). Chemical stratigraphy of lake sediments as a record of environmental change. In Y. Haworth & J. Lund (Eds.), *Lake sediments and environmental history: Studies in palaeolimnology and palaeoecology in honour of Winifred Tutin*.
- Esler, A. E. (1962). The Banks Lecture: Forest remnants of the Manawatu lowlands. *New Zealand Plants and Gardens*, 4, 255-268.
- Esler, A. E. (1964). The vegetation of early Manawatu. In B. Saunders & A. Anderson (Eds.), *Introducing Manawatu* (pp. 33-44). Massey University, New Zealand: Department of Geography.
- Esler, A. E. (1978). *Botany of the Manawatu District, New Zealand*. Wellington, New Zealand: Department of Scientific and Industrial Research.
- Ewart, A., & Stipp, J. (1968). Petrogenesis of the volcanic rocks of the central North Island, New Zealand, as indicated by a study of Sr⁸⁷Sr⁸⁶ ratios, and Sr, Rb, K, U and Th abundances. *Geochimica et Cosmochimica Acta*, 32(7), 699-736.
- Faegri, K., & Iversen, J. (1989). *Textbook of pollen analysis* (4 ed.). New York, USA: Wiley.
- Fair, E. E. (1968). *Structural, tectonic and climatic control of the fluvial geomorphology of the Manawatu River west of the Manawatu Gorge*. New Zealand: Massey University.
- Fallu, M.-A., Pienitz, R., Walker, I. R., & Overpeck, J. (2004). AMS 14C dating of tundra lake sediments using chironomid head capsules. *Journal of Paleolimnology*, 31(1), 11-22.
- Flenley, J. (2000). *Vegetation: Contrasts and changes. South of the North. Manawatu and its Neighbours*: Massey University, New Zealand.
- Folk, R. L., & Ward, W. C. (1957). Brazos River bar [Texas]: A study in the significance of grain size parameters. *Journal of Sedimentary Research*, 27(1), 3-26.
- Forbes, S. (1996). *Te Waipunahau: Archaeological survey*. A report prepared for the Horowhenua Lake Trustees.
- Fox, E. G. (2016). *Disturbance in the North Island of New Zealand: A case study using floodplain cores from the Coromandel to determine anthropogenic disturbance*. (Master's thesis, Massey University, Palmerston North, New Zealand). Retrieved from <https://mro.massey.ac.nz/handle/10179/9924>
- Frangipane, G., Pistolato, M., Molinaroli, E., Guerzoni, S., & Tagliapietra, D. (2009). Comparison of loss on ignition and thermal analysis stepwise methods for determination of sedimentary organic matter. *Aquatic conservation: Marine and Freshwater Ecosystems*, 19(1), 24-33.
- Friedrich, J., Janssen, F., Aleynik, D., Bange, H. W., Boltacheva, N., Çagatay, M., . . . Geraga, M. (2014). Investigating hypoxia in aquatic environments: Diverse approaches to addressing a complex phenomenon. *Biogeosciences (BG)*, 11, 1215-1259.
- Fuller, I. C., Macklin, M. G., & Richardson, J. M. (2015). The geography of the Anthropocene in New Zealand: Differential river catchment response to human impact. *Geographical Research*, 53(3), 255-269.
- Gellatly, A. F., Chinn, T. J., & Röthlisberger, F. (1988). Holocene glacier variations in New Zealand: A review. *Quaternary Science Reviews*, 7(2), 227-242.
- Gibb, J. (1986). A New Zealand regional Holocene eustatic sea-level curve and its application to determination of vertical tectonic movements. *Royal Society of New Zealand Bulletin*, 24, 377-395.
- Gibbs, M. (2011). *Lake Horowhenua review: Assessment of opportunities to address water quality issues in Lake Horowhenua* (No. HAM 2011-046). New Zealand: NIWA.
- Gibbs, M., & Quinn, J. (2012). *Restoration plan for Lake Horowhenua* (No. HAM2012-004). New Zealand: NIWA.
- Gibbs, M., & White, E. (1994). Lake Horowhenua: A computer model of its limnology and restoration prospects. *Hydrobiologia*, 467-477.
- Gilliland, B. W. (1978). *Lake Horowhenua. Current condition, nutrient budget and future management*: Manawatu Wanganui Regional Council.

- Gilliland, B. W. (1981). *Hokio Stream water quality assessment*: Manawatu Wanganui Regional Council.
- Glade, T. (2003). Landslide occurrence as a response to land use change: A review of evidence from New Zealand. *Catena*, 51(3-4), 297-314.
- Glew, J. R., Smol, J. P., & Last, W. M. (2002). Sediment core collection and extrusion. W. Last & J. Smol (Eds.), *Tracking environmental change using lake sediments: Basin analysis, coring and chronological techniques* (Vol. 1, pp. 73-105). London, England: Dordrecht and London: Kluwer Academic, Developments in Paleoenvironmental Research.
- Goff, J., Chagué-Goff, C., & Nichol, S. (2001). Palaeotsunami deposits: A New Zealand perspective. *Sedimentary Geology*, 143(1-2), 1-6.
- Goff, J., Rouse, H., Jones, S., Hayward, B., Cochran, U., McLea, W., . . . Morley, M. (2000). Evidence for an earthquake and tsunami about 3100–3400 yr ago, and other catastrophic saltwater inundations recorded in a coastal lagoon, New Zealand. *Marine Geology*, 170(1-2), 231-249.
- Goldin, A. (1987). Reassessing the use of loss-on-ignition for estimating organic matter content in noncalcareous soils. *Communications in Soil Science and Plant Analysis*, 18(10), 1111-1116.
- Gomez, B., Carter, L., Trustrum, N. A., Palmer, A. S., & Roberts, A. P. (2004). El Niño–Southern Oscillation signal associated with middle Holocene climate change in intercorrelated terrestrial and marine sediment cores, North Island, New Zealand. *Geology*, 32(8), 653-656.
- Grant, P. J. (1963). Forests and recent climatic history of the Huiarau Range Uruwera Region, North Island. *Transactions of the Royal Society of New Zealand Botany*, 11(12), 143-172.
- Grant, P. J. (1985). Major periods of erosion and alluvial sedimentation in New Zealand during the late Holocene. *Journal of the Royal Society of New Zealand*, 15(1), 67-121.
- Gray, A. B., Pasternack, G. B., & Watson, E. B. (2010). Hydrogen peroxide treatment effects on the particle size distribution of alluvial and marsh sediments. *The Holocene*, 20(2), 293-301.
- Green, B. J., Yli-Panula, E., Dettmann, M., Rutherford, S., & Simpson, R. (2003). Airborne Pinus pollen in the atmosphere of Brisbane, Australia and relationships with meteorological parameters. *Aerobiologia*, 19(1), 47-55.
- Greenwood, T. L., Green, J. D., Hicks, B. J., & Chapman, M. A. (1999). Seasonal abundance of small Cladocerans in lake Mangakaware, Waikato, New Zealand. *New Zealand Journal of Marine and Freshwater Research*, 33(3), 399-415.
- Grimm, E. C. (2015). TILIA Software, V. 2.0.41. *Illinois State Museum*. Illinois, USA.
- Grimm, E. C. (1987). CONISS: A fortran 77 program for stratigraphically constrained cluster analysis by the method of incremental sum of squares. *Computers & Geosciences*, 13(1), 13-35.
- Haberzettl, T., Corbella, H., Fey, M., Janssen, S., Lücke, A., Mayr, C., . . . Wille, M. (2007). Lateglacial and Holocene wet–dry cycles in southern Patagonia: Chronology, sedimentology and geochemistry of a lacustrine record from Laguna Potrok Aike, Argentina. *The Holocene*, 17(3), 297-310.
- Harmsworth, G. R., & Awatere, S. (2013). *Indigenous Maori knowledge and perspectives of ecosystems*. Lincoln, New Zealand: Manaaki Whenua Press.
- Heerdegen, R., & Shepherd, M. (1982). *Manawatu landforms - product of tectonism, climate change and process*. Auckland, New Zealand: Longman Paul.
- Heerdegen, R., & Shepherd, M. (1992). *Landforms of the Manawatu*. Auckland, New Zealand: Longman Paul.
- Heiri, O., Lotter, A. F., & Lemcke, G. (2001). Loss on ignition as a method for estimating organic and carbonate content in sediments: Reproducibility and comparability of results. *Journal of Paleolimnology*, 25(1), 101-110.
- Hellstrom, J., McCulloch, M., & Stone, J. (1998). A detailed 31,000-year record of climate and vegetation change, from the isotope geochemistry of two New Zealand speleothems. *Quaternary Research*, 50(2), 167-178.

- Hemphill-Haley, E. (1996). Diatoms as an aid in identifying late-Holocene tsunami deposits. *The Holocene*, 6(4), 439-448.
- Hesp, P. (1975). *The late Quaternary geomorphology of the lower Manawatu*. (Unpublished master's thesis), Massey University, Palmerston North, New Zealand.
- Hesp, P., & Shepherd, M. (1978). Some aspects of the late Quaternary geomorphology of the lower Manawatu Valley, New Zealand. *New Zealand Journal of Geology and Geophysics*, 21(3), 403-412.
- Hesp, P. A. (2001). The Manawatu dunefield: Environmental change and human impacts. *New Zealand Geographer*, 57(2), 33-40.
- Hesp, P. A., Shepherd, M. J., & Parnell, K. (1999). Coastal geomorphology in New Zealand, 1989-99. *Progress in Physical Geography*, 23(4), 501-524.
- Higham, T., Anderson, A., & Jacomb, C. (1999). Dating the first New Zealanders: The chronology of Wairau Bar. *Antiquity*, 73(280), 420-427.
- Higham, T., Anderson, A., Ramsey, C. B., & Tompkins, C. (2005). Diet-derived variations in radiocarbon and stable isotopes: A case study from Shag River mouth, New Zealand. *Radiocarbon*, 47(3), 367-375.
- Higham, T., & Hogg, A. (1997). Evidence for late Polynesian colonization of New Zealand: University of Waikato radiocarbon measurements. *Radiocarbon*, 39(2), 149-192.
- Hogg, A. G., Hua, Q., Blackwell, P. G., Niu, M., Buck, C. E., Guilderson, T. P., . . . Reimer, R. W. (2013). SHCal13 Southern Hemisphere calibration, 0–50,000 years cal BP. *Radiocarbon*, 55(4), 1889-1903.
- Hogg, A. G., McCormac, F., Higham, T. F., Reimer, P. J., Baillie, M. G., & Palmer, J. G. (2002). High-precision radiocarbon measurements of contemporaneous tree-ring dated wood from the British Isles and New Zealand: AD 1850–950. *Radiocarbon*, 44(3), 633-640.
- Holdaway, R., & Beavan, N. (1999). Reliable ¹⁴C AMS dates on bird and Pacific rat *Rattus exulans* bone gelatin, from a CaCO₃-rich deposit. *Journal of the Royal Society of New Zealand*, 29(3), 185-211.
- Holdaway, R. N. (1996). Arrival of rats in New Zealand. *Nature*, 384(6606), 225.
- Holdaway, R. N. (1999). A spatio-temporal model for the invasion of the New Zealand archipelago by the Pacific rat *Rattus exulans*. *Journal of the Royal Society of New Zealand*, 29(2), 91-105.
- Holland, L. (1983). The shifting sands of the Manawatu. *Soil and Water*, 4, 3-5.
- Hoogsteen, M., Lantinga, E., Bakker, E., Groot, J., & Tittonell, P. (2015). Estimating soil organic carbon through loss on ignition: Effects of ignition conditions and structural water loss. *European Journal of Soil Science*, 66(2), 320-328.
- Hoogsteen, M., Lantinga, E., Bakker, E., & Tittonell, P. (2018). An evaluation of the loss-on-ignition method for determining the soil organic matter content of calcareous soils. *Communications in Soil Science and Plant Analysis*, 1-12.
- HORIBA. (2005). Applications note: Particle sizing of sediments. Retrieved from <https://faculty.washington.edu/kate1/ewExternalFiles/AN144%20Particle%20sizing%20of%20sediments.pdf>
- HORIBA. (2012). A guidebook to particle size analysis. Retrieved from https://www.horiba.com/fileadmin/uploads/Scientific/Documents/PSA/PSA_Guidebook.pdf
- Houba, V., van der Lee, J., & Novozamsky, I. (1997). *Soil analysis procedures, other procedures, syllabus soil and plant analysis*. Wageningen, Netherlands: Wageningen Agricultural University.
- HRC. (2014). *The Lake Horowhenua accord action plan* (No. 2014/EXT/1389). Retrieved from <https://www.horizons.govt.nz/HRC/media/Media/Reserves%20and%20Projects/Action-Plan-for-Lake-Horowhenua.pdf?ext=.pdf>
- HRC. (2017). *Lake Horowhenua catchment report card*. Horizons Regional Council. Retrieved from <https://www.horizons.govt.nz/HRC/media/Media/Water/Lake-Horowhenua-Report-122017.pdf?ext=.pdf>
- HRC. (2018). *Sediment legacy project results*. Horizons Regional Council. Retrieved from <https://www.horizons.govt.nz/HRC/media/Media/Agenda-Reports/Regional-Council->

Meeting-2018-25-

09/18157%20Annex%20C%20Sediment%20legacy%20project%20results.pdf

- Hua, Q., Barbetti, M., & Rakowski, A. Z. (2013). Atmospheric radiocarbon for the period 1950–2010. *Radiocarbon*, *55*(4), 2059-2072.
- Hughes, G. R. (2005). Evolution of the north Horowhenua coastal depositional system in response to Late Pleistocene sea level changes.
- Hughes, G. R., & Kennedy, D. M. (2009). Late Pleistocene sea-level oscillations (MIS 10–2) recorded in shallow marine and coastal plain sediments of the southern Wanganui Basin, New Zealand. *Quaternary Research*, *71*(3), 477-489.
- Hughes, P., Hope, G., Latham, M., & Brookfield, M. (1979). *Prehistoric man-induced degradation of the Lakeba landscape: Evidence from two inland swamps* (No. 0909596301). Retrieved from http://horizon.documentation.ird.fr/exl-doc/pleins_textes/pleins_textes_7/b_fdi_55-56/010022534.pdf
- Ireland, T. R. (1992). Crustal evolution of New Zealand: Evidence from age distributions of detrital zircons in western province paragneisses and torlesse greywacke. *Geochimica et Cosmochimica Acta*, *56*(3), 911-920.
- Issaka, S., & Ashraf, M. A. (2017). Impact of soil erosion and degradation on water quality: A review. *Geology, Ecology, and Landscapes*, *1*(1), 1-11.
- Jara, I. A., Newnham, R. M., Alloway, B. V., Wilmshurst, J. M., & Rees, A. B. (2017). Pollen-based temperature and precipitation records of the past 14,600 years in northern New Zealand (37° S) and their linkages with the Southern Hemisphere atmospheric circulation. *The Holocene*, *27*(11), 1756-1768.
- Jones, R. I. (1992). The influence of humic substances on lacustrine planktonic food chains. *Hydrobiologia*, *229*(1), 73-91.
- Joy, M., & Death, R. (2002). Predictive modelling of freshwater fish as a biomonitoring tool in New Zealand. *Freshwater Biology*, *47*(11), 2261-2275.
- Kabbashi, N. (2011). Sewage sludge composting simulation as carbon/nitrogen concentration change. *Journal of Environmental Sciences*, *23*(11), 1925-1928.
- Kennett, J. P., Kennett, D. J., Culleton, B. J., Tortosa, J. E. A., Bischoff, J. L., Bunch, T. E., . . . Firestone, R. B. (2015). Bayesian chronological analyses consistent with synchronous age of 12,835–12,735 Cal BP for Younger Dryas boundary on four continents. *Proceedings of the National Academy of Sciences*, *112*(32), E4344-E4353.
- Kershaw, A. P. (1997). A modification of the Troels-Smith system of sediment description and portrayal. *Quaternary Australasia*, *15*(2), 63-68.
- Kirch, P. V. (2005). Archaeology and global change: The Holocene record. *Annual Review of Environment and Resources*, *30*, 409-440.
- Konert, M., & Vandenberghe, J. (1997). Comparison of laser grain size analysis with pipette and sieve analysis: A solution for the underestimation of the clay fraction. *Sedimentology*, *44*(3), 523-535.
- Kortekaas, S. (2002). *Tsunamis, storms and earthquakes: Distinguishing coastal flooding events*. (Unpublished doctoral dissertation), Coventry University, Coventry, United Kingdom.
- Kortekaas, S., & Dawson, A. G. (2007). Distinguishing tsunami and storm deposits: An example from Martinhal, SW Portugal. *Sedimentary Geology*, *200*(3-4), 208-221.
- Kylander, M. E., Ampel, L., Wohlfarth, B., & Veres, D. (2011). High-resolution x-ray fluorescence core scanning analysis of Les Echets (France) sedimentary sequence: New insights from chemical proxies. *Journal of Quaternary Science*, *26*(1), 109-117.
- Lamarque, G., Proust, J. N., & Nodder, S. D. (2005). Long-term slip rates and fault interactions under low contractional strain, Wanganui Basin, New Zealand. *Tectonics*, *24*(4).
- Large, M., & Braggins, J. (1991). *Spore atlas of New Zealand ferns and fern allies*. Wellington, New Zealand: New Zealand Journal of Botany.
- Last, W. M. (2002). Textural analysis of lake sediments. In W. Last & J. Smol (Eds.), *Tracking environmental change using lake sediments: Physical and geochemical methods* (Vol. 2, pp. 41-81). London, England: Dordrecht and London: Kluwer Academic, Developments in Paleoenvironmental Research.
- LAWA. (n.d.). Land cover. Retrieved from <https://www.lawa.org.nz/explore-data/land-cover/>

- Leathwick, J., & Whitehead, D. (2001). Soil and atmospheric water deficits and the distribution of New Zealand's indigenous tree species. *Functional Ecology*, 15(2), 233-242.
- Lee, J. M., Begg, J., & Forsyth, P. (2002). *Geology of the Wairarapa area*. New Zealand: GNS.
- Lees, C. M. (1986). Late Quaternary palynology of the southern Ruahine Range North Island, New Zealand. *New Zealand Journal of Botany*, 24(2), 315-329.
- Li, X., Rapson, G., & Flenley, J. R. (2008). Holocene vegetational and climatic history, Sponge Swamp, Haast, south-western New Zealand. *Quaternary International*, 184(1), 129-138.
- Li, Y., Qiang, M., Jin, Y., Liu, L., Zhou, A., & Zhang, J. (2018). Influence of aquatic plant photosynthesis on the reservoir effect of Genggahai Lake, northeastern Qinghai-Tibetan Plateau. *Radiocarbon*, 60(2), 561-569.
- Litchfield, N. (2003). *Maps, stratigraphic logs and age control data for river terraces in the Eastern North Island* (No. 2003/31). New Zealand: GNS.
- Livingstone, D. (1955). A lightweight piston sampler for lake deposits. *Ecology*, 36(1), 137-139.
- Loizeau, J. L., Arbouille, D., Santiago, S., & Vernet, J. P. (1994). Evaluation of a wide range laser diffraction grain size analyser for use with sediments. *Sedimentology*, 41(2), 353-361.
- Lorrey, A., & Bostock, H. (2017). The climate of New Zealand through the Quaternary. In *Advances in Quaternary science: The New Zealand landscape* (pp. 67-139.). Paris, France: Atlantis Press.
- Lorrey, A., Fowler, A. M., & Salinger, J. (2007). Regional climate regime classification as a qualitative tool for interpreting multi-proxy palaeoclimate data spatial patterns: A New Zealand case study. *Palaeogeography, Palaeoclimatology, Palaeoecology*, 253(3-4), 407-433.
- Lorrey, A., Williams, P., Salinger, J., Martin, T., Palmer, J., Fowler, A., . . . Neil, H. (2008). Speleothem stable isotope records interpreted within a multi-proxy framework and implications for New Zealand palaeoclimate reconstruction. *Quaternary International*, 187(1), 52-75.
- Lowe, D. J., Blaauw, M., Hogg, A. G., & Newnham, R. M. (2013). Ages of 24 widespread tephras erupted since 30,000 years ago in New Zealand, with re-evaluation of the timing and palaeoclimatic implications of the Lateglacial cool episode recorded at Kaipo bog. *Quaternary Science Reviews*, 74, 170-194.
- Lowe, D. J., Shane, P. A., Alloway, B. V., & Newnham, R. M. (2008). Fingerprints and age models for widespread New Zealand tephra marker beds erupted since 30,000 years ago: A framework for NZ-INTIMATE. *Quaternary Science Reviews*, 27(1-2), 95-126.
- Lowe, J. J., & Walker, M. J. (2014). *Reconstructing Quaternary environments*: Routledge.
- Lusk, C., & Ogden, J. (1992). Age structure and dynamics of a Podocarp-Broadleaf forest in Tongariro National Park, New Zealand. *Journal of Ecology*, 379-393.
- MacDonald-Creevey, A. M. (2011). *Late Holocene environmental record and geological history of the Lake Colenso area, north-western Ruahine Range, New Zealand*. (Master's thesis, Massey University, Palmerston North, New Zealand). Retrieved from <https://mro.massey.ac.nz/xmlui/handle/10179/2907>
- Mackereth, F. J. H. (1966). Some chemical observations on post-glacial lake sediments. *Phil. Trans. R. Soc. Lond. B*, 250(765), 165-213.
- MacLachlan, S., Hunt, J., & Croudace, I. (2015). Optimization of ITRAX core scanner measurement conditions for sediments from submarine mud volcanoes. In I. Croudace & R. Rothwell (Eds.), *Micro-XRF studies of sediment cores: Applications of a non-destructive tool for the environmental sciences* (pp. 103-127): Springer.
- Maclean, C., & Maclean, J. (1988). *Waikanae: Past & present*: Whitcombe Press.
- MacPhail, M. (n.d.). *Photographic record of the pollen flora of New Zealand*.
- Macphail, M., & McQueen, D. (1983). The value of New Zealand pollen and spores as indicators of Cenozoic vegetation and climates. *Tuatara*, 26(2), 37-59.
- Marty, J., & Myrbo, A. (2014). Radiocarbon dating suitability of aquatic plant macrofossils. *Journal of Paleolimnology*, 52(4), 435-443.
- Matisoo-Smith, E. (2016). The human landscape: Population origins, settlement and the impact of human arrival in Aotearoa/New Zealand. In J. Shulmeister (Ed.), *Landscape and Quaternary Environmental Change in New Zealand* (Vol. 3): Springer.

- McCave, I., Bryant, R., Cook, H., & Coughanowr, C. (1986). Evaluation of a laser-diffraction-size analyzer for use with natural sediments. *Journal of Sedimentary Research*, 56(4).
- McCull, R. (1978). Lake Tutira: The use of phosphorus loadings in a management study. *New Zealand Journal of Marine and Freshwater Research*, 12(3), 251-256.
- McDonald, R., & O'Donnell, E. (1929). *Te Hekenga: Early days in Horowhenua: Being the reminiscences of Mr. Rod McDonald*. Palmerston North, New Zealand: GH Bennett.
- McFadgen, B. (1994). *Archaeology of the Wellington Conservancy: Wairarapa*. Wellington, New Zealand: Department of conservation.
- McFadgen, B. (1997). *Archaeology of the Wellington Conservancy: Kapiti-Horowhenua*. Wellington, New Zealand: Department of Conservation.
- McGlone, M. (1978). Forest destruction by early Polynesians, Lake Poukawa, Hawkes Bay, New Zealand. *Journal of the Royal Society of New Zealand*, 8(3), 275-281.
- McGlone, M. (1983). Polynesian deforestation of New Zealand: A preliminary synthesis. *Archaeology in Oceania*, 18(1), 11-25.
- McGlone, M. (1988). New Zealand. In B. Huntley & T. Webb III (Eds.), *Vegetation history. Handbook of Vegetation Science*. (Vol. 7): Kluwer, Dordrecht, the Netherlands.
- McGlone, M. (1989). The Polynesian settlement of New Zealand in relation to environmental and biotic changes. *New Zealand Journal of Ecology*, 115-129.
- McGlone, M., Anderson, A., & Holdaway, R. (1994). *An ecological approach to the Polynesian settlement of New Zealand*.
- McGlone, M., Holdaway, R., & Gee, M. (1997). Flora and fauna. The New Zealand Islands just before human settlement, plate 8. In M. McKinnon, B. Bradley & R. Kirkpatrick (Eds.), *New Zealand historical atlas: Ko Papatuanuku e Tatoto Nei*. New Zealand: David Bateman.
- McGlone, M., Kershaw, A. P., & Markgraf, V. (1992). El Niño/Southern Oscillation climatic variability in Australasian and South American paleoenvironmental records. In H. Diaz & V. Markgraf (Eds.), *El Niño: Historical and paleoclimatic aspects of the Southern Oscillation* (pp. 435-462). Cambridge, England: Cambridge University Press.
- McGlone, M., & Moar, N. (1977). The Ascarina decline and post-glacial climatic change in New Zealand. *New Zealand Journal of Botany*, 15(2), 485-489.
- McGlone, M., Neall, V., & Clarkson, B. (1988). The effect of recent volcanic events and climatic changes on the vegetation of Mt Egmont (Mt Taranaki), New Zealand. *New Zealand Journal of Botany*, 26(1), 123-144.
- McGlone, M., Salinger, M. J., & Moar, N. T. (1993). Paleovegetation studies of New Zealand's climate since the last glacial maximum. In H. Wright, J. Kutzbach, T. Webb, W. Ruddiman, F. Strett-Perrott, & P. Bartlein (Eds.), *Global climates since the last glacial maximum* (pp. 294-317). Minneapolis, Minnesota: University of Minnesota Press.
- McGlone, M., & Topping, W. (1977). Aranuiian (post-glacial) pollen diagrams from the Tongariro region, North Island, New Zealand. *New Zealand Journal of Botany*, 15(4), 749-760.
- McGlone, M., Wilmshurst, J., & Leach, H. (2005). An ecological and historical review of bracken (*Pteridium esculentum*) in New Zealand, and its cultural significance. *New Zealand Journal of Ecology*, 165-184.
- McGlone, M., & Wilmshurst, J. M. (1999). Dating initial Maori environmental impact in New Zealand. *Quaternary International*, 59(1), 5-16.
- McGlone, M. S. (2009). Postglacial history of New Zealand wetlands and implications for their conservation. *New Zealand Journal of Ecology*, 1-23.
- McWethy, D., Higuera, P., Whitlock, C., Veblen, T., Bowman, D., Cary, G., . . . McGlone, M. (2013). A conceptual framework for predicting temperate ecosystem sensitivity to human impacts on fire regimes. *Global Ecology and Biogeography*, 22(8), 900-912.
- McWethy, D. B., Whitlock, C., Wilmshurst, J. M., McGlone, M. S., Fromont, M., Li, X., . . . Cook, E. R. (2010). Rapid landscape transformation in South Island, New Zealand, following initial Polynesian settlement. *Proceedings of the National Academy of Sciences*.

- McWethy, D. B., Whitlock, C., Wilmshurst, J. M., McGlone, M. S., & Li, X. (2009). Rapid deforestation of South Island, New Zealand, by early Polynesian fires. *The Holocene*, 19(6), 883-897.
- McWethy, D. B., Wilmshurst, J. M., Whitlock, C., Wood, J. R., & McGlone, M. S. (2014). A high-resolution chronology of rapid forest transitions following Polynesian arrival in New Zealand. *PLoS One*, 9(11).
- Meyers, P. A., & Ishiwatari, R. (1993). Lacustrine organic geochemistry - an overview of indicators of organic matter sources and diagenesis in lake sediments. *Organic Geochemistry*, 20(7), 867-900.
- Meyers, P. A., & Teranes, J. L. (2002). Sediment organic matter. In W. Last & J. Smol (Eds.), *Tracking environmental change using lake sediments: Physical and geochemical methods* (Vol. 2, pp. 239-269). London, England: Dordrecht and London: Kluwer Academic, Developments in Paleoenvironmental Research.
- MfE. (2001). *Case Study 3. Waipunahau (Lake Horowhenua): Restoring the mauri*. New Zealand Ministry for the Environment.
- MfE. (2017a). Lake Horowhenua Report. Retrieved from <http://www.mfe.govt.nz/fresh-water/clean-projects/lake-horowhenua>
- MfE. (2017b). Te Mana o Te Wai projects. Retrieved from <http://www.mfe.govt.nz/more/funding/funding-fresh-water/te-mana-o-te-wai-fund/te-mana-o-te-wai-projects>
- Mikutta, R., Kleber, M., Kaiser, K., & Jahn, R. (2005). Review: Organic matter removal from soils using hydrogen peroxide, sodium hypochlorite, and disodium peroxodisulfate. *Soil Science Society of America Journal*, 69(1), 120-135.
- Moar, N. (1967). Contributions to the Quaternary history of the New Zealand flora: Pollen diagrams from No Man's Land bog, northern Ruahine Range. *New Zealand Journal of Botany*, 5(3), 394-399.
- Moar, N., Wilmshurst, J., & McGlone, M. (2011). Standardizing names applied to pollen and spores in New Zealand Quaternary palynology. *New Zealand Journal of Botany*, 49(2), 201-229.
- Moar, N. T. (1993). Pollen grains of New Zealand dicotyledonous plants.
- Moore, P. D., Webb, J. A., & Collison, M. E. (1991). *Pollen analysis*: Blackwell Scientific Publications.
- Moreno, A., Giralt, S., Valero-Garcés, B., Sáez, A., Bao, R., Prego, R., . . . Taberner, C. (2007). A 14 kyr record of the tropical Andes: The Lago Chungará sequence (18 S, northern Chilean Altiplano). *Quaternary International*, 161(1), 4-21.
- Morgenstern, U., Martindale, H., Stewart, M., Trompeter, V., Raaij, R. v. d., Toews, R., . . . Townsend, D. (2015). *Groundwater dynamics and hydrochemical evolution as inferred from Horizon's regional age tracer data* (No. 2015/32). New Zealand: GNS.
- Morton, R. A., Gelfenbaum, G., & Jaffe, B. E. (2007). Physical criteria for distinguishing sandy tsunami and storm deposits using modern examples. *Sedimentary Geology*, 200(3-4), 184-207.
- Morton, R. A., & White, W. A. (1997). Characteristics of and corrections for core shortening in unconsolidated sediments. *Journal of Coastal Research*, 761-769.
- Moss, B., Kosten, S., Meerhoff, M., Battarbee, R. W., Jeppesen, E., Mazzeo, N., . . . De Meester, L. (2011). Allied attack: Climate change and eutrophication. *Inland Waters*, 1(2), 101-105.
- Moy, C. M., Seltzer, G. O., Rodbell, D. T., & Anderson, D. M. (2002). Variability of El Niño/Southern Oscillation activity at millennial timescales during the Holocene epoch. *Nature*, 420(6912), 162.
- Müller-Solger, A. B., Jassby, A. D., & Müller-Navarra, D. C. (2002). Nutritional quality of food resources for zooplankton (*Daphnia*) in a tidal freshwater system (Sacramento-San Joaquin River Delta). *Limnology and Oceanography*, 47(5), 1468-1476.
- Murray-McIntosh, R. P., Scrimshaw, B. J., Hatfield, P. J., & Penny, D. (1998). Testing migration patterns and estimating founding population size in Polynesia by using human mtDNA sequences. *Proceedings of the National Academy of Sciences*, 95(15), 9047-9052.

- Murray, M. R. (2002). Is laser particle size determination possible for carbonate-rich lake sediments? *Journal of Paleolimnology*, 27(2), 173-183.
- MWRC. (1984). *Manawatu-Wanganui regional management plan*: Manawatu-Wanganui Regional Council, New Zealand.
- MWRC. (2008). *Lake Horowhenua and Hokio Stream catchment management strategy*: Manawatu-Wanganui Regional Council, New Zealand.
- Nelson, C., Hendy, I., Neil, H., Hendy, C., & Weaver, P. (2000). Last glacial jetting of cold waters through the Subtropical Convergence zone in the Southwest Pacific off eastern New Zealand, and some geological implications. *Palaeogeography, Palaeoclimatology, Palaeoecology*, 156(1), 103-121.
- Nelson, D. W., & Sommers, L. E. (1996). *Total carbon, organic carbon, and organic matter*. In A.L. Page, R.H. Miller and D.R. Keeney, *Methods of soil analysis. Part 2 Chemical and Microbiological Properties* (pp. 539-579).
- Newnham, R., Lowe, D. J., Gehrels, M., & Augustinus, P. (2018). Two-step human-environmental impact history for northern New Zealand linked to late-Holocene climate change. *The Holocene*, 0959683618761545.
- Newnham, R. M. (1992). A 30,000 year pollen, vegetation and climate record from Otakairangi (Hikurangi), Northland, New Zealand. *Journal of Biogeography*, 541-554.
- Newnham, R. M., Lowe, D., McGlone, M., Wilmshurst, J., & Higham, T. (1998b). The Kaharoa Tephra as a critical datum for earliest human impact in northern New Zealand. *Journal of Archaeological Science*, 25(6), 533-544.
- Newnham, R. M., & Lowe, D. J. (2000). Fine-resolution pollen record of late-glacial climate reversal from New Zealand. *Geology*, 28(8), 759-762.
- Newnham, R. M., Lowe, D. J., & Green, J. D. (1989). Palynology, vegetation and climate of the Waikato lowlands, North Island, New Zealand, since c. 18,000 years ago. *Journal of the Royal Society of New Zealand*, 19(2), 127-150.
- Newnham, R. M., Lowe, D. J., & Matthews, B. W. (1998a). A late-Holocene and prehistoric record of environmental change from Lake Waikaremoana, New Zealand. *The Holocene*, 8(4), 443-454.
- Newnham, R. M., Lowe, D. J., & Wigley, G. (1995). Late Holocene palynology and palaeovegetation of tephra-bearing mires at Papamoa and Waihi Beach, western Bay of Plenty, North Island, New Zealand. *Journal of the Royal Society of New Zealand*, 25(2), 283-300.
- NIWA. (n.d). National and regional climate maps Manawatu. Retrieved from <https://www.niwa.co.nz/climate/national-and-regional-climate-maps/manawatu>
- Ogden, J., Basher, L., & McGlone, M. (1998). Botanical Briefing: Fire, forest regeneration and links with early human habitation: Evidence from New Zealand. *Annals of Botany*, 81(6), 687-696.
- Ogle, C., & West, C. J. (1997). *Some revegetation options for Lake Horowhenua*, Levin: New Zealand: Department of Conservation.
- Orr, T. O. H., Korsch, R. J., & Foley, L. A. (1991). Structure of melange and associated units in the Torlesse accretionary wedge, Tararua Range, New Zealand. *New Zealand Journal of Geology and Geophysics*, 34(1), 61-72.
- Pacheco, F. S., Roland, F., & Downing, J. A. (2014). Eutrophication reverses whole-lake carbon budgets. *Inland Waters*, 4(1), 41-48.
- Page, M., Trustrum, N., Orpin, A., Carter, L., Gomez, B., Cochran, U., . . . Palmer, A. (2010). Storm frequency and magnitude in response to Holocene climate variability, Lake Tutira, North-Eastern New Zealand. *Marine Geology*, 270(1-4), 30-44.
- Palmer, S. M., Hope, D., Billett, M. F., Dawson, J. J., & Bryant, C. L. (2001). Sources of organic and inorganic carbon in a headwater stream: Evidence from carbon isotope studies. *Biogeochemistry*, 52(3), 321-338.
- Patterson, R. T., Dalby, A., Kumar, A., Henderson, L. A., & Boudreau, R. E. (2002). Arcellaceans (thecamoebians) as indicators of land-use change: Settlement history of the Swan Lake area, Ontario as a case study. *Journal of Paleolimnology*, 28(3), 297-316.

- Pawson, E., & Brooking, T. (2002). *Environmental histories of New Zealand* (Vol. 342). Melbourne, Australia: Oxford University Press.
- Penny, D., & Murray-Mcintosh, R. (2002). Estimating the number of females in the founding population of New Zealand: Analysis of mtDNA variation. *The Journal of the Polynesian Society*, 111(3), 207-221.
- Perry, G. L., Wilmshurst, J. M., & McGlone, M. S. (2014). Ecology and long-term history of fire in New Zealand. *New Zealand Journal of Ecology*, 157-176.
- Perry, G. L., Wilmshurst, J. M., McGlone, M. S., McWethy, D. B., & Whitlock, C. (2012b). Explaining fire-driven landscape transformation during the initial burning period of New Zealand's prehistory. *Global Change Biology*, 18(5), 1609-1621.
- Perry, G. L., Wilmshurst, J. M., McGlone, M. S., & Napier, A. (2012a). Reconstructing spatial vulnerability to forest loss by fire in pre-historic New Zealand. *Global Ecology and Biogeography*, 21(10), 1029-1041.
- Peters, B., Jaffe, B., Peterson, C., Gelfenbaum, G., & Kelsey, H. (2001). *An overview of tsunami deposits along the Cascadia margin*. Paper presented at the Proceedings of the international tsunami symposium.
- Peters, R., Jaffe, B., & Gelfenbaum, G. (2007). Distribution and sedimentary characteristics of tsunami deposits along the Cascadia margin of western North America. *Sedimentary Geology*, 200(3-4), 372-386.
- Petersen, G. C. (1952). *The pioneering days of Palmerston North*. Levin, New Zealand: Kerslake, Billens and Humphrey.
- Philippsen, B. (2013). The freshwater reservoir effect in radiocarbon dating. *Heritage Science*, 1(1), 24.
- Porter, S. C. (2000). Onset of neoglaciation in the Southern Hemisphere. *Journal of Quaternary Science: Published for the Quaternary Research Association*, 15(4), 395-408.
- Pulido-Villena, E., Reche, I., & Morales-Baquero, R. (2005). Food web reliance on allochthonous carbon in two high mountain lakes with contrasting catchments: A stable isotope approach. *Canadian Journal of Fisheries and Aquatic Sciences*, 62(11), 2640-2648.
- PYLONEX. (n.d.). HTH sediment corer. Retrieved from <https://www.pylonex.com/files/2016-06/leaflet-hth-corer-ny.pdf>
- Rich, C. C. (1959). *Late Cenozoic geology of the lower Manawatu Valley, New Zealand*. (Unpublished doctoral dissertation), Harvard University, Cambridge, USA.
- Roche, M. (1997). From forest to pasture. The clearance of the lower North Island bush, plate 47. In M. McKinnon, B. Bradley & R. Kirkpatrick (Eds.), *New Zealand historical atlas: Ko Papatuanuku e Takoto Nei*. New Zealand: David Bateman.
- Roche, M. (2000). *Taming the land – a complete transformation*. (B. Saunders Ed.). Palmerston North, New Zealand: Geography Programme, Massey University, New Zealand.
- Rogers, G., & McGlone, M. (1989). A postglacial vegetation history of the southern-central uplands of North Island, New Zealand. *Journal of the Royal Society of New Zealand*, 19(3), 229-248.
- Rogers, K., & Cochran, U. (2017). Detecting environmental change using stable isotopes. In *Quaternary Techniques Short Course, 2017, National Isotope Centre*. New Zealand: GNS.
- Rolett, B., & Diamond, J. (2004). Environmental predictors of pre-European deforestation on Pacific Islands. *Nature*, 431(7007), 443.
- Rolston, R. (1944). Excavations at pa-site Lake Horowhenua. *The Journal of the Polynesian Society*, 53(4), 163-174.
- Rolston, R. (1947). Further excavations at pa-site, Lake Horowhenua. *The Journal of the Polynesian Society*, 56(3), 256-265.
- Rolston, R. (1948). Results of further excavations at pa-site, Lake Horowhenua. *The Journal of the Polynesian Society*, 57(4), 279-300.
- Rothwell, R., & Croudace, I. (2015a). Micro-XRF studies of sediment cores: A perspective on capability and application in the environmental sciences. In I. Croudace & R. Rothwell (Eds.), *Micro-XRF studies of sediment cores: Applications of a non-destructive tool for the environmental sciences* (pp. 1-21): Springer.

- Rothwell, R. G., & Croudace, I. (2015b). Twenty years of XRF core scanning marine sediments: What do geochemical proxies tell us? In I. Croudace & R. Rothwell (Eds.), *Micro-XRF studies of sediment cores: Applications of a non-destructive tool for the environmental sciences* (pp. 25-102): Springer.
- Roygard, J., Brown, L., Ferguson, L., Deverall, A., & Cooper, A. (2015). *Lake Horowhenua accord and clean-up fund - progress report*. Horizons Regional Council. Retrieved from http://flrc.massey.ac.nz/workshops/15/Manuscripts/Paper_Roygard_2015.pdf
- Rühland, K. M., Paterson, A. M., & Smol, J. P. (2015). Lake diatom responses to warming: Reviewing the evidence. *Journal of Paleolimnology*, *54*(1), 1-35.
- Salas, M. (1983). Long-distance pollen transport over the southern Tasman Sea: Evidence from Macquarie Island. *New Zealand Journal of Botany*, *21*(3), 285-292.
- Sayer, C., Roberts, N., Sadler, J., David, C., & Wade, P. (1999). Biodiversity changes in a shallow lake ecosystem: A multi-proxy palaeolimnological analysis. *Journal of Biogeography*, *26*(1), 97-114.
- Schaefer, J. M., Denton, G. H., Kaplan, M., Putnam, A., Finkel, R. C., Barrell, D. J., . . . Chinn, T. (2009). High-frequency Holocene glacier fluctuations in New Zealand differ from the northern signature. *Science*, *324*(5927), 622-625.
- Schumacher, B. A. (2002). Methods for the determination of total organic carbon (TOC) in soils and sediments. Las Vegas, USA: United States Environmental Protection Agency.
- Shennan, S. (2009). Evolutionary demography and the population history of the European early Neolithic. *Human Biology*, *81*(3), 339-355.
- Shulmeister, J., & Lees, B. G. (1995). Pollen evidence from tropical Australia for the onset of an ENSO-dominated climate at c. 4000 BP. *The Holocene*, *5*(1), 10-18.
- Simmons, D. R. (1969). A New Zealand myth: Kupe, Toi and the "fleet". *New Zealand Journal of History*, *3*(1), 14-31.
- Smale, M. (1984). White Pine Bush and an alluvial kahikatea (*Dacrycarpus dacrydioides*) forest remnant, eastern Bay of Plenty, New Zealand. *New Zealand Journal of Botany*, *22*(2), 201-206.
- Smirnov, N. (2014). *Physiology of the Cladocera*. Oxford, UK: Elsevier.
- Smol, J. P. (2008). *Pollution of lakes and rivers: A paleoenvironmental perspective* (2nd ed.): John Wiley & Sons.
- Sommerfield, C., Nittrouer, C., & Alexander, C. (1999). ⁷Be as a tracer of flood sedimentation on the northern California continental margin. *Continental Shelf Research*, *19*(3), 335-361.
- Søndergaard, M., Jensen, J. P., & Jeppesen, E. (2003). Role of sediment and internal loading of phosphorus in shallow lakes. *Hydrobiologia*, *506*(1-3), 135-145.
- Sperazza, M., Moore, J. N., & Hendrix, M. S. (2004). High-resolution particle size analysis of naturally occurring very fine-grained sediment through laser diffractometry. *Journal of Sedimentary Research*, *74*(5), 736-743.
- Spriggs, M., & Anderson, A. (1993). Late colonization of east Polynesia. *Antiquity*, *67*(255), 200-217.
- Steffen, W., Crutzen, P. J., & McNeill, J. R. (2007). The Anthropocene: Are humans now overwhelming the great forces of nature. *AMBIO: A Journal of the Human Environment*, *36*(8), 614-621.
- Stephens, T., Atkin, D., Augustinus, P., Shane, P., Lorrey, A., Street-Perrott, A., . . . Snowball, I. (2012). A late glacial Antarctic climate teleconnection and variable Holocene seasonality at Lake Pupuke, Auckland, New Zealand. *Journal of Paleolimnology*, *48*(4), 785-800.
- Stuiver, M., & Reimer, P. J. (1993). Extended ¹⁴C data base and revised CALIB 3.0 ¹⁴C age calibration program. *Radiocarbon*, *35*(1), 215-230.
- Sutton, D. G., Flenley, J. R., Li, X., Todd, A., Butler, K., Summers, R., & Chester, P. I. (2008). The timing of the human discovery and colonization of New Zealand. *Quaternary International*, *184*(1), 109-121.
- Swales, A., Ovenden, R., Wadhwa, S., & Rendle, D. (2010). *Bay of Islands OS20/20 survey report. Chapter 4: Recent sedimentation rates (over the last 100-150 years)*. New Zealand. New Zealand: NIWA.










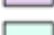




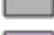






- Swales, A., Williamson, R. B., Van Dam, L. F., Stroud, M. J., & McGlone, M. S. (2002). Reconstruction of urban stormwater contamination of an estuary using catchment history and sediment profile dating. *Estuaries*, 25(1), 43-56.
- Talbot, M. (2001). Nitrogen isotopes in paleolimnology. In W. Last & J. Smol (Eds.), *Tracking environmental change using lake sediments: Physical and geochemical methods* (Vol. 2, pp. 401-440). London, England: Dordrecht and London: Kluwer Academic, Developments in Paleoenvironmental Research.
- Tana, R., & Tempero, G. W. (2013). *Life-history of Lake Horowhenua common smelt: Analysis of otolith chemistry and vertebral counts* (No. ERI Report Number 16): Hamilton, New Zealand: The University of Waikato, Environmental Research Institute.
- Te Punga, M. T. (1953). *The geology of Rangitikei valley*. New Zealand: Department of Scientific and Industrial Research, New Zealand Geological Survey.
- Tempero, G. W. (2013). *Assessment of fish populations in Lake Horowhenua, Levin*. Hamilton, New Zealand: The University of Waikato, Environmental Research Institute.
- TMPR. (2017). *The Muaūpoko priority report* (No. WAI 2200). Waitangi Tribunal.
- Trodahl, M. (2010). *Late Holocene sediment deposition of Lake Wairarapa, North Island, New Zealand*. (Master's thesis, Victoria University of Wellington, Wellington, New Zealand). Retrieved from <http://researcharchive.vuw.ac.nz/xmlui/handle/10063/1677>
- Turnbull, J. (2017). Radiocarbon dating. In *Quaternary Techniques Short Course, 2017, National Isotope Centre*. New Zealand: GNS.
- Ummerhofer, C. C., Sen Gupta, A., & England, M. H. (2009). Causes of late twentieth-century trends in New Zealand precipitation. *Journal of Climate*, 22(1), 3-19.
- Vaasma, T. (2008). Grain-size analysis of lacustrine sediments: A comparison of pre-treatment methods. *Estonian Journal of Ecology*, 57(4).
- Vandergoes, M., & Cochran, U. (2017). Paleoenvironmental reconstruction using microfossils: Terrestrial. In *Quaternary Techniques Short Course, 2017, National Isotope Centre*. New Zealand: GNS.
- Vandergoes, M. J., Fitzsimons, S. J., & Newnham, R. M. (1997). Late glacial to Holocene vegetation and climate change in the eastern Takitimu Mountains, western Southland, New Zealand. *Journal of the Royal Society of New Zealand*, 27(1), 53-66.
- Vandergoes, M. J., Howarth, J. D., Dunbar, G. B., Turnbull, J. C., Roop, H. A., Levy, R. H., . . . Keller, L. D. (2018). Integrating chronological uncertainties for annually laminated lake sediments using layer counting, independent chronologies and Bayesian age modelling (Lake Ohau, South Island, New Zealand). *Quaternary Science Reviews*, 188, 104-120.
- Vant, W. (1985). *Discussion of some aspects of Wanganui-Manawatu coastal dune lakes relevant to enhancement proposals for Lake Horowhenua*. Unpublished report to Manawatu Catchment Board, Palmerston North, New Zealand.
- Vant, W., & Gilliland, B. (1991). Changes in water quality in Lake Horowhenua following sewage diversion. *New Zealand Journal of Marine and Freshwater Research*, 25, 57-61.
- Vasskog, K., Kvisvik, B. C., & Paasche, Ø. (2016). Effects of hydrogen peroxide treatment on measurements of lake sediment grain-size distribution. *Journal of Paleolimnology*, 56(4), 365-381.
- Verburg, P., Hamill, K., Unwin, M., & Abell, J. (2010). *Lake water quality in New Zealand 2010: Status and trends*. New Zealand: NIWA. Retrieved from <https://www.mfe.govt.nz/sites/default/files/media/Environmental%20reporting/Lake%20water%20quality%20in%20New%20Zealand%202010%20Status%20and%20trends.pdf>
- Waksman, S. A., & Stevens, K. R. (1930). A critical study of the methods for determining the nature and abundance of soil organic matter. *Soil Science*, 30(2), 97-116.
- Wardle, P. (1991). *Vegetation of New Zealand*. Cambridge, UK: Cambridge University Press.
- Waters, C. N., Zalasiewicz, J. A., Williams, M., Ellis, M. A., & Snelling, A. M. (2014). A stratigraphical basis for the Anthropocene? *Geological Society, London, Special Publications*, 395.

- Whaley, P., Clarkson, B., & Smale, M. (1997). Claudelands Bush: Ecology of an urban kahikatea (*Dacrycarpus dacrydioides*) forest remnant in Hamilton, New Zealand. *Tane*, 36, 131-155.
- White, B. (1998). *Inland waterways: Lakes*. Waitangi Tribunal. Retrieved from <https://www.waitangitribunal.govt.nz/assets/Documents/Publications/wt-theme-q-inland-waterways-lakes.pdf>
- White, E., Payne, G., Pickmere, S., & Woods, P. (1991). Seasonal variation in nutrient limitation of the algal community in Lake Horowhenua, New Zealand. *New Zealand Journal of Marine and Freshwater Research*, 25(3), 311-316.
- Whyte, A., Marshall, S., & Chambers, G. (2005). Human evolution in Polynesia. *Human Biology*, 157-177.
- Williams, P., King, D., Zhao, J.-X., & Collerson, K. D. (2004). Speleothem master chronologies: Combined Holocene 18O and 13C records from the North Island of New Zealand and their palaeoenvironmental interpretation. *The Holocene*, 14(2), 194-208.
- Wilmshurst, J. (2007). Human effects on the environment: Pre-European deforestation. In *Te Ara - the Encyclopedia of New Zealand*. Retrieved from <https://teara.govt.nz/en/human-effects-on-the-environment/page-2>
- Wilmshurst, J. M. (1995). *A 2000 year history of vegetation and landscape change in Hawke's Bay, North Island, New Zealand*. (Unpublished doctoral dissertation), University of Canterbury, Christchurch, New Zealand.
- Wilmshurst, J. M. (1997). The impact of human settlement on vegetation and soil stability in Hawke's Bay, New Zealand. *New Zealand Journal of Botany*, 35(1), 97-111.
- Wilmshurst, J. M., Anderson, A. J., Higham, T. F., & Worthy, T. H. (2008). Dating the late prehistoric dispersal of Polynesians to New Zealand using the commensal Pacific rat. *Proceedings of the National Academy of Sciences*, 105(22), 7676-7680.
- Wilmshurst, J. M., Eden, D. N., & Froggatt, P. C. (1999). Late Holocene forest disturbance in Gisborne, New Zealand: A comparison of terrestrial and marine pollen records. *New Zealand Journal of Botany*, 37(3), 523-540.
- Wilmshurst, J. M., & Higham, T. F. (2004). Using rat-gnawed seeds to independently date the arrival of Pacific rats and humans in New Zealand. *The Holocene*, 14(6), 801-806.
- Wilmshurst, J. M., Higham, T. F., Allen, H., Johns, D., & Phillips, C. (2004). Early Maori settlement impacts in northern coastal Taranaki, New Zealand. *New Zealand Journal of Ecology*, 167-179.
- Wilmshurst, J. M., & McGlone, M. S. (2005a). Corroded pollen and spores as indicators of changing lake sediment sources and catchment disturbance. *Journal of Paleolimnology*, 34(4), 503-517.
- Wilmshurst, J. M., & McGlone, M. S. (2005b). Origin of pollen and spores in surface lake sediments: Comparison of modern palynomorph assemblages in moss cushions, surface soils and surface lake sediments. *Review of Palaeobotany and Palynology*, 136(1-2), 1-15.
- Wilmshurst, J. M., McGlone, M. S., & Partridge, T. R. (1997). A late Holocene history of natural disturbance in lowland Podocarp/hardwood forest, Hawke's Bay, New Zealand. *New Zealand Journal of Botany*, 35(1), 79-96.
- Wood, J. R., Wilmshurst, J. M., Newnham, R. M., & McGlone, M. (2016). Evolution and ecological change during the New Zealand Quaternary. In *Landscape and Quaternary Environmental Change in New Zealand* (Vol. 3): Springer.
- Woodward, C., & Shulmeister, J. (2005). A Holocene record of human induced and natural environmental change from Lake Forsyth (Te Wairewa), New Zealand. *Journal of Paleolimnology*, 34(4), 481-501.
- Woodward, C., & Shulmeister, J. (2006). New Zealand Chironomids as proxies for human-induced and natural environmental change: Transfer functions for temperature and lake production (chlorophyll a). *Journal of Paleolimnology*, 36(4), 407-429.
- WRC. (2018). Maori history of the greater Wellington region. Retrieved from <http://www.gw.govt.nz/maori-history-of-the-greater-wellington-region>

- Yaldwyn, J. (2002). The match box - the rat bone: The Hukanui #7b excavations 1959. *Archaeology in New Zealand*, 45(2), 118-127.
- Yasuda, Y., Kitagawa, H., & Nakagawa, T. (2000). The earliest record of major anthropogenic deforestation in the Ghab Valley, northwest Syria: A palynological study. *Quaternary International*, 73, 127-136.
- Yearbook. (1990). The New Zealand official 1990 year book. Retrieved from https://www3.stats.govt.nz/New_Zealand_Official_Yearbooks/1990/NZOYB_1990.htm 1?_ga=2.36207977.839827635.1526960634-1968496129.1526958794
- Zabowski, D., Rygiewicz, P., & Skinner, M. (1996). Site disturbance effects on a clay soil under radiata pine. *Plant and Soil*, 186(2), 343-351.

Appendices

Appendix A: Legend for Figure 1.

	Q1af Alluvial fan
	Q1al Holocene flood plain gravels
	Q1as Swamp deposit over flood gravel
	Q1dm Active sand dunes
	Q1ds Inactive sand dunes
	Q2af Alluvial sand deposits
	Q2al Ashhurst/Ohakea Fluvial Terrace
	Q3al Milson/Rata Fluvial Terrace
	Q4al Alluvial deposits Forrest Hill/Porewa Fluvial Terrace
	Q5b Tokomaru Marine Terrace
	Q6af Alluvial fan
	Q6al Alluvial gravel and terrace
	Q8al Alluvial gravel and terrace
	Te Torlesse Basement Greywacke
	Tt Rakaia Basement Greywacke
	eQal Undifferentiated early Quaternary loess covered fan and alluvial gravel
	mQal Undifferentiated mid Quaternary gravel with loess or tephra cover beds
	uQal Undifferentiated loess covered alluvial gravel
	Koputaroa Syncline
	Levin Anticline
	Levin Fault

Appendix C: Obscuration values

Sample #	cm	Obscuration values %	Notes
1	0.5	4	
2	6.5	6	
3	12.5	6	
4	18.5	6	
5	24.5	7	
6	31	6	
7	37	4	
8	43	6	
9	49	6	
10	55	6	
11	61	6	
12	67	11	
13	73	4	
14	79	3	
15	85	3	
17	103	5	
18	109	6	
19	115	4	
21	121	4	
20	127	4	
22	134	6	
23	139	5	
24	145	5	
25	151	2	
25	151	3	
26	163	7	
27	175	5	
28	187	8	
29	203	5	
30	215	7	
31	227	9	
32	239	12	Fines drained
33	251	11	Fines drained
34	263	10	Fines drained
35	275	12	Fines drained
36	287	10	Fines drained
37	303	12	Fines drained
38	315	12	Fines drained
39	333	12	Fines drained
40	351	11	Fines drained
41	363	12	Fines drained
42	375	14	Fines drained
43	387	15	Fines drained



Rafter Radiocarbon

Accelerator Mass Spectrometry Result

This result for the sample submitted is for the exclusive use of the submitter. All liability whatsoever to any third party is excluded.

NZA 65134

R 41178/1

Job No: 209794

Report issued: 27 Jun 2018

Sample ID Core S_0-30cm_2-12cm
Description Cladocera Ehippia
Fraction dated Other organic material
Submitter Marcus Vandergoes
 GNS Science

Conventional Radiocarbon Age	Modern	±		(years BP)
$\delta^{13}\text{C}$ (‰)	-29.9	±	0.2	from IRMS
Fraction modern	1.1255	±	0.0026	
$\Delta^{14}\text{C}$ (‰) and collection date		±		
Measurement Comment				

Sample Treatment Details

Description of sample when received: The sample was submitted suspended in water in a vial containing cladocera ehippia. Sample prepared by: Wet Sieve. Pre-treatment description: A number of blue fibres were hand picked out and then the sample was sieved to 200 microns to remove cellular detritus and algae (*B. braunii*) which was contaminating the sample. Chemical pre-treatment was by acid, alkali, acid. Weight obtained after chemical pre-treatment was 2.2 mg. Carbon dioxide was generated by sealed tube combustion and 1 mgC was obtained. Sample carbon dioxide was converted to graphite by reduction with hydrogen over iron catalyst.

Conventional Radiocarbon Age and $\Delta^{14}\text{C}$ are reported as defined by Stuiver and Polach (*Radiocarbon* 19:355-363, 1977). $\Delta^{14}\text{C}$ is reported only if collection date was supplied and is decay corrected to that date. Fraction modern (F) is the blank corrected fraction modern normalized to $\delta^{13}\text{C}$ of -25‰, defined by Donahue et al. (*Radiocarbon*, 32(2):135-142, 1990). $\delta^{13}\text{C}$ normalization is always performed using $\delta^{13}\text{C}$ measured by AMS, thus accounting for AMS fractionation. Although not used in the ^{14}C calculations, the environmental $\delta^{13}\text{C}$ measured offline by IRMS is reported if sufficient sample material was available. The reported errors comprise statistical errors in sample and standard determinations, combined in quadrature with a system error based on the analysis of an ongoing series of measurements of standard materials. Further details of pretreatment and analysis are available on request.



Rafter Radiocarbon

NZA 65135

R 41178/2

Job No: 209795

Report issued: 27 Jun 2018

Accelerator Mass Spectrometry Result

This result for the sample submitted is for the exclusive use of the submitter. All liability whatsoever to any third party is excluded.

Sample ID Horo 10_0-0.9m_85cm
Description Seed
Fraction dated Plant Material
Submitter Marcus Vandergoes
GNS Science

Conventional Radiocarbon Age	480	±	19	(years BP)
$\delta^{13}\text{C}$ (‰)	-21.9	±	0.2	from IRMS
Fraction modern	0.9420	±	0.0022	
$\Delta^{14}\text{C}$ (‰) and collection date		±		
Measurement Comment				

Sample Treatment Details

Description of sample when received: The sample was submitted in a vial as a single small hard complete seed. Sample prepared by: Cut/Scrape, Picking. Pre-treatment description: The detritus was cleaned off of the surface of the seed and cut in half to confirm that no contaminants had penetrated the inside of the seed. The sample appeared free of contamination. Chemical pre-treatment was by acid, alkali, acid. Weight obtained after chemical pre-treatment was 73.8 mg. Carbon dioxide was generated by sealed tube combustion and 1 mgC was obtained. Sample carbon dioxide was converted to graphite by reduction with hydrogen over iron catalyst.

Conventional Radiocarbon Age and $\Delta^{14}\text{C}$ are reported as defined by Stuiver and Polach (*Radiocarbon* 19:355-363, 1977). $\Delta^{14}\text{C}$ is reported only if collection date was supplied and is decay corrected to that date. Fraction modern (F) is the blank corrected fraction modern normalized to $\delta^{13}\text{C}$ of -25‰, defined by Donahue et al. (*Radiocarbon*, 32(2):135-142, 1990). $\delta^{13}\text{C}$ normalization is always performed using $\delta^{13}\text{C}$ measured by AMS, thus accounting for AMS fractionation. Although not used in the ^{14}C calculations, the environmental $\delta^{13}\text{C}$ measured offline by IRMS is reported if sufficient sample material was available. The reported errors comprise statistical errors in sample and standard determinations, combined in quadrature with a system error based on the analysis of an ongoing series of measurements of standard materials. Further details of pretreatment and analysis are available on request.



Rafter Radiocarbon

NZA 65136

R 41178/3

Job No: 209796

Report issued: 27 Jun 2018

Accelerator Mass Spectrometry Result

This result for the sample submitted is for the exclusive use of the submitter. All liability whatsoever to any third party is excluded.

Sample ID Horo 10_0-0.9m_80-90cm
Description Cladocera Ehippia
Fraction dated Other organic material
Submitter Marcus Vandergoes
GNS Science

Conventional Radiocarbon Age	1094	±	20	(years BP)
$\delta^{13}\text{C}$ (‰)	-33.3	±	0.2	from IRMS
Fraction modern	0.8726	±	0.0021	
$\Delta^{14}\text{C}$ (‰) and collection date		±		
Measurement Comment				

Sample Treatment Details

Description of sample when received: The sample was submitted suspended in water in a vial containing cladocera ehippia. Sample prepared by: Wet Sieve. Pre-treatment description: A number of blue fibres were hand picked out, then the sample was sieved to 200 microns to remove cellular detritus and algae (*B. braunii*) which was contaminating the sample. Chemical pre-treatment was by acid, alkali, acid. Weight obtained after chemical pre-treatment was 1.9 mg. Carbon dioxide was generated by sealed tube combustion and 0.9 mgC was obtained. Sample carbon dioxide was converted to graphite by reduction with hydrogen over iron catalyst.

Conventional Radiocarbon Age and $\Delta^{14}\text{C}$ are reported as defined by Stuiver and Polach (*Radiocarbon* 19:355-363, 1977). $\Delta^{14}\text{C}$ is reported only if collection date was supplied and is decay corrected to that date. Fraction modern (F) is the blank corrected fraction modern normalized to $\delta^{13}\text{C}$ of -25‰, defined by Donahue et al. (*Radiocarbon*, 32(2):135-142, 1990). $\delta^{13}\text{C}$ normalization is always performed using $\delta^{13}\text{C}$ measured by AMS, thus accounting for AMS fractionation. Although not used in the ^{14}C calculations, the environmental $\delta^{13}\text{C}$ measured offline by IRMS is reported if sufficient sample material was available. The reported errors comprise statistical errors in sample and standard determinations, combined in quadrature with a system error based on the analysis of an ongoing series of measurements of standard materials. Further details of pretreatment and analysis are available on request.



Rafter Radiocarbon

NZA 65079

R 41178/4

Job No: 209797

Report issued: 27 Jun 2018

Accelerator Mass Spectrometry Result

This result for the sample submitted is for the exclusive use of the submitter. All liability whatsoever to any third party is excluded.

Sample ID Horo 10_0-0.9m_80-85cm
Description Lake Margin Plant material
Fraction dated Plant Material
Submitter Marcus Vandergoes
GNS Science

Conventional Radiocarbon Age	780	±	50	(years BP)
$\delta^{13}\text{C}$ (‰)		±		from
Fraction modern	0.9075	±	0.0056	
$\Delta^{14}\text{C}$ (‰) and collection date		±		

Measurement Comment

This sample contained <0.3 mg carbon and has therefore been treated as a "small sample". Small samples are sensitive to contamination during sample collection, processing and measurement, which we correct for using concurrently measured size-matched modern and 14C-free blank materials. This correction and the lower number of 14C counts obtained necessarily produce lower precision than larger samples. Nonetheless, measurement of known-age materials shows that the results are accurate within the reported precision

Sample Treatment Details

Description of sample when received: The sample was submitted as wet bulk sediment in a tube. Sample prepared by: Wet Sieve, Picking. Pre-treatment description: The sample was sieved to 90 micron and several flakes of flax or lake margin plant material were retrieved along with other organic materials which were separated. The contaminants were scraped off with a spatula and blue fibres were removed with tweezers to prepare the flax pieces for dating. Chemical pre-treatment was by acid, alkali, acid. Weight obtained after chemical pre-treatment was 0.4 mg. Carbon dioxide was generated by sealed tube combustion and 0.2 mgC was obtained. Sample carbon dioxide was converted to graphite by reduction with hydrogen over iron catalyst.

Conventional Radiocarbon Age and $\Delta^{14}\text{C}$ are reported as defined by Stuiver and Polach (*Radiocarbon* 19:355-363, 1977). $\Delta^{14}\text{C}$ is reported only if collection date was supplied and is decay corrected to that date. Fraction modern (F) is the blank corrected fraction modern normalized to $\delta^{13}\text{C}$ of -25‰, defined by Donahue et al. (*Radiocarbon*, 32(2):135-142, 1990). $\delta^{13}\text{C}$ normalization is always performed using $\delta^{13}\text{C}$ measured by AMS, thus accounting for AMS fractionation. Although not used in the ^{14}C calculations, the environmental $\delta^{13}\text{C}$ measured offline by IRMS is reported if sufficient sample material was available. The reported errors comprise statistical errors in sample and standard determinations, combined in quadrature with a system error based on the analysis of an ongoing series of measurements of standard materials. Further details of pretreatment and analysis are available on request.



Rafter Radiocarbon

NZA 65080

R 41178/5

Job No: 209798

Report issued: 27 Jun 2018

Accelerator Mass Spectrometry Result

This result for the sample submitted is for the exclusive use of the submitter. All liability whatsoever to any third party is excluded.

Sample ID Horo 10_0-0.9m_80-85cm
Description Cladocera Ehippia
Fraction dated Other organic material
Submitter Marcus Vandergoes
GNS Science

Conventional Radiocarbon Age	1077	±	108	(years BP)
$\delta^{13}\text{C}$ (‰)		±		from
Fraction modern	0.8745	±	0.0118	
$\Delta^{14}\text{C}$ (‰) and collection date		±		

Measurement Comment

This sample contained <0.3 mg carbon and has therefore been treated as a "small sample". Small samples are sensitive to contamination during sample collection, processing and measurement, which we correct for using concurrently measured size-matched modern and 14C-free blank materials. This correction and the lower number of 14C counts obtained necessarily produce lower precision than larger samples. Nonetheless, measurement of known-age materials shows that the results are accurate within the reported precision

Sample Treatment Details

Description of sample when received: The sample was submitted as wet bulk sediment in a tube. Sample prepared by: Picking, Wet Sieve. Pre-treatment description: The sample was sieved to 90 micron and a small amount of cladocera ehippia were retrieved along with other organic materials which were separated from the ehippia. The contaminants were scraped off with a spatula and blue fibres were removed with tweezers to prepare ehippia for dating. Chemical pre-treatment was by acid, alkali, acid. Weight obtained after chemical pre-treatment was 0.2 mg. Carbon dioxide was generated by sealed tube combustion and 0.1 mgC was obtained. Sample carbon dioxide was converted to graphite by reduction with hydrogen over iron catalyst.

Conventional Radiocarbon Age and $\Delta^{14}\text{C}$ are reported as defined by Stuiver and Polach (*Radiocarbon* 19:355-363, 1977). $\Delta^{14}\text{C}$ is reported only if collection date was supplied and is decay corrected to that date. Fraction modern (F) is the blank corrected fraction modern normalized to $\delta^{13}\text{C}$ of -25‰, defined by Donahue et al. (*Radiocarbon*, 32(2):135-142, 1990). $\delta^{13}\text{C}$ normalization is always performed using $\delta^{13}\text{C}$ measured by AMS, thus accounting for AMS fractionation. Although not used in the ^{14}C calculations, the environmental $\delta^{13}\text{C}$ measured offline by IRMS is reported if sufficient sample material was available. The reported errors comprise statistical errors in sample and standard determinations, combined in quadrature with a system error based on the analysis of an ongoing series of measurements of standard materials. Further details of pretreatment and analysis are available on request.



Rafter Radiocarbon

NZA 65137

R 41178/6

Job No: 209799

Report issued: 27 Jun 2018

Accelerator Mass Spectrometry Result

This result for the sample submitted is for the exclusive use of the submitter. All liability whatsoever to any third party is excluded.

Sample ID Horo 10_1.9-2.9m_10-20cm
Description Cladocera Ehippia
Fraction dated Other organic material
Submitter Marcus Vandergoes
GNS Science

Conventional Radiocarbon Age	3410	±	21	(years BP)
$\delta^{13}\text{C}$ (‰)	-32.8	±	0.2	from IRMS
Fraction modern	0.6541	±	0.0017	
$\Delta^{14}\text{C}$ (‰) and collection date		±		
Measurement Comment				

Sample Treatment Details

Description of sample when received: The sample was submitted suspended in water in a vial containing cladocera ehippia. Sample prepared by: Wet Sieve. Pre-treatment description: A number of blue fibres were hand picked out, then the sample was sieved to 200 microns to remove cellular detritus and algae (*B. braunii*) which was contaminating the sample. Chemical pre-treatment was by acid, alkali, acid. Weight obtained after chemical pre-treatment was 1.7 mg. Carbon dioxide was generated by sealed tube combustion and 0.8 mgC was obtained. Sample carbon dioxide was converted to graphite by reduction with hydrogen over iron catalyst.

Conventional Radiocarbon Age and $\Delta^{14}\text{C}$ are reported as defined by Stuiver and Polach (*Radiocarbon* 19:355-363, 1977). $\Delta^{14}\text{C}$ is reported only if collection date was supplied and is decay corrected to that date. Fraction modern (F) is the blank corrected fraction modern normalized to $\delta^{13}\text{C}$ of -25‰, defined by Donahue et al. (*Radiocarbon*, 32(2):135-142, 1990). $\delta^{13}\text{C}$ normalization is always performed using $\delta^{13}\text{C}$ measured by AMS, thus accounting for AMS fractionation. Although not used in the ^{14}C calculations, the environmental $\delta^{13}\text{C}$ measured offline by IRMS is reported if sufficient sample material was available. The reported errors comprise statistical errors in sample and standard determinations, combined in quadrature with a system error based on the analysis of an ongoing series of measurements of standard materials. Further details of pretreatment and analysis are available on request.



Rafter Radiocarbon

NZA 65138

R 41178/7

Job No: 209800

Report issued: 27 Jun 2018

Accelerator Mass Spectrometry Result

This result for the sample submitted is for the exclusive use of the submitter. All liability whatsoever to any third party is excluded.

Sample ID Horo 10_2.9-3.9m_7-17cm
Description Cladocera Ehippia
Fraction dated other organic material
Submitter Marcus Vandergoes
GNS Science

Conventional Radiocarbon Age	2259	±	20	(years BP)
$\delta^{13}\text{C}$ (‰)	-34.1	±	0.2	from IRMS
Fraction modern	0.7549	±	0.0019	
$\Delta^{14}\text{C}$ (‰) and collection date		±		
Measurement Comment				

Sample Treatment Details

Description of sample when received: The sample was submitted suspended in water in a vial containing cladocera ehippia. Sample prepared by: Wet Sieve. Pre-treatment description: A number of blue fibres were hand picked out, then the sample was sieved to 200 microns to remove cellular detritus and algae (*B. braunii*) which was contaminating the sample. Chemical pre-treatment was by acid, alkali, acid. Weight obtained after chemical pre-treatment was 2.7 mg. Carbon dioxide was generated by sealed tube combustion and 1.2 mgC was obtained. Sample carbon dioxide was converted to graphite by reduction with hydrogen over iron catalyst.

Conventional Radiocarbon Age and $\Delta^{14}\text{C}$ are reported as defined by Stuiver and Polach (*Radiocarbon* 19:355-363, 1977). $\Delta^{14}\text{C}$ is reported only if collection date was supplied and is decay corrected to that date. Fraction modern (F) is the blank corrected fraction modern normalized to $\delta^{13}\text{C}$ of -25‰, defined by Donahue et al. (*Radiocarbon*, 32(2):135-142, 1990). $\delta^{13}\text{C}$ normalization is always performed using $\delta^{13}\text{C}$ measured by AMS, thus accounting for AMS fractionation. Although not used in the ^{14}C calculations, the environmental $\delta^{13}\text{C}$ measured offline by IRMS is reported if sufficient sample material was available. The reported errors comprise statistical errors in sample and standard determinations, combined in quadrature with a system error based on the analysis of an ongoing series of measurements of standard materials. Further details of pretreatment and analysis are available on request.



Rafter Radiocarbon

NZA 65822

R 41211/3

Job No: 210535

Report issued: 17 Sep 2018

Accelerator Mass Spectrometry Result

This result for the sample submitted is for the exclusive use of the submitter. All liability whatsoever to any third party is excluded.

Sample ID Horo10 1.9-2.9-12-18cm
Description Cladocera Ehippia
Fraction dated Other organic material
Submitter Marcus Vandergoes
GNS Science

Conventional Radiocarbon Age	2369	±	22	(years BP)
$\delta^{13}\text{C}$ (‰)	-33.6	±	0.2	from IRMS
Fraction modern	0.7446	±	0.0020	
$\Delta^{14}\text{C}$ (‰) and collection date		±		
Measurement Comment				

Sample Treatment Details

Description of sample when received: The sample was submitted in a plastic bottle as a small clump of damp sediment. The sediment was sieved to 150 micron and some cladocera ehippia were observed in the >150 fraction along with mineral grains, algae and bulk fine organics including cladocera body shells. Sample prepared by: Wet Sieve, Picking. Pre-treatment description: As much c. ehippia was picked out as possible with tweezers. The </> 150 fraction was combined and stored separately. The cladocera ehippia mass was not large, but the concentrate was pure. To prepare for treatment and to obtain a sizeable mass for measurement, the collected ehippia from sample depths 12-14 cm, 14-16 cm, and 16-18 cm were combined for a sample ranging from 12-18 cm. Chemical pre-treatment was by acid, alkali, acid. Weight obtained after chemical pre-treatment was 8.6 mg. Carbon dioxide was generated by sealed tube combustion and 0.7 mgC was obtained. Sample carbon dioxide was converted to graphite by reduction with hydrogen over iron catalyst.

Conventional Radiocarbon Age and $\Delta^{14}\text{C}$ are reported as defined by Stuiver and Polach (*Radiocarbon* 19:355-363, 1977). $\Delta^{14}\text{C}$ is reported only if collection date was supplied and is decay corrected to that date. Fraction modern (F) is the blank corrected fraction modern normalized to $\delta^{13}\text{C}$ of -25‰, defined by Donahue et al. (*Radiocarbon*, 32(2):135-142, 1990). $\delta^{13}\text{C}$ normalization is always performed using $\delta^{13}\text{C}$ measured by AMS, thus accounting for AMS fractionation. Although not used in the ^{14}C calculations, the environmental $\delta^{13}\text{C}$ measured offline by IRMS is reported if sufficient sample material was available. The reported errors comprise statistical errors in sample and standard determinations, combined in quadrature with a system error based on the analysis of an ongoing series of measurements of standard materials. Further details of pretreatment and analysis are available on request.



Rafter Radiocarbon

NZA 65823

R 41211/6

Job No: 210538

Report issued: 17 Sep 2018

Accelerator Mass Spectrometry Result

This result for the sample submitted is for the exclusive use of the submitter. All liability whatsoever to any third party is excluded.

Sample ID Horo10 2.9-3.9-9-15cm
Description Cladocera Ehippia
Fraction dated Other organic material
Submitter Marcus Vandergoes
GNS Science

Conventional Radiocarbon Age	3484	±	23	(years BP)
$\delta^{13}\text{C}$ (‰)	-32.1	±	0.2	from IRMS
Fraction modern	0.6481	±	0.0018	
$\Delta^{14}\text{C}$ (‰) and collection date		±		
Measurement Comment				

Sample Treatment Details

Description of sample when received: The sample was submitted in a plastic bottle as a small clump of damp sediment. The sediment was sieved to 150 micron and some cladocera ehippia were observed in the >150 fraction along with mineral grains, algae and bulk fine organics including cladocera body shells. Sample prepared by: Wet Sieve, Picking. Pre-treatment description: As much c. ehippia was picked out as possible with tweezers. The </> 150 fraction was combined and stored separately. The cladocera ehippia mass was not large, but the concentrate was pure. To prepare for treatment and to obtain a sizeable mass for measurement, the collected ehippia from sample depths 9-11 cm, 11-13 cm, and 13-15 cm were combined for a sample ranging from 9-15 cm. Chemical pre-treatment was by acid, alkali, acid. Weight obtained after chemical pre-treatment was 12.8 mg. Carbon dioxide was generated by sealed tube combustion and 0.7 mgC was obtained. Sample carbon dioxide was converted to graphite by reduction with hydrogen over iron catalyst.

Conventional Radiocarbon Age and $\Delta^{14}\text{C}$ are reported as defined by Stuiver and Polach (*Radiocarbon* 19:355-363, 1977). $\Delta^{14}\text{C}$ is reported only if collection date was supplied and is decay corrected to that date. Fraction modern (F) is the blank corrected fraction modern normalized to $\delta^{13}\text{C}$ of -25‰, defined by Donahue et al. (*Radiocarbon*, 32(2):135-142, 1990). $\delta^{13}\text{C}$ normalization is always performed using $\delta^{13}\text{C}$ measured by AMS, thus accounting for AMS fractionation. Although not used in the ^{14}C calculations, the environmental $\delta^{13}\text{C}$ measured offline by IRMS is reported if sufficient sample material was available. The reported errors comprise statistical errors in sample and standard determinations, combined in quadrature with a system error based on the analysis of an ongoing series of measurements of standard materials. Further details of pretreatment and analysis are available on request.



Rafter Radiocarbon

NZA 65824

R 41211/7

Job No: 210539

Report issued: 17 Sep 2018

Accelerator Mass Spectrometry Result

This result for the sample submitted is for the exclusive use of the submitter. All liability whatsoever to any third party is excluded.

Sample ID Horo10 80-85cm <90um
Description Sediment
Fraction dated Sediment
Submitter Marcus Vandergoes
GNS Science

Conventional Radiocarbon Age	961	±	21	(years BP)
$\delta^{13}\text{C}$ (‰)	-27.7	±	0.2	from IRMS
Fraction modern	0.8873	±	0.0023	
$\Delta^{14}\text{C}$ (‰) and collection date		±		
Measurement Comment				

Sample Treatment Details

Description of sample when received: The sample was stored in a centrifuge tube containing damp sediment. Cladocera had already been extracted from the sediment for dating. Pre-treatment description: Approximately half of the sediment was selected for a bulk date. The remaining untreated sediment was stored. Chemical pre-treatment was by acid, alkali which was repeated three times in total, acid. Weight obtained after chemical pre-treatment was 95.5 mg. Carbon dioxide was generated by sealed tube combustion and 13.4 mgC was obtained. Sample carbon dioxide was converted to graphite by reduction with hydrogen over iron catalyst.

Conventional Radiocarbon Age and $\Delta^{14}\text{C}$ are reported as defined by Stuiver and Polach (*Radiocarbon* 19:355-363, 1977). $\Delta^{14}\text{C}$ is reported only if collection date was supplied and is decay corrected to that date. Fraction modern (F) is the blank corrected fraction modern normalized to $\delta^{13}\text{C}$ of -25‰, defined by Donahue et al. (*Radiocarbon*, 32(2):135-142, 1990). $\delta^{13}\text{C}$ normalization is always performed using $\delta^{13}\text{C}$ measured by AMS, thus accounting for AMS fractionation. Although not used in the ^{14}C calculations, the environmental $\delta^{13}\text{C}$ measured offline by IRMS is reported if sufficient sample material was available. The reported errors comprise statistical errors in sample and standard determinations, combined in quadrature with a system error based on the analysis of an ongoing series of measurements of standard materials. Further details of pretreatment and analysis are available on request.

